PRESSING FORCE CONTROL OF TABLETTING MACHINE

PIJIRAWUCH WIENGCHANDA

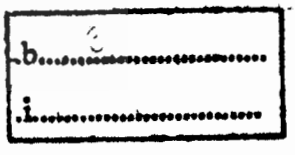

A THESIS SUBMITTED IN PARTIAL FULFILLMENT
OF THE REQUIREMENT FOR THE DEGREE OF
MASTER OF ENGINEERING IN MECHANICAL ENGINEERING
FACULTY OF ENGINEERING
KING MONGKUT'S INSTITUTE OF TECHNOLOGY LADKRABANG
2011

KMITL-2011-EN-M-030-133

หัวข้อวิทยานิพนธ์	การควบคุมแรงกดของเครื่องกดอัดเม็ดยา
นักศึกษา	เรือเอกปิจิราวุช เวียงจันดา
รหัสประจำตัว	52610518
ปริญญา	วิศวกรรมศาสตรมหาบัณฑิต
สาขาวิชา	วิศวกรรมเครื่องกล
พ.ศ.	2554
อาจารย์ที่ปรึกษาวิทยานิพนธ์	ผศ.ดร.ณัฐวุฒิ เดไปวา

บทคัดย่อ

งานวิจัยนี้ทำการศึกษา ออกแบบระบบอิเลคโทร – ไฮโดรลิคแบบควบคุมแรงของเครื่องกดอัดเม็ดยา และทำการปรับปรุงประสิทธิภาพของแบบจำลอง/ระบบโดยการใช้การควบคุมแบบย้อนกลับ ในขั้นตอนแรกนั้นระบบไฮโดรลิคได้ถูกจัดสร้างและทำการทดลอง โดยพรอพโพชั่นนอลวาล์วได้ถูกทำการทดสอบเพื่อหาคุณลักษณะของวาล์ว ซึ่งได้แก่ความสัมพันธ์ของสัญญาณการควบคุมและพื้นที่ช่องการเปิดของวาล์ว แบบจำลองของระบบอิเลคโทร – ไฮโดรลิคได้พัฒนาโดยโปรแกรม Matlab/Simulink ตรวจสอบและปรับปรุงความถูกต้องโดยการเปรียบเทียบผลการจำลองกับผลการทดลองจริง ระบบควบคุมแบบพีไอดีและระบบควบคุมแบบตรรกะคลุมเครือถูกใช้เพื่อควบคุมระบบอิเลคโทร – ไฮโดรลิคแบบควบคุมแรงกด ตัวควบคุมแบบพีไอดีนั้นได้รับการออกแบบสำหรับระบบแบบเชิงเส้นที่จุดสมดุลซึ่งในงานวิจัยนี้ได้ทำการแปลงระบบที่ไม่เป็นเชิงเส้นให้เป็นเชิงเส้นโดยใช้ทฤษฎี Taylor series และออกแบบปรับแต่งตัวควบคุมพีไอดีโดยใช้ทฤษฎี Ziegler – Nichols ในส่วนของการออกแบบตัวควบคุมแบบตรรกะคลุมเครือนั้นออกแบบให้มีผลการตอบสนองของระบบที่ใกล้เคียงกับผลการตองสนองของระบบที่ใช้ตัวควบคุมแบบพีไอดี การจำลองของแบบจำลองถูกพัฒนาโดยใช้โปรแกรม Matlab/Simulink และผลของการจำลองจะถูกเปรียบเทียบกับผลการทดลองในแต่ละตัวควบคุม ผลการตอบสนองทั้งประสิทธิภาพและความเสถียรของระบบจะถูกนำมาเปรียบเทียบกันระหว่างแบบจำลองและผลการทดลองจริงของแต่ละตัวควบคุมในแต่ละแรงกดที่ต้องการ

Thesis Title	Pressing Force Control of Tabletting Machine
Student	Lieutenant Pijirawuch Wiengchanda
Student ID	52610518
Degree	Master of Engineering
Program	Mechanical Engineering
Year	2011
Thesis Advisor	Asst.Prof.Dr.Nattawoot Depaiwa

ABSTRACT

The objective of this thesis is to model an electro – hydraulic servo system (EHSS) using force control for tabletting machine and then improve upon the performance of the model/system through feedback control design. The hydraulic system is first constructed and tested. The proportional valve is tested for finding the characteristics of valve that is curve between signal input voltages and opening area of valve. The model of electro – hydraulic servo system is improved using Matlab/Simulink and checked for accuracy by comparing with the dynamic system test results. Proportional – Integral – Differential (PID) controller and Fuzzy Logic Controllers (FLC) have been applied in order to control the electro – hydraulic servo system using force control. PID controller are designed specifically for the linear models at equilibrium point that linearized from non – linear model to linear model by using Taylor series theorem, and tuned using Ziegler – Nichols theory. In the case of FLC designed to response as well as the response of designed PID controller. Simulation is performed using Matlab/Simulink and some of the results are compared graphically with experimental results. The nominal stability and performance of each control system is found and compared for the models and system.

Acknowledgments

I would like to express my profound gratitude to my advisor, Asst.Prof.Dr.Nattawoot Depaiwa, for his guidance, encouragement, patience and constructive criticisms during the supervision of this thesis and thanks a lot of lecturer, Asst.Prof.Dr.Unnut Pinsopon, for his suggested in ideal and commendation in this thesis. I am very grateful to all of committees; Asst.Prof.Dr.Unnut Pinsopon, Dr.Akapot Tantrapiwat, Dr.Amnart Kanarat, Asst.Prof.Dr.Nattawoot Depaiwa and Dr.Thitaphol Huyanan for their evolutions on my research.

Many thanks go to my agency, Royal Thai Navy, for allowed me to study in master degree.

Moreover, I wish to give special thanks to Dr.Duangratana Shuwisitkul from Srinakrarinwirot university Onkarak branch and a countless number of students in Department of Mechanical Engineering and Automotive club at King Mongkut's Institute of Technology Ladkrabang, especially, Mr.Naren Chaitanee, Mr.Prathan Srichai, Mr.Songtam Laowsuwan, Mr.Wittawat Imerb, Mr.Pattanit Nomthongthai, Mr.Piyaboot Ornman and Mr.Yuttana Songsaengchan for sharing of their discussion.

Finally, I really appreciate my family for their great supports and encouragement over the past year.

Lieutenant Pijirawuch Wiengchanda

Contents

Contents (Cont.)

Contents (Cont.)

List of Table

List of Figures

List of Figures (Cont.)

List of Figures (Cont.)

Figures **Page**

Chapter 1
Introduction

1.1 Background

Many tabletting machines used for experiment with pressing process the tablet in some Pharmacy Department of Thailand imported from foreign countries. The conventional machine cannot control a pressing force that may cause directly to the quality of the tablet, for example, the solubility, hardness, rough of surface, etc. In this research, the tabletting machine, which can control the pressing force, will be developed and used to analyze the effect of controller–parameter onto the quality of the tablet.

The electro-hydraulic servo system has been widely used in various fields of industrial process control for force or position servo application because it has the characteristics of small volume, quick response, controlling signals flexibly, high stiffness and large output power [1]. Along with the accelerated process of manufacturing information, to bring up more and higher request for the electro-hydraulic force servo control system. However, there are also many challenges in the design of electro-hydraulic control systems. For example, there are highly nonlinear phenomenon, the flow-pressure relationship and the dead band due to the internal leakage and hysteresis, and many uncertainties of hydraulic systems due to linearization. Therefore, the electro-hydraulic servo system, it is almost impossible to build an accurate mathematical model theoretically and it is difficult for conventional PID controller to realize effective control in electro - hydraulic servo control system.

1.2 Purpose and Scope of the Thesis

The goals of this thesis are as follows; construct and model the electro – hydraulic servo system for tabletting press machine test with pressing force control and then improve upon the performance of the model/system through feedback control design, perform lab tests to create a dynamic model of the servo valve, and test and analyze for nominal stability and performance in the time domain. The differencing schemes control used in this research are PID controller and Fuzzy logic controller.

1.3 Layout of the Thesis

This research is basic organized into seven parts including this introduction. Here is the brief description of the remaining chapters.

Chapter 2 deals with the literature for the development of electro – hydraulic servo system models and controller.

Chapter 3 models the dynamic model of Electro – hydraulic servo system for tabletting pressing machine. This system contains two cases, in the case of cylinder extend and in the case of cylinder retract. The linearization of system method and implementation of model of electro – hydraulic servo system in the Matlab – Simulink is represented.

Chapter 4 briefs the controller design for electro – hydraulic servo system for tabletting press machine. In this chapter, present the PID controller that design by using Ziegler – Nichols method and Fuzzy logic controller that design by using phase - plane method.

Chapter 5 presents the equipment in the system and the method for experimental the servo valve and the nominal stability and performance of the system.

Chapter 6 presents the result of valve modulation test, the accuracy of mathematic model that compare with the real system and the nominal stability and performance of the system that is rising time, settling time and steady state error.

Chapter 7 discusses the conclusions of the present work and the further issues that it raises.

Chapter 2
Literature Review

The application of hydraulic actuation to heavy duty equipment reflects the ability of the hydraulic circuit to transmit larger forces and to be easily controlled. It has many distinct advantages such as the fast response speed, very high system stiffness and a higher force to weight ratio [2-3]. The electro-hydraulic servo system, among others, is perhaps the most important system for force servo applications because it takes the advantages of both the large output power of traditional hydraulic systems and the rapid response of electric systems. Typical applications of Electro-Hydraulic Servo Systems (EHSS) include injection molding machines, different kinds of machine tools and construction machinery, etc. However, there are also many challenges in the design of electro-hydraulic control system [2–4]. For example, they are the highly nonlinear phenomena such as fluid compressibility, the flow/pressure relationship and dead band due to the internal leakage and hysteresis and the many uncertainties of hydraulic systems due to linearization. Therefore, it seems to be quite difficult to perform a high precision servo control by using linear control method.

The study of electro-hydraulic force servo control strategy which was done by scholar home and abroad is as follows: classical control [5], adaptive control [6-7], predictive control [8], neural network control [9] and so on, and scholar got certain achievements in these fields.

B. Šulc, J. A. Jan [10] deals with non-linear modeling and control of a differential hydraulic actuator. Then on linear state space equations are derived from basic physical laws. They are more powerful than the transfer function in the case of linear models, and they allow the application of an object oriented approach in simulation programs. The effects of all friction forces (static, Coulomb and viscous) have been modeled, and many phenomena that are usually neglected are taken in to account, e.g., the static term of friction, the leakage between the two chambers and external space. Proportional Differential (PD) and Fuzzy Logic Controllers (FLC) have been applied in order to make a comparison by means of simulation. Simulation is performed using Matlab/Simulink, and some of the results are compared graphically. FLC is tuned in such way that it produces a constant control signal close to its maximum (or minimum), where possible. In the case of PD control the occurrence of peaks cannot be avoided.

Chen et al. [11] designed a variable-structure force controller including position, velocity, acceleration, force and pressure feedback signals for a single-rod hydraulic

cylinder. The controller showed steady state errors for step inputs and the control signal was discontinuous.

Conrad and Jensen [12] used the combinations of velocity feed-forward, output feedback and a Luenberger observer with state estimate feedback for force control of a double-rod hydraulic actuator. However, variations in load were not considered in their study.

Alleyne et al. [13] showed that conventional PID controller does not yield reasonable performance over a wide range of operating condition. Meanwhile, fuzzy control, an intelligent control method imitating the logical thinking of human and being independent on accurate mathematical model of the controlled object, can overcome some shortcomings of traditional PID. This control method brings many advantages such as more powerful anti-interference, faster response and stronger robustness. But the fuzzy is a nonlinear control and output of the controller has the static error as in the presentation of J.Guo et al. [14]. Then, fuzzy-PID control which combines the traditional PID control and fuzzy control algorithm is a good solution.

Charter 3
Dynamic Systems

3.1 Background

Though the hydraulic power systems have notable drawbacks, they still find use in a wide range of industrial application. Electro – hydraulic systems are used in the machine tool industry, milling machine, automobiles, punching presses, etc.

Electro Hydraulic Servo System (EHSS) have been used in industry in a wide number of applications due to their small size to power ratio, the ability to apply a very large force and control accuracy. However, the dynamic of hydraulic system are highly nonlinear; the system may be subjected to non – smooth nonlinearities due to input saturation, directional change of valve opening, friction, and valve overlap. Aside from the nonlinear nature of hydraulic dynamics, EHSS also have large extent of model uncertainties, such as the external disturbance and leakage that cannot to be modeled exactly, and the nonlinear functions that describe them may not be known. While accurate modeling involving all the nonlinearities is helpful in identifying the complex dynamic behavior, it complicates the hydraulic system model for any nonlinear control strategy.

Industry's growing need for faster development times and more accurate manufacturing is placing new demand on the technology used in automation. Systems are becoming more and more complex, consisting of mechanisms, actuators, controller and sensors. Even simple components will contain sensors that are used as a feedback for their controllers.

This charter covers the governing equation for electro – hydraulic servo system. In section 3.2, an overview of the fluid properties and governing equations of the electro – hydraulic servo system are provided, section 3.3 demonstrates the dynamics of an electro – hydraulic servo system, section 3.4 briefs linearization of mathematical model method and section 3.5 suggest the dynamics of an electro – hydraulic servo system by using MATLAB – Simulink.

3.2 Dynamic Effects of Hydraulic System

Some of the important physical properties of fluid and governing equation of the electro – hydraulic servo system are presented here.

3.2.1 Mass Density

Mass density, defined as the mass per unit of volume is an important property of fluid. It is represented by ρ. In the SI system, it has units of kg/m^3. The density of

a liquid varies with temperature and pressure. Since the variation of density with temperature and pressure is small. Taylor's series approximate can be used

$$\rho(P,T) = \rho_0 + \left(\frac{\partial \rho}{\partial P}\right)_T (P - P_0) + \left(\frac{\partial \rho}{\partial T}\right)_P (T - T_0) \qquad (3.1)$$

where ρ, P and T are the mass density, pressure and temperature, respectively, of the liquid about initial value of ρ_0, P_0, T_0 .

3.2.2 Bulk Modulus

The mass density (ρ) is called the *isothermal bulk modulus*. It is defined as the ratio of change in pressure to the fractional change in volume at constant temperature. It has the unit of pressure (Pa, in SI system). The bulk modulus (β) varies with fluid pressure, temperature, air content, and rigidity of the container and hoses. It is an important property in determining the dynamic properties of the hydraulic system.

It is reasonable to assume the container to be rigid and the effect of temperature on bulk modulus is negligible. A theoretical equation for effective bulk modulus as given by is [15]

$$\frac{1}{\beta_\varepsilon} = -\frac{\Delta P}{\Delta V / V} = \frac{1}{\beta_{hose}} + \frac{1}{\beta_{air\ free}} + \frac{\varepsilon}{1.4(P_{chamber} + P_{atomsphere})} \qquad (3.2)$$

where ε is the percentage of air in the fluid. A small amount of entrapped air can drastically reduce the bulk modulus. Experimentally, it is possible to determine the effective bulk modulus as a function of pressure and entrained air percentage.

There are many empirical formulas for the effective bulk modulus, including the effect of entrain air and mechanical compliance, base on direct measurements. The commonly used equation for effective bulk modulus, β_e , in hydraulic cylinder is [16]

$$\beta_e = a_1 E_{max} log\left(a_2 \frac{P}{P_{max}} + a_3\right) \qquad (3.3)$$

where the constant parameter are E_{max} = 1.8x10^9 Pa and P_{max} = 2.8 MPa. The other parameter must a_1, a_2 and a_3 must be identified.

The fundamental laws and equations, which govern the flow of fluid, are described in the section. Only the equations relevant for study of hydraulic system are presented.

3.2.3 Flow Continuity Equation

Consider the fluid volume V_0 as shown in Figure 3.1, with inlet mass flow rate of m_i and outlet mass flow rate of m_o. Using the law of conservation of mass, the rate at which the mass of fluid is accumulated is equal to the input flow rate minus the output flow rate.

$$\rho_i Q_i - \rho_o Q_o = \frac{d}{dt}(\rho V) \tag{3.4}$$

where Q_i and Q_o are the inlet and outlet flows.
If the density of the fluid is assumed constant, the above equation can be rewritten as

$$Q_i - Q_o = \frac{dV}{dt} + \frac{V}{\rho}\frac{d\rho}{dt} \tag{3.5}$$

Using the following equation of bulk modulus [16]

$$\frac{d\rho}{\rho} = \frac{dP}{\beta_e} \tag{3.6}$$

Obtained the flow continuity equation

$$Q_i - Q_o = \frac{dV}{dt} + \frac{V}{\beta_e}\frac{dP}{dt} \tag{3.7}$$

The first term on the right hand side is the due to the boundary deformation and the second team is due to the fluid compressibility term.

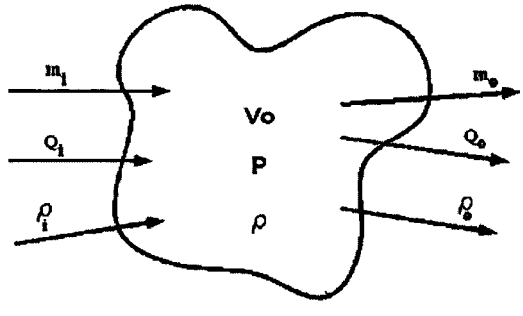

Figure 3.1 Generalized flow volume

3.2.4 Flow through an Orifice

Due to high flow rates in the hydraulic systems, most of the hydraulic flows are turbulent in nature. Using Bernoulli's equation and continuity equation, the flow through an orifice is obtained as [17]

$$Q = C_d A_0 \sqrt{\frac{2}{\rho}(\Delta P)} \tag{3.8}$$

where Q is flow rate, C_d is called the discharge coefficient, A_o is the area of cross section of orifice, ΔP is the pressure dropped across valve and It has been assumed that the orifices used in hydraulic system are sharp edged.

3.2.5 Newton's Second Law Effects

The second building block in the formulation of dynamic equations results from noting that masses subjected to unbalanced forces must accelerate according to Newton's second law, $F = ma$. This equation is commonly rearranged as

$$a = \ddot{x} = \frac{\left(\sum_{i=1}^{i=n} F_i\right)}{m} \tag{3.9}$$

As before, careful attention to signs is necessary. A direction for x must be established and the signs of forces specified accordingly. An allusion to vector concepts was made in the introduction to this chapter. It will be obvious that it is only components of force resolved in the x direction, which included in the equation. An exception to this statement might be friction force that may result from force perpendicular to the direction of motion.

The previous equation is not suitable for most standard differential equation solvers. This second order equation must be split into two first order equations

$$\frac{dx}{dt} = v \tag{3.10}$$

$$\frac{dv}{dt} = \frac{\left(\sum_{i=1}^{i=n} F_i\right)}{m} \tag{3.11}$$

The forces on the moving parts of a fluid power circuit shown in Equation 3.10 may result from pressure differences, viscous friction, coulomb friction, gravity, and flow forces to name a few.

3.3 Mathematical Model of Tableting Machine

In this study, consider a force that pressing on tablet in the die which installed in the end of actuator rod. The overall schematic representation of the system is depicted in Figure 3.2. The hydraulic flow is supplied from fixed volumetric displacement pump and flow though proportional valve is constant. The actuator that in the end installed the die presses to the tablet in the tabletting block. The system includes mainly controller, motor pump, proportional valve, piston cylinder. The control scheme is coded and run from a Pentium PC with the input/output interface using DAQ card. The force sensor that is installed upper the tabletting block directly measures the feedback control signal. (As picture of Tabletting machine is shown in Figure 5.2)

3.3.1 Model of Tabletting Machine Dynamic

The model of tabletting machine consists of three main modules, shown as Figure 3.2. These modules are power unit including AC motor and the hydraulic pump, the amplifier-embedded proportional valve and the hydraulic cylinder. Based on the law of the continuous flow and the Newton's second law, the mathematical model of the system dynamic is described as follows.

Constitutive relations of the motor – pump subsystem are

$$Q_p = V_D N_p \tag{3.12}$$

where Q_p is the practical output dynamic flow rate of the pump in m^3/s, V_D is the volumetric displacement of pump in m^3/rev, and N_p is the cycle of the pump in rev/sec.

This thesis works for mathematical modeling of the system by considering of two cases. The first, considering the piston is extending (shown as Figure 3.3) and the second, considering the piston is retracting (shown as Figure 3.4).

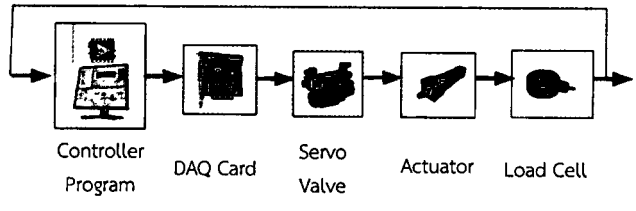

Figure 3.2 Diagram of electro – hydraulic servo system

3.3.2 Piston Extended Case

In the case of a piston is extending, applying the Equation 3.8 to consider flow rates from power unit flow though the proportional valve into the cylinder as follows

$$Q_{pahe} = \left(C_d \sqrt{\frac{2}{\rho}} \right) A_{pa} \sqrt{P_p - P_{he}} \tag{3.13}$$

where Q_{pahe} is the flow rate flow though proportional valve from port p to port a into the head end of cylinder. C_d is called the discharge coefficient and it has been assumed the orifices area is sharp edged. A_{pa} is the opening area of cross section of port p to port a. P_P is the pressure of pump, and P_{he} is the pressure on the head end of cylinder.

In addition, consider flow rates from the cylinder flow though the proportional valve into the power unit as follows:

$$Q_{btre} = \left(C_d \sqrt{\frac{2}{\rho}} \right) A_{bt} \sqrt{P_{re} - P_t} \tag{3.14}$$

where Q_{btre} is the flow rate from the rod end of cylinder flow though proportional valve from port b to port t into the power unit. C_d is called the discharge coefficient and it has been assumed the orifices area is sharp edged. A_{bt} is the opening area of cross section of port a to port t. P_{he} is the pressure on the rod end of cylinder and P_t is the pressure of ambient.

Considering the compression of hydraulic oil within the cylinder, can be write the following equation as

$$Q_p = Q_{pahe} + \frac{V_{hose}}{\beta} \dot{P}_p \tag{3.15}$$

$$Q_{pahe} = A_{he} \dot{x} + \frac{\left(V_{0he} + A_{he} x \right)}{\beta} \dot{P}_{he} \tag{3.16}$$

$$Q_{btre} = A_{re} \dot{x} - \frac{\left(V_{0re} + A_{re} \left(L_{stroke} - x \right) \right)}{\beta} \dot{P}_{re} \tag{3.17}$$

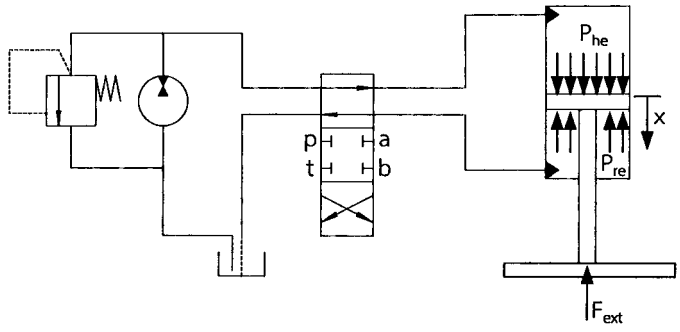

Figure 3.3 Block diagram of the electro – hydraulic servo system in case of the cylinder extend

From Equation 3.14, 3.15 and 3.16, rearranging

$$\dot{P}_p = \frac{\beta}{V_{hose}}\left(Q_p - Q_{pahe}\right) \tag{3.18}$$

$$\dot{P}_{he} = \frac{\beta}{\left(V_{0he} + A_{he}x\right)}\left(Q_{pahe} - A_{he}\dot{x}\right) \tag{3.19}$$

$$\dot{P}_{re} = \frac{\beta}{\left(V_{0re} + A_{re}\left(L_{stroke} - x\right)\right)}\left(-Q_{btre} + A_{re}\dot{x}\right) \tag{3.20}$$

Applying the Newton's second law for motion equation of cylinder

$$\ddot{x} = \frac{1}{m_{piston}}\left(P_{he}A_{he} - P_{re}A_{re} - F_{ext}\right) \tag{3.21}$$

Then, set the status variable in the state equation building, as following

$$x_1 = x \tag{3.22}$$

$$x_2 = \dot{x}_1 \tag{3.23}$$

$$x_3 = P_p \tag{3.24}$$

$$x_4 = P_{he} \tag{3.25}$$

$$x_5 = P_{re} \tag{3.26}$$

Set variables to the state equation from Equation 3.22. It can be written by

$$\dot{x}_1 = x_2 \tag{3.27a}$$

In addition, from Equation 3.18, 3.19, 3.20 and 3.21, can be rewritten as

$$\dot{x}_2 = \frac{1}{m_{piston}}\left(P_{he}A_{he} - P_{re}A_{re} - F_{ext}\right) \tag{3.27b}$$

$$\dot{x}_3 = \frac{\beta}{V_{hose}}\left(Q_p - Q_{pahe}\right) \tag{3.27c}$$

$$\dot{x}_4 = \frac{\beta}{\left(V_{0he} + A_{he}x_1\right)}\left(Q_{pahe'} - A_{he}x_2\right) \tag{3.27d}$$

$$\dot{x}_5 = \frac{\beta}{\left(V_{0re} + A_{re}\left(L_{stroke} - x_1\right)\right)}\left(-Q_{atre} + A_{re}x_2\right) \tag{3.27e}$$

Equation 3.27a, 3.27b, 3.27c, 3.27d and 3.27e is the mathematic model of the electro – hydraulic servo system in case of the cylinder extend.

3.3.3 Piston Retracted Case

In the case of a piston is retracting, applying the Equation 3.7 to consider flow rates from power unit into the cylinder as follows

$$Q_{pbre} = \left(C_d\sqrt{\frac{2}{\rho}}\right)A_{pb}\sqrt{P_p - P_{re}} \tag{3.28}$$

In addition, consider flow rates from the cylinder into the power unit as follows.

$$Q_{athe} = \left(C_d\sqrt{\frac{2}{\rho}}\right)A_{at}\sqrt{P_{he} - P_t} \tag{3.29}$$

Considering the compression of hydraulic oil within the cylinder, we can write the following equation as in case of the cylinder retracts.

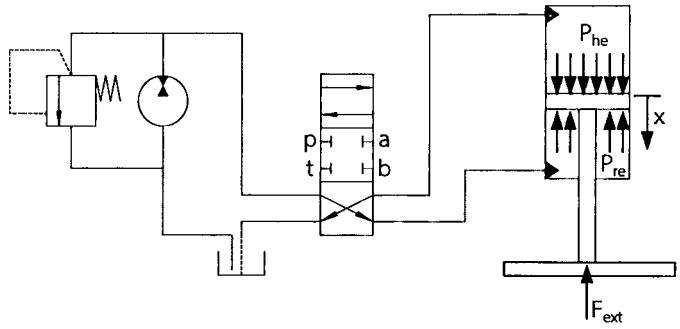

Figure 3.4 Block diagram of the electro – hydraulic servo system in case of the cylinder retracts

$$Q_p = Q_{pbre} + \frac{V_{hose}}{\beta}\dot{P}_p \tag{3.30}$$

$$Q_{athe} = A_{he}\dot{x} - \frac{\left(V_{0he} + A_{he}x\right)}{\beta}\dot{P}_{he} \tag{3.31}$$

$$Q_{pbre} = A_{re}\dot{x} - \frac{\left(V_{0re} + A_{re}\left(L_{stroke} - x\right)\right)}{\beta}\dot{P}_{re} \tag{3.32}$$

From Equation 3.30, 3.31 and 3.32, rearranging

$$\dot{P}_p = \frac{\beta}{V_{hose}}\left(Q_p - Q_{pbhe}\right) \tag{3.33}$$

$$\dot{P}_{he} = \frac{\beta}{\left(V_{0he} + A_{he}x\right)}\left(-Q_{athe} + A_{he}\dot{x}\right) \tag{3.34}$$

$$\dot{P}_{re} = \frac{\beta}{\left(V_{0re} + A_{re}\left(L_{stroke} - x\right)\right)}\left(Q_{pbre} - A_{re}\dot{x}\right) \tag{3.35}$$

Applying the Newton's second law for motion equation of cylinder

$$\ddot{x} = \frac{1}{m_{piston}}\left(P_{he}A_{he} - P_{re}A_{re} - F_{ext}\right) \tag{3.36}$$

Then, set the status variable in the state equation building, as following

$$x_1 = x \tag{3.37}$$

$$x_2 = \dot{x}_1 \tag{3.38}$$

$$x_3 = P_p \tag{3.39}$$

$$x_4 = P_{he} \tag{3.40}$$

$$x_5 = P_{re} \tag{3.41}$$

Set variables to the state equation from Equation 3.38. It can be written by

$$\dot{x}_1 = x_2 \tag{3.42a}$$

In addition, from Equation 3.33, 3.34, 3.35 and 3.36, we can be rewritten as

$$\dot{x}_2 = \frac{1}{m_{piston}}\left(P_{he}A_{he} - P_{re}A_{re} - F_{ext}\right) \tag{3.42b}$$

$$\dot{x}_3 = \frac{\beta}{V_{hose}}\left(Q_p - Q_{pbre}\right) \tag{3.42c}$$

$$\dot{x}_4 = \frac{\beta}{\left(V_{0he} + A_{he}x_1\right)}\left(-Q_{athe} + A_{he}x_2\right) \tag{3.42d}$$

$$\dot{x}_5 = \frac{\beta}{\left(V_{0re} + A_{re}\left(L_{stroke} - x_1\right)\right)}\left(Q_{pbre} - A_{re}x_2\right) \tag{3.42e}$$

Equation 3.42a, 3.42b, 3.42c, 3.42d and 3.42e is the mathematic model of the electro – hydraulic servo system in case of the cylinder retracts.

3.4 Linearization of Mathematical model

In the section 3.2 and 3.3, the mathematical model was considered but it is the non – linear equation. In this section, we show how to perform linearization of systems described by nonlinear differential equations. The procedure introduced is based on the Taylor series expansion and on knowledge of nominal system trajectories and nominal system inputs.

In order to liberalize general nonlinear systems, we will use the Taylor Series expansion of functions. Consider a function *f(x)* of a single variable *x*, and suppose that $\bar{x}$ is a point such that $f(\bar{x}) = 0$. In this case, the point $\bar{x}$ is called an equilibrium point of the system $\dot{x} = f(x)$, since we have $\dot{x} = 0$ when $x = \bar{x}$ (i.e., the system reaches an equilibrium at $\bar{x}$). Recall that the Taylor Series expansion of *f(x)* around the point $\bar{x}$ is given by

$$f(x) = f(\bar{x}) + \left.\frac{df}{dx}\right|_{x=\bar{x}} (x-\bar{x}) + \frac{1}{2}\left.\frac{d^2 f}{dx^2}\right|_{x=\bar{x}} (x-\bar{x})^2 + \frac{1}{6}\left.\frac{d^3 f}{dx^3}\right|_{x=\bar{x}} (x-\bar{x})^3 + \ldots \quad (3.43)$$

This can be written as

$$f(x) = f(\bar{x}) + \left.\frac{df}{dx}\right|_{x=\bar{x}} (x-\bar{x}) + \textit{high order term} \quad (3.44)$$

For *x* sufficiently close to $\bar{x}$, these higher order terms will be very close to zero, and so we can drop them to obtain the approximation

$$f(x) \approx f(\bar{x}) + a(x-\bar{x}) \quad (3.45)$$

Since $f(x) = 0$, then on linear differential equation $\dot{x} = f(x)$ can be approximate near the equilibrium point by

$$\dot{x} = a(x-\bar{x}) \quad (3.46)$$

To complete the linearization, we define the perturbation state (also known as delta state) $\delta x = x - \bar{x}$ and using the fact that $\delta\dot{x} = \dot{x}$, we obtain the literalized mode

$$\delta\dot{x} = a\delta x \quad (3.47)$$

That this linear model is valid only near the equilibrium point, (how "near" depends on how non-linear the function is).

The extension to functions of multiple state and inputs is very similar to the above procedure. Suppose the evolution of state x_i is given by

$$\dot{x}_i = f_i(x_1, x_2, \ldots, x_n, u_1, u_2, \ldots u_m) \quad (3.48)$$

For some general function f_i suppose that the equilibrium points are given by $x_1, x_2, \ldots, x_n, u_1, u_2, \ldots u_m$ so that

$$f_i(x_1, x_2, \ldots, x_n, u_1, u_2, \ldots u_m) = 0 \qquad \forall i \in \{1,2,\ldots,n\} \tag{3.49}$$

that the equilibrium point should make all of the functions f_i equal to zero, so that all states in the systems top moving when they reach equilibrium. The linearization of f_i about the equilibrium point is then given by

$$f_i(x_1, x_2, \ldots, x_n, u_1, u_2, \ldots u_m) \approx \sum_{j=1}^{n} \left.\frac{\partial f_i}{\partial x_j}\right|_{x_j=\overline{x}_j} \delta x_j + \sum_{j=1}^{m} \left.\frac{\partial f_i}{\partial u_j}\right|_{u_j=\overline{u}_j} \delta u_j \tag{3.50}$$

If we define the delta states and inputs $\delta x_j = x_j - \overline{x}_j$ (for $1 \leq j \leq n$) and $\delta u_j = u_j - \overline{u}_j$ (for $1 \leq j \leq m$), the literalized dynamics of state x_i are given by

$$\delta \dot{x}_i = \sum_{j=1}^{n} \left.\frac{\partial f_i}{\partial x_j}\right|_{x_j=\overline{x}_j} \delta x_j + \sum_{j=1}^{m} \left.\frac{\partial f_i}{\partial u_j}\right|_{u_j=\overline{u}_j} \delta u_j \tag{3.51}$$

Sometimes, the "δ" notation is dropped in the linearize equation, with the implicit understanding that are working with a literalized system.

From the theorem above, will be linearization the equation of electro – hydraulic servo system in state space model around the equilibrium point $\overline{x}_1(0), \overline{x}_2(0), \overline{x}_3(0), \overline{x}_4(0), \overline{x}_5(0)$

$$\begin{bmatrix} \dot{x}_1 \\ \dot{x}_2 \\ \dot{x}_3 \\ \dot{x}_4 \\ \dot{x}_5 \end{bmatrix} = \begin{bmatrix} 0 & 1 & 0 & 0 & 0 \\ 0 & 0 & 0 & \dfrac{A_{he}}{m_{piston}} & -\dfrac{A_{re}}{m_{piston}} \\ 0 & 0 & f_{33} & f_{34} & 0 \\ f_{41} & f_{42} & f_{43} & f_{44} & 0 \\ f_{51} & f_{52} & 0 & 0 & f_{55} \end{bmatrix} \begin{bmatrix} x_1 \\ x_2 \\ x_3 \\ x_4 \\ x_5 \end{bmatrix} + \begin{bmatrix} 0 \\ 0 \\ B_{31} \\ B_{41} \\ B_{51} \end{bmatrix} [U] \tag{3.52}$$

where

$$f_{33} = -\left(\frac{\beta}{V_{hose}} C_d \sqrt{\frac{2}{\rho}} A_{pa}\right) \frac{1}{2\sqrt{x_3 - x_4}}$$

$$f_{34} = \left(\frac{\beta}{V_{hose}} C_d \sqrt{\frac{2}{\rho}} A_{pa}\right) \frac{1}{2\sqrt{x_3 - x_4}}$$

$$f_{41} = -\left(\beta C_d \sqrt{\frac{2}{\rho}} A_{pa} \sqrt{x_3 - x_4} + \beta A_{he} x_2\right) \frac{V_{0he}}{\left(V_{0he} + A_{he} x_1\right)^2}$$

$$f_{42} = -\frac{A_{he}\beta}{\left(V_{0he} + A_{he} x_1\right)}$$

$$f_{43} = \left(\frac{\beta}{\left(V_{0he} + A_{he} x_1\right)} C_d \sqrt{\frac{2}{\rho}} A_{pa}\right) \frac{1}{2\sqrt{x_3 - x_4}}$$

$$f_{44} = -\left(\frac{\beta}{\left(V_{0he} + A_{he} x_1\right)} C_d \sqrt{\frac{2}{\rho}} A_{pa}\right) \frac{1}{2\sqrt{x_3 - x_4}}$$

$$f_{51} = -\left(\beta C_d \sqrt{\frac{2}{\rho}} A_{pa} \sqrt{x_5} + \beta A_{re} x_2\right) \frac{A_{re}}{\left(V_{0re} + A_{re}\left(L_{stroke} - x_1\right)\right)^2}$$

$$f_{52} = \frac{\beta A_{re}}{\left(V_{0re} + A_{re}\left(L_{stroke} - x_1\right)\right)}$$

$$f_{55} = -\frac{\beta}{\left(V_{0re} + A_{re}\left(L_{stroke} - x_1\right)\right)} C_d \sqrt{\frac{2}{\rho}} A_{pa} \frac{1}{2\sqrt{x_5}}$$

$$B_{31} = \frac{\beta C_d}{\left(V_{0he} + A_{he} x_1\right)} \sqrt{\frac{2}{\rho}} \sqrt{x_3 - x_4}$$

$$B_{41} = \frac{\beta C_d}{\left(V_{0he} + A_{he} x_1\right)} \sqrt{\frac{2}{\rho}} \sqrt{x_3 - x_4}$$

$$B_{51} = -\frac{\beta C_d}{\left(V_{0re} + A_{re}\left(L_{stroke} - x_1\right)\right)}\sqrt{\frac{2}{\rho}}\sqrt{x_5}$$

3.5 Implementation of EHSS model in MATLAB – Simulink

The following section describes the implementation of the mathematical model of electro – hydraulic servo system (EHSS) in MATLAB – Simulink. Appendix B-1 shows the MATLAB – Simulink real-time control environment used implement the model.

The main disadvantages of hydraulic servo-system are a nonlinear dynamical behavior of system, which stems from the compressibility of liquids, properties of complex flow valves and friction in hydraulic actuators. They depend on factors, which are difficult to measure, such as oil bulk modulus, viscosity and temperature. General availability of increasingly sophisticated computer hardware and computer software with a better mathematical and simulation programs allow simulation of very complex systems. MATLAB-Simulink [18] is often used in simulation tests because of the following advantages [19].

Simplified procedure that allows the designer to encode mathematical models in the appropriate programming language

The possibility of multiple use of the basic mathematical model, using specific libraries and their combinations,

A possibility of examining systems with models having appreciably extended ranges of coefficients, in particular for hydraulic systems.

This section is aimed at presenting modeling of hydraulic servo – systems, directional control valve and differential cylinder, by means of MATLAB – Simulink. First, the basic mathematical models of valve and cylinder and phenomena occurring in hydraulic servo – systems have been considered in the section 3.2 – 3.3. The models are shown both as block and detailed diagrams adapted to the requirements of the MATLAB – Simulink graphical editor. Then, there have been described a laboratory hydraulic system and laboratory measurements of pressure in the cylinder chambers.

Chapter 4
Controller Design

4.1 Introduction

The electro – hydraulic servo system has several characteristics such as having some uncertain parameters, cylinder position, velocity changing with working environments and conditions. One new control method is needed urgently, which has the strong compatibility to the change of system parameter.

The traditional PID controller has the characteristics of simple algorithm, well stability and high reliability. Fuzzy control is the intelligent control technology based on natural language control rules and fuzzy logic inference. The control rules fully reflect some human's intelligence. In this chapter, we present the method for design the controller and make the reconstruction to the controller.

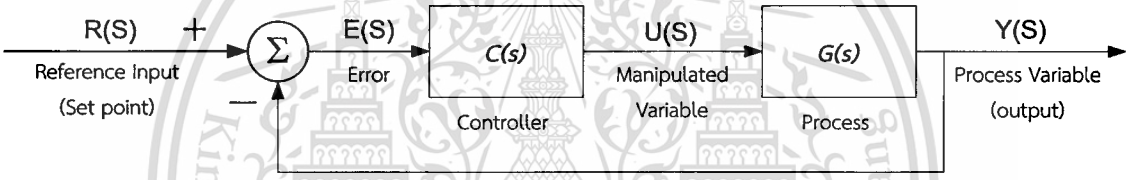

Figure 4.1 Feedback Control Process Diagram

4.2 Proportional – Integral – Derivative Controller (PID Controller)

4.2.1 Introduction

"PID" is an acronym for "proportional, integral, and derivative. A PID controller is a controller that includes elements with those three functions. In the literature on PID controllers, acronyms are also used at the element level: the proportional element is referred to as the "P element", the integral element as the "I element", and the derivative element as the "D element". The PID controller is first place on the market in 1939 and has remained the most widely used controller in process control until today.

4.2.2 PID Controller Structure

The PID controller encapsulates three of the most important controller structures in a single package. The parallel form of a PID controller (shown as in Figure 4.2 and Table 4.1) has transfer function:

$$C(s) = k_p + \frac{k_i}{s} + k_d s = k_p\left(1 + \frac{1}{T_i} + T_d s\right) \qquad (4.1)$$

where k_p, k_i, k_d, T_i *and* T_d are proportional gain, integral gain, derivative gain, rise time and rate time.

The proportional term (k_p) in the controller generally helps in establishing system stability and improving the transient response while the derivative term is often used when it is necessary to improve the closed loop response speed even further. Conceptually, the effect of the derivative term (k_d) makes a process adjustment based on the current rate of change of the process control error. Derivative control is typically used in cases where there is a large time lag between the controlled device and the sensor used for the feedback. This term has the overall effect of preventing the actuator signal from going too far in one direction or another, and can be used to limit excessive overshoot. And the most important term in the controller is the integrator term (k_i) that makes a process adjustment based on the cumulative error not its current value. The integral term (k_i) is the reciprocal of the reset time, T_r, of the system. The reset time is the duration of each error-summing cycle. Integral control can cancel any steady-state offsets that would occur when using purely proportional control. This is sometimes called *reset* control.

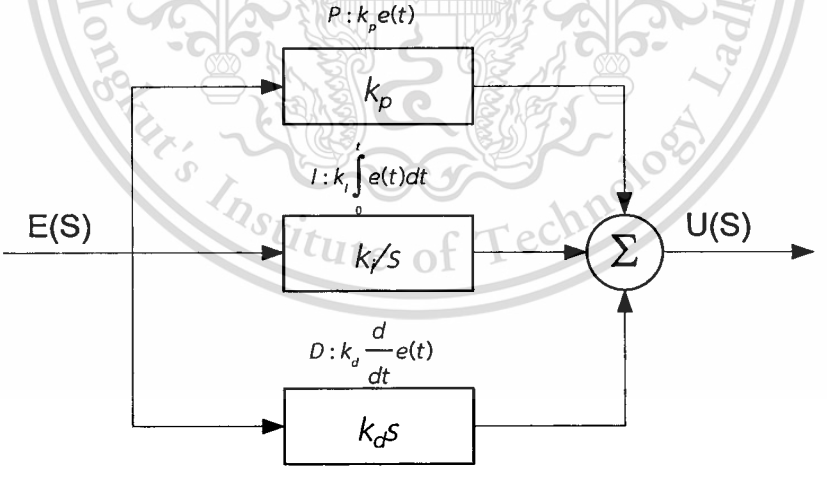

Figure 4.2 Parallel From of the PID Compensator

4.2.3 Ziegler – Nichols Tuning

In 1942 Ziegler and Nichols, both employees of Taylor Instruments, described simple mathematical procedures, the first and second methods respectively, for tuning PID controllers. These procedures are now accepted as standard in control systems practice. Both techniques make a priori assumptions on the system model,

but do not require that these models be specifically known. Ziegler – Nichols formulae for specifying the controllers are based on plant step responses.

4.2.3.1 The First Method

The first method applied to plants with step responses of the form displayed in Figure 4.3. This type of response is typical of a first order system with transportation delay, such as that induced by fluid flow from a tank along a pipeline. It is also typical of a plant made up of a series of first order systems. The response is characterized by two parameters, L the delay time and T the time constant. These are found by drawing a tangent to the step response at its point of inflection and noting its intersections with the time axis and the steady state value. The plant model is therefore

$$G(s) = \frac{Ke^{-sL}}{Ts+1} \tag{4.5}$$

Ziegler and Nichols derived the following control parameters based on this model as shown in Table 4.2

Table 4.1 PID Controller Type

Controller Type	k_p	k_i	k_d	$C(s)$
P (Proportional)	≠0	zero	zero	k_p
I (Integral)	zero	≠0	zero	$\frac{k_i}{s}$
PI (Proportional plus Integral)	≠0	≠0	zero	$k_p + \frac{k_i}{s} = \frac{k_p\left(s+\frac{k_i}{k_p}\right)}{s}$
PD (Proportional plus Derivative)	≠0	zero	≠0	$k_p + k_d s = k_d\left(\frac{k_p}{k_d}+s\right)$
PID (Proportional+Integral+Derivative)	≠0	≠0	≠0	$\frac{k_d s^2 + k_p s + k_i}{s} = \frac{k_d\left(s^2+\frac{k_p}{k_d}s+\frac{k_i}{k_d}\right)}{s}$

Table 4.2 Ziegler – Nichols Recipe – First Method

PID Type	k_p	$T_i=k_p/k_i$	$T_d=k_d/k_p$
P	$\frac{T}{L}$	∞	0
PI	$0.9\frac{T}{L}$	$\frac{T}{0.3}$	0
PID	$1.2\frac{T}{L}$	$2L$	$0.5L$

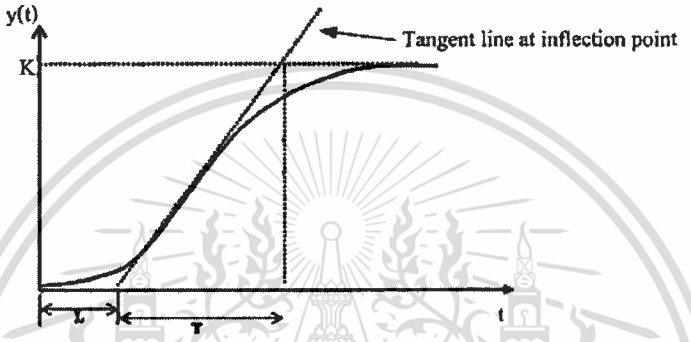

Figure 4.3 Response curve for Ziegler – Nichols – First method

4.2.3.2 The Second Method

The second method targets plants that can be rendered unstable under proportional control. The technique is designed to result in a closed loop system with 25% overshoot. This is rarely achieved as Ziegler and Nichols determined the adjustments based on a specific plant model.

The steps for tuning a PID controller via the 2nd method are as follows:

Using only proportional feedback control:

(i) Reduce the integrator and derivative gains to 0.

(ii) Increase k_p from 0 to some critical value $k_p = K_{cr}$ at which sustained scillations occur. If it does not occur then another method has to be applied.

(iii) Note the value K_{cr} and the corresponding period of sustained oscillation, P_{cr}

The controller gains are now specified as follows in Table 4.3

4.2.4 PID Controller Design for Tabletting Machine

In this research, performance criteria requirement for used target design the PID controller are approximately 3.0 - 4.0 second of settling time, ±5 kg error of pressing force in every force desired no overshoot and range of operation is between 100 kg to 2000 kg. And, PID controller is designed and tuned based on mathematical system modeling and simulation results. Modeling error, uncertainties and hydraulic

nonlinear dynamic are obstacles in obtaining an accurate mathematical model. Therefore, the PID controller is finally fine-tuned in actual experiments.

The gains of PID controller results that are designed and tuned are as shown in chapter 6.

Table 4.3 Ziegler – Nichols Recipe – Second Method

PID Type	k_p	$T_i=k_p/k_i$	$T_d=k_d/k_p$
P	$0.5K_{cr}$	∞	0
PI	$0.45K_{cr}$	$\frac{P_{cr}}{1.2}$	0
PID	$0.6K_{cr}$	$\frac{P_{cr}}{2}$	$\frac{P_{cr}}{8}$

4.3 Fuzzy Logic Controller

4.3.1 Introduction

In order to design fuzzy logic controller for controlling the desired processes, fuzzy set and fuzzy logic controller theory must know. First, the basic of fuzzy set and fuzzy logic will be useful in explaining fuzzy logic system. It is reviewed in this chapter.

4.3.2 Fuzzy Set Theory

In traditional set or crisp set theory, membership value of an object can defined exactly with two values: 0 or 1, when the object belongs to set completely or it does not belong at all. However, in general, countless vague objects cannot be described easily and certainly by crisp set theory. Though, the membership values of interested objects are found, it is not fairly. Fuzzy set theory is a tool, which used to remedy this dilemma.

Fuzzy set was first proposed by Professor L. A. Zadeh in 1965. The theory has laid the foundation for computing with words by generalizing 0 and 1 membership value of a crisp set to a membership function of a fuzzy set. The explanation of fuzzy set is as follows:

Definition 1 Fuzzy Set

Let U be a collection of objects and be called the universe of discourse. X is any member in U and defined by $x \in U$. A fuzzy set A in U is characterized by membership function $\mu_A(x)$, which associates with each objects in U a real number

in the interval [0 1] with the value of $\mu_A(x)$ at x representing the "grade of membership" of x in A. When A is a set in the ordinate sense of the term, its membership function can take on only two values 0 and 1, with $\mu_A(x)$ reduces of the familiar characteristic function of a set A. Fuzzy set A can be written by

$$A=\{(x,\mu_A(x))\mid x\in U\} \tag{4.6}$$

When the membership function of fuzzy set is continuous, the fuzzy set A is defined as

$$A=\int_U \mu_A(x)/x \tag{4.7}$$

And when the membership function of fuzzy set is discrete, the fuzzy set A is as

$$A=\{(x_1,\mu_A(x_1)),(x_2,\mu_A(x_2)),...,(x_n,\mu_A(x_n))\} \tag{4.8}$$

or

$$A=\mu_A(x_1)/x_1+\mu_A(x_2)/x_2+...+\mu_A(x_n)/x_n=\sum_{n=1}^{n}\mu_A(x_i)/x_i \tag{4.9}$$

Here, $\int$ and + mean unionizing the member x and the member $\mu_A(x)$ to be a set. They have no meaning of general mathematical operation as integration and summation. And / means relation between the member x and the member $\mu_A(x)$. It is not relate to division of the member.

For explaining the concepts of the crisp set and the fuzzy set clearly, the membership function of crisp set and fuzzy set can illustrated in Figure 4.4.

Definition 2 Singleton Set

Singleton is a fuzzy set which has nonzero membership values for one only element of the universe of discourse. Figure 4.5 shows a singleton fuzzy set whose membership value is 0 everywhere except at x=30. The majority of typical fuzzy controllers and model employs singleton fuzzy set in consequent of fuzzy rules.

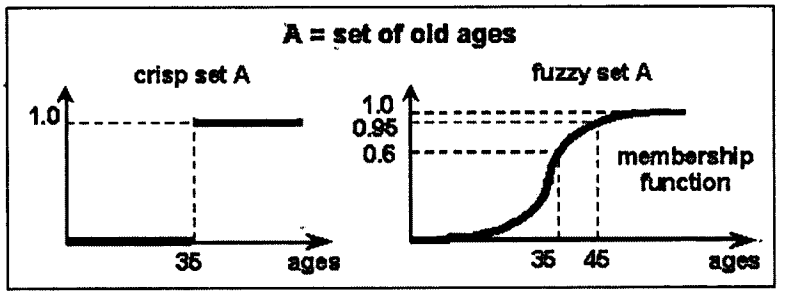

Figure 4.4 The membership functions of crisp set and fuzzy set.

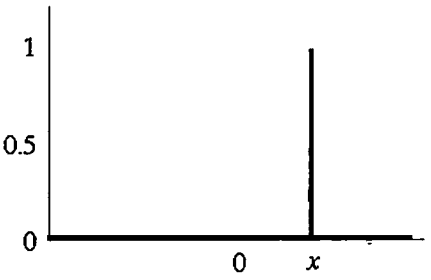

Figure 4.5 Fuzzy singleton

Definition 3 Support

The support of a fuzzy set A is set of all element x in the universe of discourse U such that $\mu_A(x) > 0$. It is definite by

$$\text{supp}(A) = \{x \in U \mid \mu_A(x) > 0\} \tag{4.10}$$

4.3.3 Fuzzy Logic Operation

Let A and B are fuzzy set in the universe of discourse U whose membership functions are $\mu_A(x)$ and $\mu_A(x)$ respectively. The basic operations are defined in this subsection.

Definition 4 Complement

The complement of a fuzzy set A whose $\mu_A(x) \in [0,1]$ in the universe of discourse U is represented by $\overline{A}$. Its membership function for all element $x \in U$ are defined as

$$\mu_{\overline{A}}(x) = 1 - \mu_A(x) \qquad ;\forall x \in U \tag{4.11}$$

Definition 5 Intersection

The intersection of a fuzzy set A and B in the universe of discourse U is represented by $A \cap B$. Its membership function for all element $x \in U$ are defined as

$$\mu_{A \cap B}(x) = \min\{\mu_A(x), \mu_B(x)\} \qquad ;\forall x \in U \tag{4.12}$$

Definition 6 Union

The union of a fuzzy set A and B in the universe of discourse U is represented by $A \cup B$. Its membership function for all element $x \in U$ are defined as

$$\mu_{A \cup B}(x) = \max\{\mu_A(x), \mu_B(x)\} \qquad ;\forall x \in U \tag{4.13}$$

Definition 7 Equality

The fuzzy set A equals to the fuzzy set B when their grades of membership are equivalent.

$$A = B \leftrightarrow \mu_A(x) \neq \mu_A(x) \qquad ;\forall x \in U \tag{4.14}$$

when the grade of membership function A and B are equal. If the grade of membership A and B are unequal, it can be symbolized by $A \subset B$.

Definition 8 Double – Negation Law

Double – negation law is defined to be

$$\bar{\bar{A}} = A \tag{4.15}$$

Definition 9 DeMorgan's Law

DeMorgan's law is rule for inference. It was defined as follows:

$$\overline{A \cup B} = \bar{A} \cup \bar{B}, \tag{4.16}$$

$$\overline{A \cap B} = \bar{A} \cap \bar{B}, \tag{4.17}$$

$$\bar{A} \cup B \neq U, \tag{4.18}$$

$$A \cap \bar{A} \neq \varnothing. \tag{4.19}$$

Definition 10 Cartesian Product

Let $A_1, A_2, \ldots, A_n$ are fuzzy sets in universe of discourse $U_1, U_2, \ldots, U_n$, respectively. Cartesian product of $A_1, A_2, \ldots, A_n$ are fuzzy sets in product space $U_1 \times U_2 \times \ldots \times U_n$ whose membership function is expressed by

$$\mu_{A_1 \times A_2 \times \ldots \times A_n}(x_1, x_2, \ldots, x_n) = \min\left[\mu_{A_1}(x_1), \mu_{A_2}(x_2), \ldots, \mu_{A_n}(x_n)\right] \tag{4.20}$$

when

$$x_1 \in U_1, x_2 \in U_2, \ldots, x_n \in U_n$$

Definition 11 Algebraic Product

Algebraic product of fuzzy set A and fuzzy set B expressed by $A \times B$. Its membership function is defined as follows:

$$\mu_{A \times B}(x) = \mu_A(x) \times \mu_B(x) \tag{4.21}$$

Definition 12 Algebraic Summation

Algebraic Summation of fuzzy set A and fuzzy set B expressed by $A+B$. Its membership function is defined as follows:

$$\mu_{A+B}(x)=\mu_A(x)+\mu_B(x)-\mu_A(x)\times\mu_B(x) \tag{4.22}$$

Definition 13 Bounded Summations

Bounded summation of fuzzy set A and fuzzy set B is expressed by $A\oplus B$. Its membership function is defined as follows:

$$\mu_{A\oplus B}(x)=\min\left\{1,\mu_A(x)+\mu_B(x)\right\} \tag{4.23}$$

Definition 14 Bounded Differences

Bounded difference of fuzzy set A and fuzzy set B is expressed by $A\Theta B$. Its membership function is defined as follows:

$$\mu_{A\Theta B}(x)=\max\left\{0,\mu_A(x)-\mu_B(x)\right\} \tag{4.24}$$

4.3.4 Linguistic Variable

A linguistic variable is characterized by a quintuple $(x,\ T(x),\ U,\ G,\ M)$

Here, x is the term set of linguistic,

$T(x)$ is the term set of linguistic variable x,

U is the term set of discourse,

G is the syntactic rule for generating the name of the value of x and

M is the semantic rules for associating each value with its meaning.

The term of linguistic variable can be presented as shown in Figure 4.6 with three term; "slow", "medium", and "high"

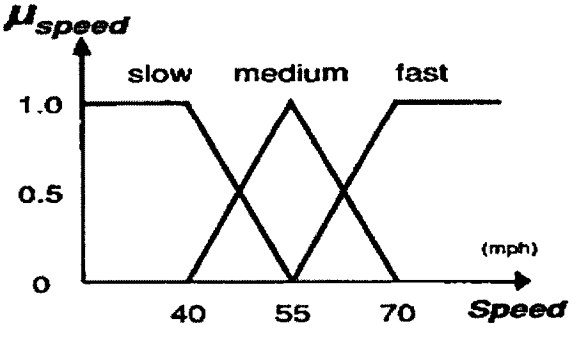

Figure 4.6 Linguistic variable called *"speed"*

4.3.5 Fuzzy Logic Controller

Basic configuration of fuzzy logic controller (FLC) shown in Figure 4.7 consists of fuzzification, fuzzy rules, fuzzy inference and defuzzifier, where x_1, x_2,...,x_n are inputs of fuzzy logic controller and z is output of fuzzy logic controller.

4.3.5.1 Fuzzification

Fuzzification is mathematical procedure that is used to convert the input of the fuzzy controller to be the membership value of the fuzzy set. It can be defined as

$$\mu_A(x) = fuzzification(x_0) \tag{4.25}$$

The number of fuzzy sets, their linguistic names and design parameters are determined by the fuzzy controller developer's decision included the control operator's knowledge and experience about characteristic of the system.

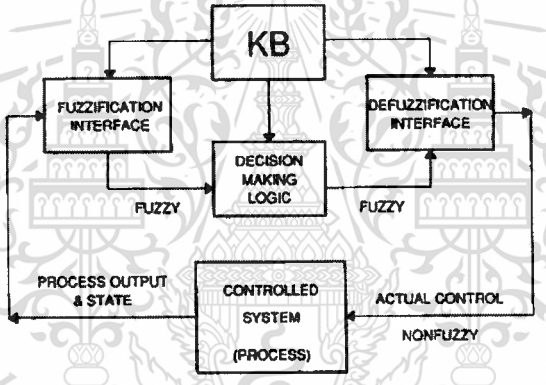

Figure 4.7 Basic configuration of fuzzy logic controller

4.3.5.2 Fuzzy Rule

A fuzzy controller is use fuzzy rule which are linguistic IF – THEN statement. Fuzzy rule acts like a key in liking the input variables of fuzzy controller to the output variable. There are 2 major types of fuzzy rules. There are namely Mamdani fuzzy rule and Takagi – Sugeno (TS) fuzzy rule.

4.3.5.2.1 Mamdani Fuzzy Rule

Mamdani fuzzy rule is fuzzy control rule whose the rule outcome is linguistic variable. The expression of a general Mamdani fuzzy rule for a fuzzy controller involving n inputs and m outputs can be described as follows:

$$\begin{aligned} &\text{IF } x_1 \text{ is } A_1 \text{ AND } x_2 \text{ is } A_2 \text{ AND ... AND } x_n \text{ is } A_n \\ &\text{THEN } y_1 \text{ is } B_1 \text{ AND } y_2 \text{ is } B_2 \text{ AND ... AND } y_n \text{ is } B_n \end{aligned} \tag{4.26}$$

where $x_1, x_2, ..., x_n$ are input variables, $y_1, y_2, ..., y_n$ are output variables, *AND* are fuzzy logic *AND* operations, $A_1, A_2, ..., A_n$ are fuzzy set of inputs, $B_1, B_2, ..., B_n$ are fuzzy set of outputs.

4.3.5.2.2 TS Fuzzy Rule

TS fuzzy rule is fuzzy control rule whose the rule outcome is function of input variables. TS fuzzy rule for a fuzzy controller involving *n* inputs and *m* outputs can be described as follows:

$$\begin{aligned} &\text{IF } x_1 \text{ is } A_1 \text{ AND } x_2 \text{ is } A_2 \text{ AND ... AND } x_n \text{ is } A_n \\ &\text{THEN } y_1 = f_1(x_1, x_2, ..., x_n), y_2 = f_2(x_1, x_2, ..., x_n), ..., y_n = f_n(x_1, x_2, ..., x_n) \end{aligned} \tag{4.27}$$

where

$f_1(x_1, x_2, ..., x_n), f_2(x_1, x_2, ..., x_n), ..., f_n(x_1, x_2, ..., x_n)$ are functions of input variables. In theory $f_n(x_1, x_2, ..., x_n)$ can be choosing as any real function, linear or nonlinear function. However, in practical, proper choosing or determining the mathematical formalism of nonlinear functions for every fuzzy rule is extremely difficult. Consequently, linear function seems to be the easy option.

Fuzzy controller can be divided into two types by using fuzzy rule. They are Mamdani fuzzy controller and TS fuzzy controller.

4.3.5.3 Fuzzy Inference

Fuzzy inference or fuzzy reasoning is used in a fuzzy rule to determine the rule outcome from the information of rule input. Mamdani fuzzy rule and TS fuzzy rule use the different inference method.

For Mamdani fuzzy rule, the most popular inference methods are Mamdani minimum inference, Larsen product inference, drastic product inference and Bounded product inference. Let $\mu_{B_i}(y_i)$ be the membership function of the fuzzy set B_i, the four popular inference methods are defined by the following Table 4.4.

For making the meaning of the definitions of the popular fuzzy inference methods whose mathematical definitions given in Table 4.4 easy to understand, graphical illustration are used and are shown Figure 4.8.

It can be seen from Figure 4.8 that when the different inference method is used for fuzzy rule consequent which is fuzzy set, the rule outcome formed in the shaded areas are not similar. However, when the different inference method is used for fuzzy rule consequent that is fuzzy singleton, the rule outcome is identifiably as shown in Figure 4.9.

Table 4.4 Defined of four Popular Inference methods for Mamdani fuzzy rule

Fuzzy Inference Method	Definition
Mamdani minimum inference, R_M	$\min(\mu_i, \mu_B(y_i))$
Larsen product inference, R_L	$\mu_i \times \mu_{B_i}(y_i)$
Drastic product inference, R_{DP}	$\begin{cases} \mu_i & for \quad \mu_{B_i}(y_i)=1 \\ \mu_{B_i} & for \quad \mu_i=1 \\ 0 & for \quad \mu_i<1 \quad and \quad \mu_{B_i}(y_i)<1 \end{cases}$
Bounded product inference, R_{BP}	$\max\left(0, \mu_i + \mu_{B_i}(y_i) - 1\right)$

For TS fuzzy rule, the result of the fuzzy inference is $\mu_i \times f_1(x_1, x_2, ..., x_n)$. Every rule outcome is weighted by membership values of the inputs. So, the result of the fuzzy inference for TS fuzzy rule can be represented mathematical equations easier than Mamdani fuzzy rule.

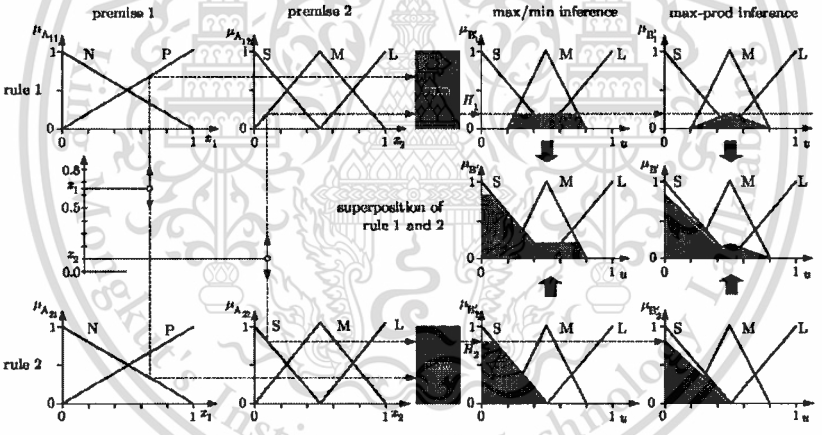

Figure 4.8 Fuzzy Inference method

4.3.5.4 Defuzzification

The resulting fuzzy set must be converted to a number that can be sent to the process as a control signal. This operation is called *defuzzification*, and in Figure 4.11 the *x*-coordinate marked by a white, vertical dividing line becomes the signal control. The resulting fuzzy set is thus defuzzifier in to a crisp control signal. There are several defuzzification methods.

4.3.5.4.1 Centre of Gravity (COA)

The crisp output value *u* (white line in Figure 4.11) is the abscissa under the center of gravity of the fuzzy set.

$$u = \frac{\sum_i \mu(x_i) x_i}{\sum_i \mu(x_i)} \tag{4.28}$$

Here x_i is a running point in a discrete universe, and $\mu(x_i)$ is its membership value in the membership function. The expression can be interpreted as the weighted average of the elements in the support set. For the continuous case, replace the summations by integrals. It is a much-used method although its computational complexity is relatively high. This method is also called *centroid of area*.

4.3.5.4.2 Centre of Gravity Method for Singleton (COGS)

If the membership functions of the conclusions are singletons (Figure 4.7), the output value is

$$u = \frac{\sum_i \mu(s_i) s_i}{\sum_i \mu(s_i)} \tag{4.29}$$

Here s_i is the position of singleton *i* in the universe, and $\mu(s_i)$ is equal to the firing strength α_i of rule *i*. This method has a relatively good computational complexity, and *u* is differentiable with respect to the singletons s_i, which is useful in neuron fuzzy systems.

4.3.5.4.3 Bisector of Area (BOA)

This method picks the abscissa of the vertical line that divides the area under the curve in two equal halves. In the continuous case,

$$u = \left\{ x \mid \int_{\min}^{x} \mu(x)dx = \int_{x}^{\max} \mu(x)dx \right\} \tag{4.30}$$

Here *x* is the running point in the universe, $\mu(x)$, is its membership, *Min* is the left most value of the universe, and *Max* is the right most value. Its computational complexity is relatively high, and it can be ambiguous. For example, if the fuzzy set consists of two singletons, any point between the two would divide the area in two halves; consequently it is safer to say that in the discrete case, BOA is not defined.

4.3.5.4.4 Mean of Maxima (MOM)

An intuitive approach is to choose the point with the strongest possibility, i.e. maximal membership. It may happen, though, that several such points exist, and a common practice is to take the mean of maxima (MOM). This method disregards the shape of the fuzzy set, but the computational complexity is relatively good.

4.3.5.4.5 Leftmost Maximum (LM), and Rightmost Maximum (RM)

Another possibility is to choose the left most maximum (LM), or the right most maximum (RM). In the case of a robot, for instance, it must choose between left and right to avoid an obstacle in front of it. The defuzzifier must then choose one or the other, not something in between. These methods are in different to the shape of the fuzzy set, but the computational complexity is relatively small.

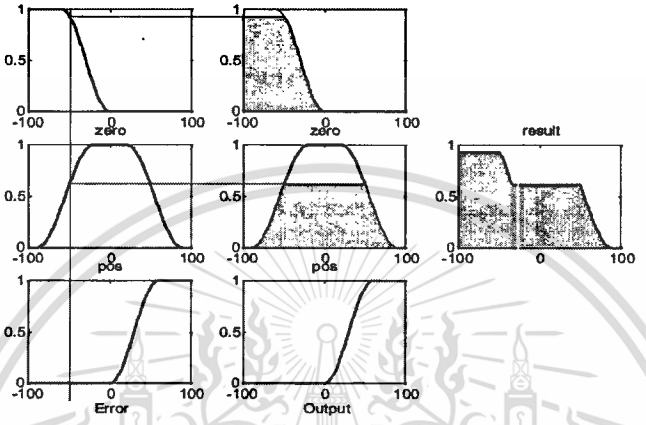

Figure 4.9 One input, one output rule base with non – singleton output set

4.4 Design of the Electro – Hydraulic Servo System Fuzzy Controller

In this research, performance criteria requirement used for target design the fuzzy logic controller are approximately 3.0 - 4.0 second of settling time, ±5 kg error of pressing force in every force desired, no overshoot and range of operation is between 100 kg to 2000 kg. And, Fuzzy logic controller is designed and tuned based on mathematical system modeling and simulation results. Modeling error, uncertainties and hydraulic nonlinear dynamic are obstacles in obtaining an accurate mathematical model. Therefore, the fuzzy controller is finally fine-tuned in actual experiments.

The first step of fuzzy controller design is to select the number of controller inputs and corresponding number of input membership functions required for the fuzzification process. In the case of the EHSS controller with pressing force control, it was believed that the force error (e) and change in the force error (de) would be sufficient input to the fuzzy controller. Traditional fuzzy controller design suggests that 3-7 input membership functions per input are sufficient [20]. It was decided to employ seven input member functions per input membership function.

Both error and change of error inputs membership function, it was known that the input to the controller would fall into four main categories. They were given the linguistic labels "zero", "big", "medium" and "small" according to the magnitude of force error (e) and change of error (de) that represented. It was decided to assign

two membership to the big category that are “positive big (PB)” and “negative big (NB)”, two to the medium category that are “positive medium (PM)” and “negative medium (NM)”, two to the small category that are “positive small (PS)” and “negative small (NS)”, and one to the "zero" category that is “zero (ZE)”. The error (e) in pressing force is expressed by the number in the universe [-10, 10] volt, it equivalents to [-5000, 5000] kg-force and the universe of change of error (de) is [-2, 2] volt, it equivalents to [-1000, 1000] kg-force. These input membership functions are shown below in Figure 4.10 and Figure 4.11.

It was decided to use Gaussian membership functions rather than triangular or trapezoidal membership functions in order to achieve the desired smooth interpolation of the output signal command. Triangular and trapezoidal membership functions contain discontinuities in their derivatives, which can result in abrupt changes in the output of the controller. This is undesirable, as it would cause the actuator to exert unnecessary, large, transient forces as it tried to accelerate to match the abrupt changes in controller output [20].

The second step of the fuzzy controller design process was to define the output membership functions. It was decided to use seven member functions; it was known that the output to the controller would fall into four main categories. They were given the linguistic labels "zero", "big", "medium" and "small" according to the magnitude of signal control (CI) that represented. It was decided to assign two membership to the big category that are “positive big (PB)” and “negative big (NB)”, two to the medium category that are “positive medium (PM)” and “negative medium (NM)”, two to the small category that are “positive small (PS)” and “negative small (NS)”, and one to the "zero" category that is “zero (ZE)”. The signal control (CI) is expressed by the number in the universe [-2, 2] volt.

Since it was decided to use a Mamdani inference fuzzy controller, the output membership functions are Gaussian membership functions. This can be observed in Figure 4.12. The four output membership functions are labeled "zero", "small", "medium" and "big" according to the signal command that they represent.

The third step of the fuzzy controller design was the specification of the rule base that links the fuzzifier and the defuzzifier. There are 49 rules that correspond to the same number of input and output membership functions. These rules are implied by the desired output of the controller. The following is the rule base that used in the EHSS fuzzy controller is shown in Table 4.5.

The input membership functions, the output membership function, and the rule base have been designed; all that remained was to select the operations used in the inference process and the defuzzification method. It was decided to select the most widely – used operations for simplicity. Therefore, the MIN operator was chosen for

the AND operation, and the MAX operator was chosen for the OR operation employed. The former is used to truncate the Gaussian output membership functions the value of the premise corresponding to each of the 49 rules. The latter was not used in this controller, as the rule bases contain any OR conditions to be evaluated.

The final step of the controller design process was the selection of a defuzzification method. It was decided to use center of gravity method (COA) for solution the output controller. Since a Mamdani inference engine with Gaussian output membership functions were employed, the equation used to calculate the crisp output (signal command) is as presented in Equation 4.28.

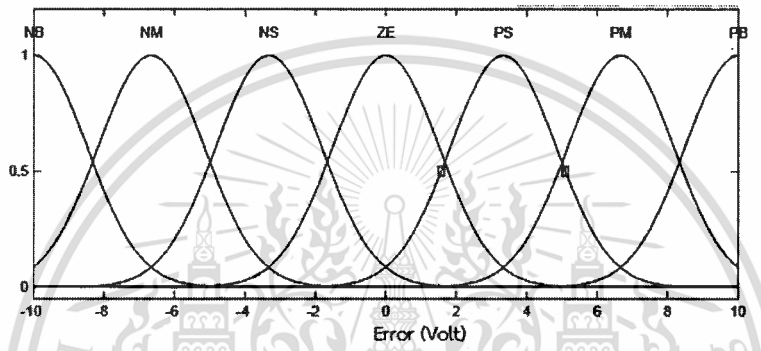

Figure 4.10 Input membership functions (Error Function)

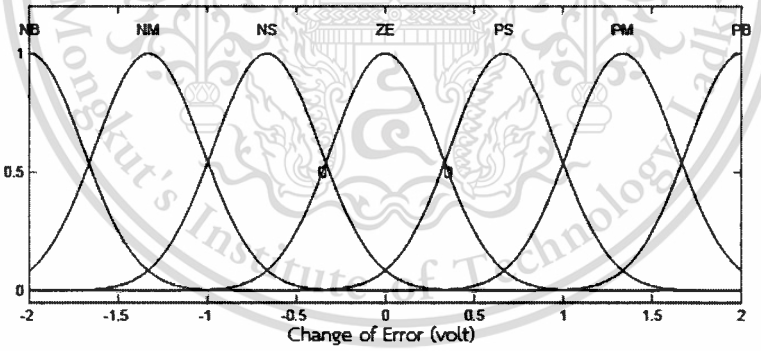

Figure 4.11 Input membership functions (Change of Error Function)

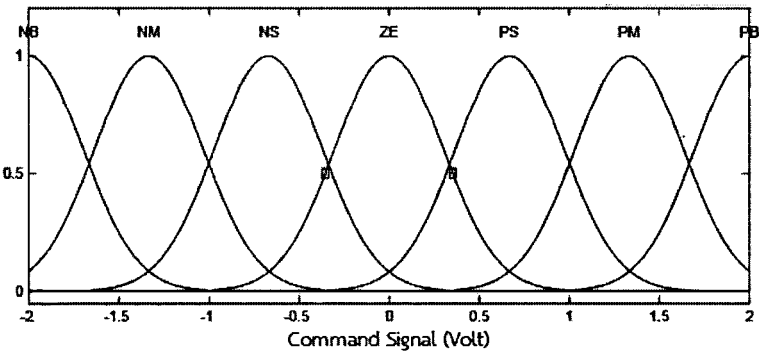

Figure 4.12 Output membership functions

Table 4.5 Rule Base

	Change of Error							
Error		NB	NM	NS	ZE	PS	PM	PB
	NB	ZE	ZE	ZE	NB	NM	NM	NB
	NM	ZE	ZE	ZE	NM	NS	NM	NM
	NS	ZE	ZE	ZE	NS	ZE	NS	NM
	ZE	NB	NM	NS	ZE	PS	PM	PB
	PS	PM	PS	ZE	PS	ZE	ZE	ZE
	PM	PB	PM	PS	PM	ZE	ZE	ZE
	PB	PB	PM	PM	PB	ZE	ZE	ZE

4.5 Implementation of the EHSS Fuzzy Controller

The following section describes the implementation of the Mamdani fuzzy controller. Figure 4.13 shows the Matlab/Simulink real-time control environment used implement the various controllers, the results of which are presented in Chapter 6. The fuzzy controller was developed using the Matlab/Simulink Fuzzy Logic Toolbox, which contains tools designed to aid in creating fuzzy controllers.

The Matlab/Simulink Fuzzy Logic Toolbox contains two tools intended to aid in the visualization of the operation of the FLC. The first is the rule viewer. It allows the control designer to specify an arbitrary input to the controller, as illustrated by the vertical line over laid on the input membership functions on the left side of Figure 4.14. The degree of activation of the input membership functions is illustrated by the highlighted area under each input function. The corresponding controller output is indicated by the short vertical line over laid on the output membership functions on the right side of the figure. The degree of activation of the output membership functions is illustrated by the crisp value that calculates by center of gravity method that is highlighted.

The second tool provided to visualize the operation of the FLC is the surface viewer, which shown in Figure 4.15. This tool plots the output of the controller over the entire range of inputs

The two different controllers (PID controller and Fuzzy controller) presented in Chapters 4 will have a significant impact on the performance of the EHSS. This impact is investigated quantitatively and qualitatively in Chapter 6.

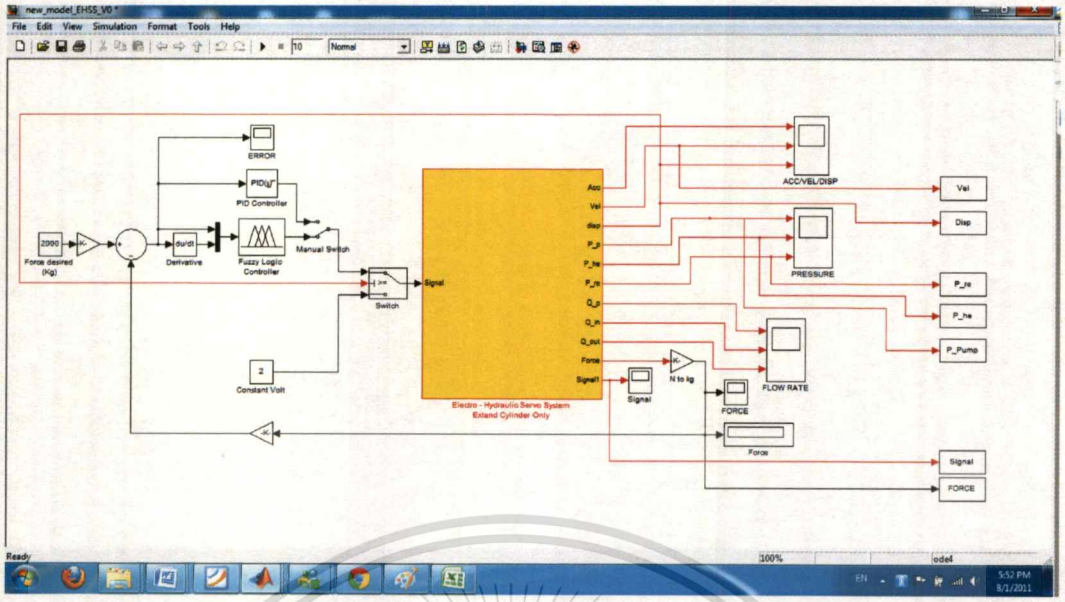

Figure 4.13 Matlab - Simulink control environment

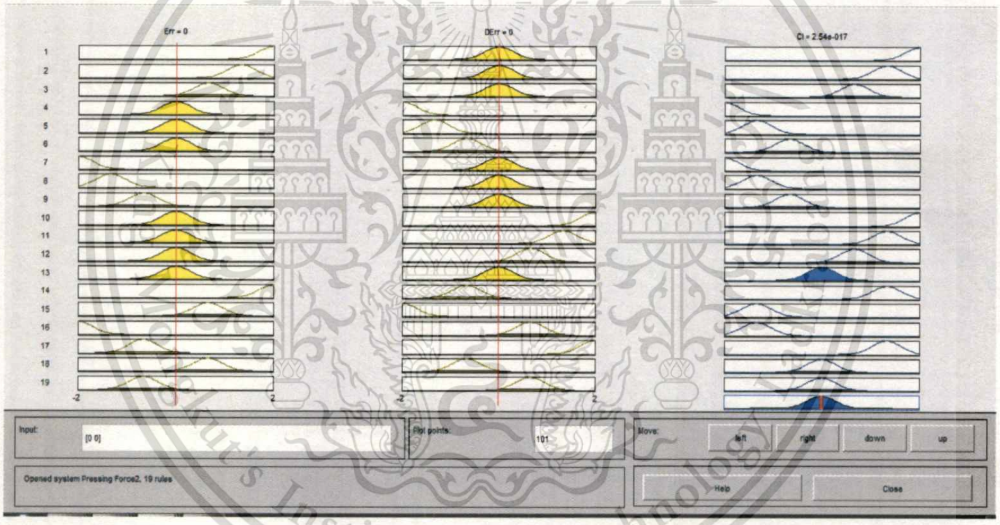

Figure 4.14 FLC Rule Viewer

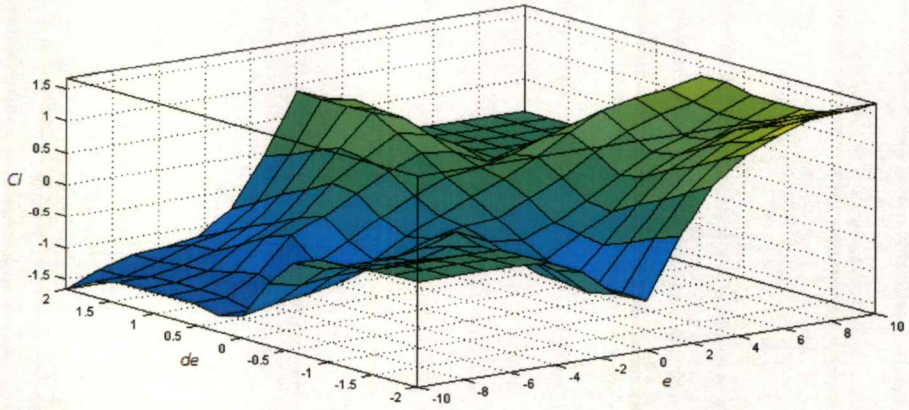

Figure 4.15 FLC Surface Viewer

Chapter 5
Experimental Setup

In this chapter, briefing perform lab of valve modulation test to create a dynamic model of the servo valve system, laboratory of dynamic system test for analyze the mathematic model compare with the EHSS, and test for nominal stability and performance with control system.

5.1 Valve Modulation Test

5.1.1 Mechanical Setup

Figure 5.1 shows a picture of valve modulation test for create a dynamic model of the servo valve system. Visible are the major components of the system such as proportional valve, the power unit, flow rate meter, pressure sensor and computer control system.

A picture show as a hydraulic line connects between of the proportional valve and the power unit. Two pressure sensors are placed on either side of the proportional valve to record pressures drop across proportional valve. One flow rate meter is placed on the outlet of proportional valve to record fluid flow rate that flow though proportional valve. A personal computer sends the signal command to proportional valve and record data form pressure sensors and flow rate meter.

Figure 5.1 Mechanical setup of valve modulation test

5.1.2 Valve Modulation Test Method

Sending varies the input voltage signal from minus eight to eight voltages to the proportional valve cause the flow of hydraulic oil though the proportional valve. Record the flow rate flow though the valve and pressure drop across valve at each input signal. Using data for calculate the area which the valve open at each input

signal by orifice equation. Therefore, with each input signal, a given the modulation curve between input signal and area of opening vale. The results are shown as chapter 6.

5.2 Dynamic System Test

5.2.1 Mechanical Setup

Figure 5.2 shows a picture of dynamic system test for analyze the mathematic model compare with the EHSS. Visible are the major components of the system such as the power unit, proportional valve, actuator, potential sensor, pressure sensor and computer control system.

A picture show as a single – rod actuator (head end and rod end piston areas are not equal) is connected to proportional valve. One potential sensor are placed on the actuator to record displacement of actuator when movement. Two pressure sensors are placed on either side of the piston to record fluid pressures within the actuator. A third pressure sensor record the supply pressure, P_P, from the hydraulic power unit. A personal computer sends the signal command to proportional valve and record data form pressure sensors and potential sensor.

5.2.2 Dynamic System Test Method

Sending varies the input voltage signal from 0.0 to +4.0 voltages to the proportional valve cause movement of the actuator rod. Record the fluid pressures and displacement of actuator rod at each input signal. Using data from experimental compare with simulation data for analyze the accuracy of mathematic model of electro – hydraulic servo system for tabletting machine with force control. The results are shown as in chapter 6.

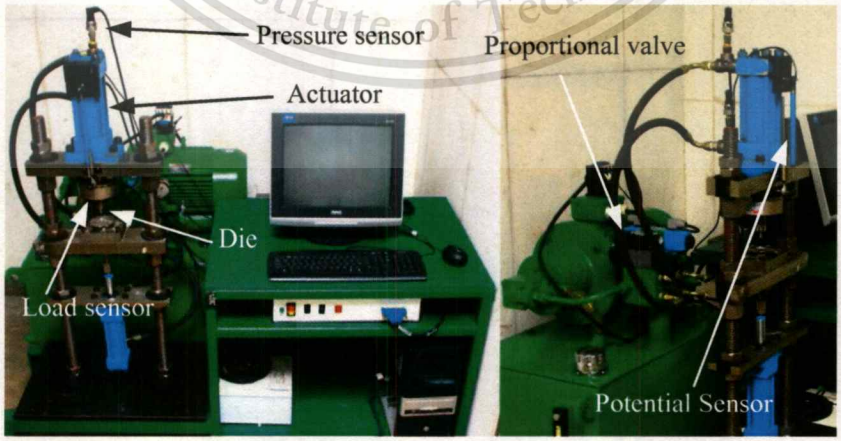

Figure 5.2 Mechanical setup of dynamic system test

5.3 Nominal Stability and Performance Test

5.3.1 Mechanical Setup

The electro – hydraulic servo system for tabletting machine with force control is shown as Figure 5.2. Visible are the major components of the system such as the actuator, proportional valve, motor, pump, load sensor, potential sensor, pressure sensor, control box and computer control system.

The mechanical setup is same as the dynamic system test expect on the end of cylinder is placed load sensor and dies for stamping the powder of tablet.

5.3.2 Data Acquisition Setup

A block diagram of the electro – hydraulic servo system for tabletting pressing machine with force control is shown in Figure 5.3. The hydraulic pump supplies the proportional valve/actuator with a constant P_p. The PC sends an input voltage signal through an analog output port on the data acquisition card (DAQ card) where it is converted from a digital-to-analog signal, to the servo amplifier. The input signal is then sent from the amplifier to the proportional valve. A power supply provides the load cell and pressure sensors with a required 24 VDC. The output voltage from each sensor is sent to the PC through analog input ports on the DAQ card where it is converted from an analog-to-digital signal (the output signal from the load cell is passed through an amplifier before it is sent to the DAQ card. The load cell signal, along with some type of control system, can then be used to create closed-loop (CL) force control for the system, and then be used to create closed-loop (CL) force control for the system. LabView program is used as the user interface to generate and analyze all data to and from the PC. The front panel and block diagram of LabView appears to the end user are shown as Appendix B.

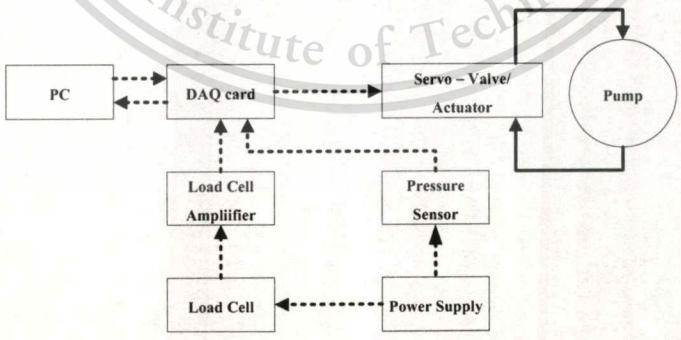

Figure 5.3 Block diagram of the EHSS
(dotted and bold arrows represent electric and hydraulic connections, respectively)

5.4 Test Rig

5.4.1 The Hydraulic Power Unit

The hydraulic power unit, shown as Figure 5.4 , consists of motor (380 VAC, 3Ø, max 1450 rpm), 1.81 cm^3/rev fix volumetric displacement pump and hydraulic oil (AW68). It supplies the hydraulic oil to servo system with a constant flow rate of 3.16×10^{-4} m^3/s.

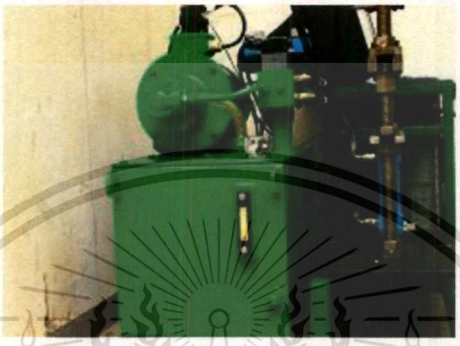

Figure 5.4 Hydraulic power unit

5.4.2 Proportional Valve

This research uses COM-3-2C-30-CH-11 that product by Tokyo Keiki Inc., shown as in Figure 5.5. It is controlled by ±10 volt of input, max 30 L/min of control flow rate, 13.7 MPa of allowable tank port backpressure, 50 ms of response time and 10 ms of acceleration–deceleration time setting.

Figure 5.5 COM-3-2C-30-CH-11 proportional valves

5.4.3 Hydraulic Actuator

This research uses a single rod actuator, shown as Figure 5.6. It has 63 mm bore of head end diameter, 27 mm bore of rod end diameter and 0.10 m of stroke.

Figure 5.6 Hydraulic actuator

5.4.4 Load Cell Sensor

This research uses LTM-590 series load sensor, shown as Figure 5.7. It has 5000 kg of rate capacity, 0 – 10 VDC output, 15 VDC of maximum input voltage and ± 0.0017% *Sn*. of error.

Figure 5.7 Load sensor

5.4.5 Potential Sensor

This research uses Penny Giles model SLS – 130 series, shown as Figure 5.1. It has 125 mm stroke, 0 to 10 VDC output, 74 VDC applied voltage maximum input, and ±0.25% error.

Figure 5.8 Potential sensor

5.4.6 Pressure Sensor

This research uses Duplomatic PTH – 400/20E0 – K10, shown as Figure 5.9. It has 400 bar of max pressure, 0 to 10 VDC output and 0.5%P_N of accuracy.

Figure 5.9 Pressure sensor

5.4.7 Data Acquisition Card

This research uses National Instrument - DAQmx model PCI – 6221 (37 – pin), shown as Figure 5.10. It has 16 bit, 833 kS/s max analog output rate, 16 analog inputs, 2 analog outputs, 24 digital input/output, and ±10 volt analog output range. Using for sent and receive signal from proportional vale and sensor to PC.

Figure 5.10 NI-DAQmx PCI – 6221 (37 – pin)

5.4.8 Flow Rate Meter

This research uses SFI – 800 – ½ - A712 sight flow indicator, shown as Figure 5.11. It has 150 psi max pressure, 8 to 28 VDC power supply, 0 to 100 Hz frequency output range, 1 to 10 VDC output signal and ±5% of F.S. accuracy.

Figure 5.11 Flow rate meter

Chapter 6
Results

In this chapter, the results from experimental test in the chapter 5 are shown. The results are divided in three parts, valve modulation test result, dynamic system test compare with simulation results and nominal stability and performance with control system compare with simulation results.

6.1 Valve Modulation Test Result

In this section, the results of valve modulation experimental test are shown as Table 6.1, Table 6.2 and Figure 6.1.

From the Figure 5.1, the power unit supplies 13.7 MPa of hydraulic oil pressure to the proportional valve. Difference pressure across proportional valve that called pressure drop across valve of port p to port a and port p to port b in every signal are approximately 11.0 MPa, and pressure drop across valve of port b to port t and port a to port t in every signal are approximately 9.0 MPa. Using flow rate data and pressure drop across valve data that record form sensor calculate the open area port by orifice equation (using Equation 3.8). Table 6.1 shows the result in case of positive signal input and Table 6.2 shows the result in case of negative signal input.

Figure 6.1 shows valve modulation curve that plots between signal and open area port. This valve modulation curve is characteristic of proportional valve, which used in this research and used it for valve block in Matlab – Simulink.

Table 6.1 Valve modulation test result in case of positive signal input

Volt	Port p - a			Port b - t		
	Flow rate (mm^3/s)	ΔP (MPa)	Opening Gap (mm^2)	Flow rate (mm^3/s)	ΔP (MPa)	Opening Gap (mm^2)
0	0.000	13.647	0.000	0.000	12.835	0.000
1	16584.851	10.260	0.126	48273.082	9.147	0.389
2	40805.781	10.363	0.309	96641.670	9.045	0.784
3	56489.596	10.139	0.433	131599.916	9.266	1.055
4	78103.682	10.244	0.595	171602.395	9.005	1.396
5	103778.878	10.211	0.792	210440.639	9.099	1.703
6	129683.336	10.184	0.992	248042.545	8.913	2.028
7	155233.056	10.165	1.188	294419.334	9.087	2.384
8	180241.015	10.190	1.378	338612.099	9.065	2.745

Table 6.2 Valve modulation test result in case of negative signal input

Volt	Port p - b			Port a - t		
	Flow rate (mm^3/s)	ΔP (MPa)	Opening Gap (mm^2)	Flow rate (mm^3/s)	ΔP (MPa)	Opening Gap (mm^2)
0	0.000	13.652	0.000	0.000	13.156	0.000
-1	16584.916	9.947	0.128	47396.333	8.936	0.387
-2	40805.940	10.393	0.309	93333.132	9.113	0.755
-3	56489.817	10.263	0.430	121453.591	9.024	0.987
-4	78103.987	10.321	0.593	163838.029	9.058	1.329
-5	103779.284	10.211	0.793	213535.010	9.298	1.709
-6	129683.843	10.184	0.992	249778.457	8.947	2.039
-7	155233.662	10.165	1.1889	287718.416	8.997	2.342
-8	180241.719	10.190	1.379	343514.387	9.055	2.787

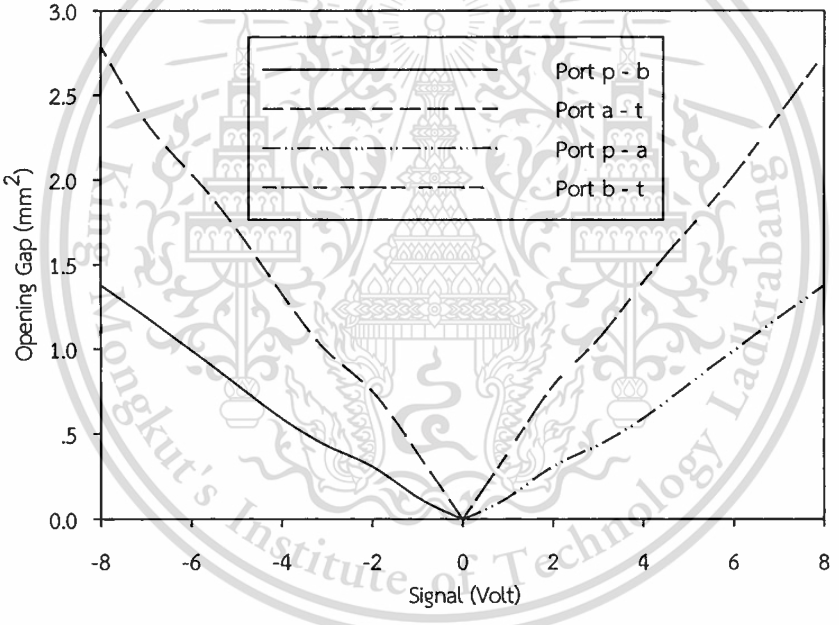

Figure 6.1 Valve modulation curve

6.2 Dynamic System Test Result

In this section, dynamic system test results compare with simulation with Matlab/Simulink result are shown as Figure 6.2 to Figure 6.6.

Figure 6.2 displays the simulation results compare with experimental results of displacement of actuator movement. It can be seen that in simulation result, it used approximately 16, 7, 5 and 3.5 second for 1, 2, 3 and 4 volt input case, respective, for 100 mm stroke that the end of stroke point, and in experimental result, it take a close time with simulation result.

Figure 6.3 displays the simulation results compare with experimental results of velocity of actuator movement. It can be seen that the actuator have approximately 6, 15, 20 and 30 mm/s velocity for 1, 2, 3 and 4 volt input case, respective, in both simulation and experimental results.

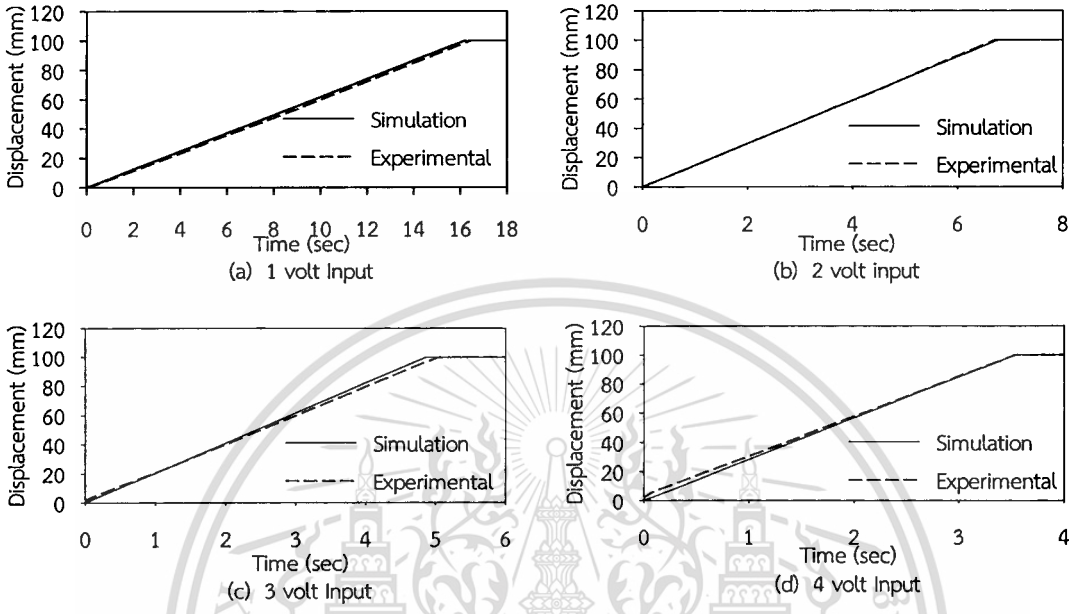

Figure 6.2 Comparison between simulation and experimental results of displacement of actuator movement

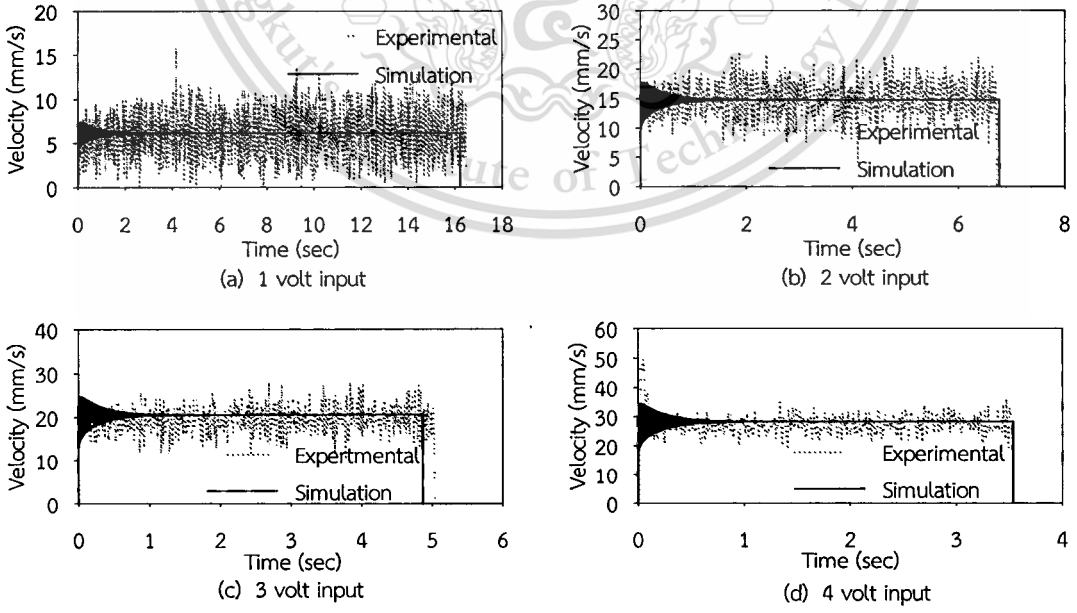

Figure 6.3 Comparison between simulation and experimental results of velocity of actuator movement

Figure 6.4 displays the simulation results compare with experimental results of head end pressure of actuator movement. It can be seen that the head end pressure in simulation result are approximately 0.5 MPa for every input signal case when actuator movement and increasing to 13.7 MPa when the actuator stops at the end of stroke point. In the experimental result, the head end pressures are approximately 2.0 MPa for every input signal case when actuator movement and increasing to 13.7 MPa when the actuator stops at the end of stroke point.

Figure 6.5 displays the simulation results compare with experimental results of rod end pressure of actuator movement. It can be seen that in simulation results, the rod end pressures are approximately 1.5, 2.2, 2.5 and 2.7 MPa for 1, 2, 3 and 4 volt input case, respective, when actuator movement and decreasing to 0.0 MPa , immediately, when the actuator stops at the end of stroke point in every volt input case. In experimental result, the rod end pressure increase to 1.2 MPa, immediately for 1 volt input case, then the pressure increase from 1.2 MPa to 1.6 MPa when actuator movement and decreasing immediately to 0.0 MPa when the actuator stops at the end of stroke point. In the same, the rod end pressure increase to 1.8, 2.2 and 2.5 MPa, immediately, for 2, 3 and 4 volt input case, respective, and then the pressure increase from 1.8, 2.2 and 2.5 MPa to 2.3, 2.5 and 2.7 MPa when actuator movement and decreasing to 0.0 MPa, immediately, when the actuator stops at the end of stroke point.

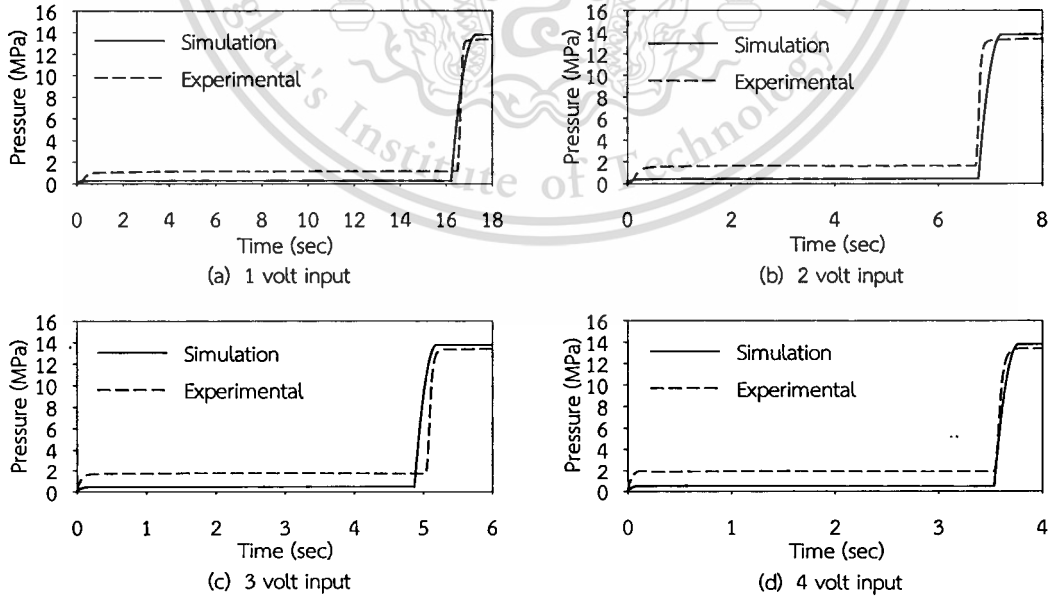

Figure 6.4 Comparison between simulation and experimental results of head end pressure of actuator movement

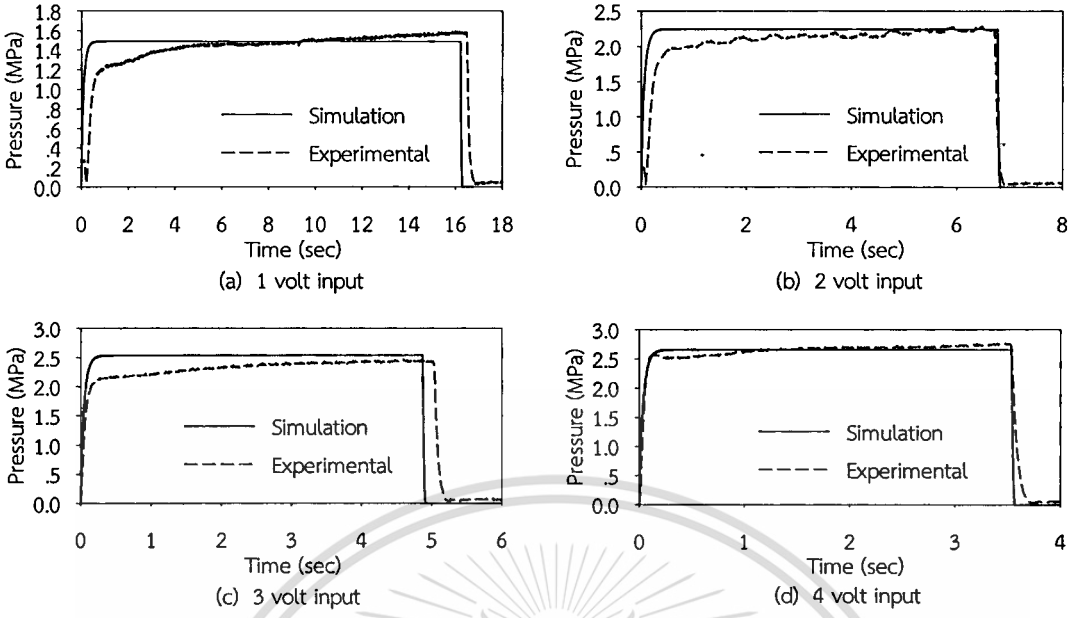

Figure 6.5 Comparison between simulation and experimental results of rod end pressure of actuator movement

Figure 6.6 displays the simulation results compare with experimental results of pump pressure. It can be seen that the pressure increase to 13.7 MPa, immediately (relief valve open at 13.7 MPa) for every input signal case and constant pressure at 13.7 MPa in the both simulation and experimental result.

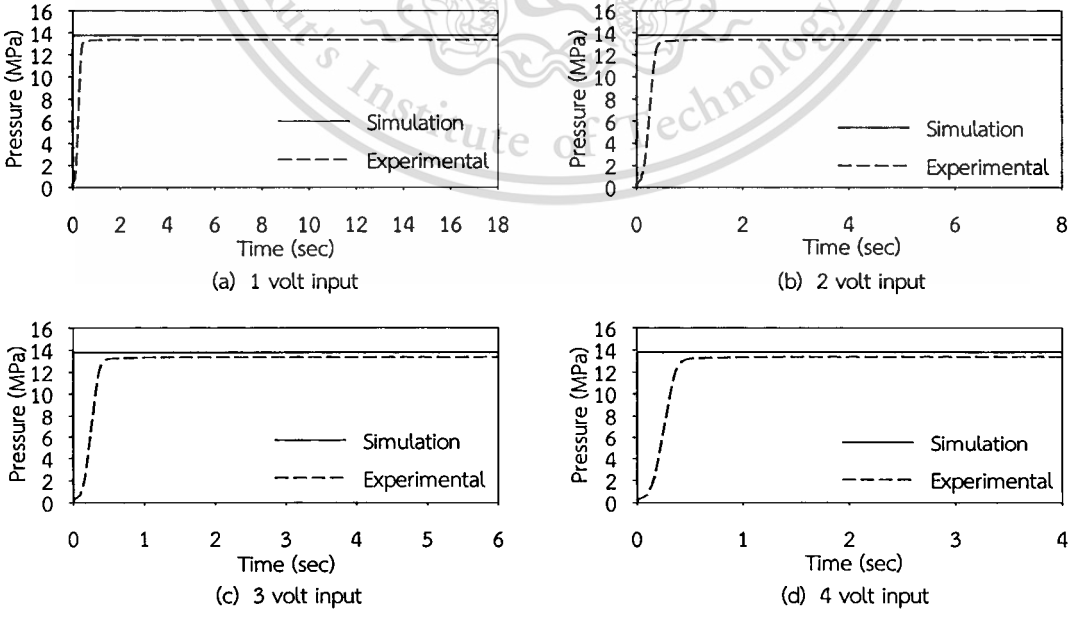

Figure 6.6 Comparison between simulation and experimental results of pump pressure

Considering mathematical model of electro – hydraulic servo system in chapter 3, there are five state in the equation, displacement (x_1), velocity (x_2), pump pressure (x_3), head end pressure (x_4) and rod end pressure (x_5). From result in Figure 6.2 to Figure 6.6, it can be seen that the simulation result is similarly with the experimental result in the every valve for 0 to 4 volt input (the volt input in this research active in range of application between from 0 volt to 4 volt). Therefore, the mathematical model of electro – hydraulic servo system is accuracy and used it for design the controller.

6.3 Nominal Stability and Performance Results

6.3.1 Nominal Stability and Performance with PID Controller

In this section, shows the gain of PID controller at equilibrium point that designed and the nominal stability and performance with controller system. In this research, designed controllers at equilibrium point that 500, 1000, 1500 and 2000 kg-force and settling time recommend is approximately 3.0 – 4.0 second.

6.3.1.1 500 kg-force Equilibrium point

From equation 3.27 in chapter 3, defined the equilibrium point from simulation dynamic system result shown as Table 6.3

Table 6.3 Equilibrium point value at 500 kg-force

State point	Symbol	Value	Unit
Displacement	x, (x_1)	45.0	mm
Velocity	v, (x_2)	10.0	mm/s
Pump pressure	P_p, (x_3)	13.700	MPa
Head end pressure	P_{he},(x_4)	1.572	MPa
Rod end pressure	P_{re}, (x_5)	0.100	MPa

Substituting value in Table 6.3 to equation 3.52 and using it design the PID controller by Ziegler – Nichols method (briefs as section 4.2.3) then, given the gain of PID controller, shown as Table 6.4.

Table 6.4 Gain of PID controller at 500 kg-force Equilibrium point

Gain	Value
k_p	0.0035
k_i	0.00002
k_d	0.00023

Figure 6.7 shows the response of system with PID controller that comparison between simulation and experimental response. It can be seen that in simulation response, it has approximately 3 second settling time, 2 second rising time and +1 kg-force steady state error. In experimental response, it has approximately 4 second settling time, 2.8 second rising time and – 2 kg-force steady state error.

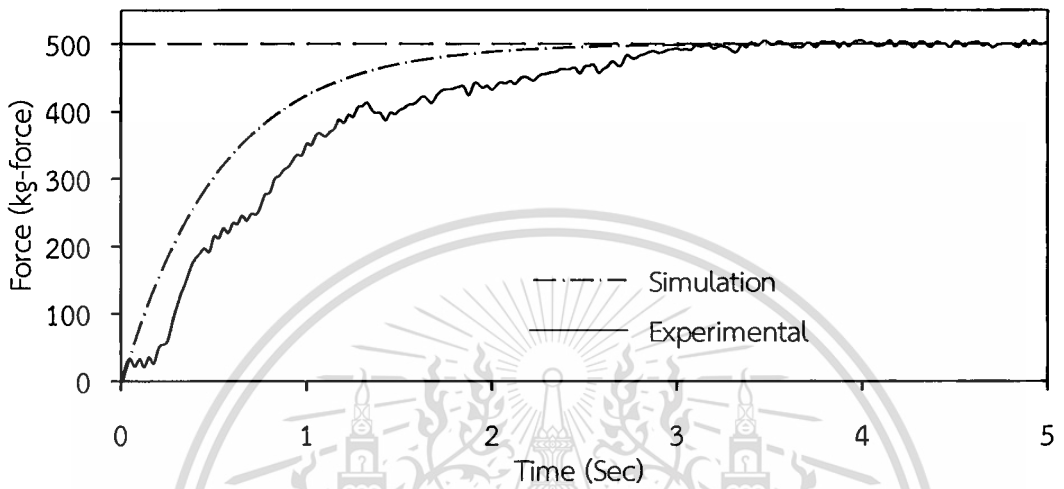

Figure 6.7 Comparison between simulation and experimental response of EHSS with PID controller at 500 kg-force equilibrium point

In electro – hydraulic servo system that control with PID controller, there are any range of operation around equilibrium point that designed. At 500 kg-force equilibrium point, ranges of operation are 300 – 800 kg-force. In this range, the response was according to controller design that uses gain of PID controller in Table 6.4.

Figure 6.8 shows the response of 300 kg-force that force desired minimum allowed used for gain of PID controller at 500 kg-force equilibrium in Table 6.4. It can be seen that it has approximately 4 second settling time, 2.5 second rising time and – 1 kg-force steady state error

Figure 6.9 shows the response and signal response of 800 kg-force that force desired maximum allowed used for gain of PID controller at 500 kg-force equilibrium in Table 6.4. It can be seen that it has approximately 5 second settling time, 4.5 second rising time and – 3 kg-force steady state error.

The other result of response which allowed used for 500 kg-force gain parameter is shown as Appendix A.

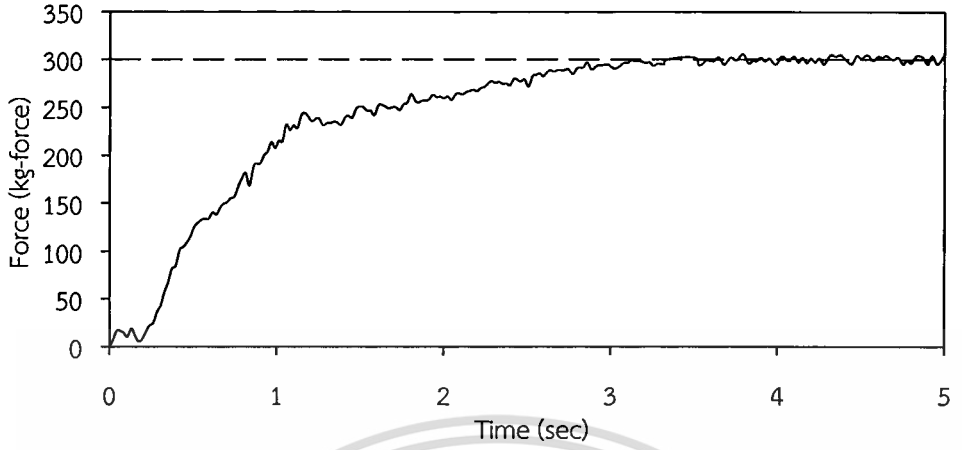

Figure 6.8 Response of 300 kg-force that force desired minimum allowed used for gain of PID controller at 500 kg-force equilibrium point

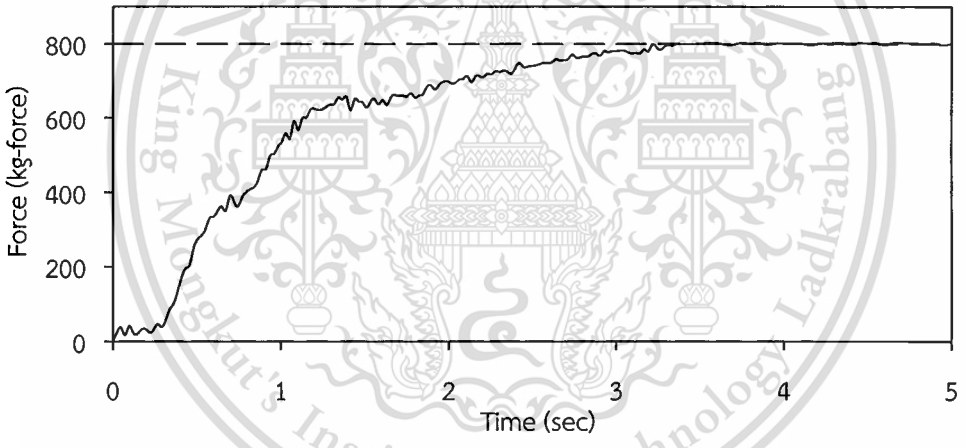

Figure 6.9 Response of 800 kg-force that force desired maximum allowed used for gain of PID controller at 500 kg-force equilibrium

6.3.1.2 The Other Equilibriums Point that 1000,1500 and 2000 kg-force

Table 6.5 shows the equilibrium point value from simulation dynamic system result that used substitute in equation 3.52 and using it design the PID controller by Ziegler – Nichols method.

Table 6.6 shows the gain of PID controller that designed at any equilibrium point. This value used for in simulation with Matlab – Simulink and in experimental with LabView program.

Table 6.7 shows the range of operation in 1000, 1500 and 2000 kg-force equilibrium point. In this range, the response was according to controller design that uses gain of PID controller in Table 6.6.

Table 6.5 Equilibrium point value at 1000, 1500 and 2000 kg-force

Point (kg-force)	x_1 (mm)	x_2 (mm/s)	x_3 (MPa)	x_4 (MPa)	x_5 (MPa)
1000	45.0	10.0	13.7	3.15	1.00
1500	45.0	10.0	13.7	4.72	1.00
2000	45.0	10.0	13.7	6.29	1.00

Table 6.6 Gain of PID controller at 1000, 1500 and 2000 kg-force equilibrium point

Gain	1000 kg-force	1500 kg-force	2000 kg-force
k_p	0.0018	0.0013	0.001
k_i	0.00015	0.00015	0.0001
k_d	0.0002	0.00013	0.00009

Table 6.7 Range of operation in 1000, 1500 and 2000 kg-force equilibrium point

Equilibrium point	Minimum force allowed	Maximum force allowed
1000	800	1200
1500	1200	1800
2000	1800	2200

Figure 6.10 shows the response of system with PID controller that comparison between simulation and experimental response at 1000 kg-force equilibrium point. It can be seen that in simulation response, it has approximately 3 second settling time, 2 second rising time and +1 kg-force steady state error. In experimental response, it has approximately 4.5 second settling time, 4 second rising time and – 2 kg-force steady state error.

Figure 6.11 shows the response of 800 kg-force that force desired minimum allowed used for gain of PID controller at 1000 kg-force equilibrium in Table 6.6. It can be seen that it has approximately 4.5 second settling time, 4 second rising time and – 2 kg-force steady state error.

Figure 6.12 shows the response of 1200 kg-force that force desired maximum allowed used for gain of PID controller at 1000 kg-force equilibrium in Table 6.6. It can be seen that it has approximately 4.5 second settling time, 3.5 second rising time and – 3 kg-force steady state error.

Figure 6.13 shows the response of system with PID controller that comparison between simulation and experimental response at 1500 kg-force equilibrium point. It

can be seen that in simulation response, it has approximately 3 second settling time, 2 second rising time and –1 kg-force steady state error. In experimental response, it has approximately 5.5 second settling time, 4 second rising time and – 3 kg-force steady state error.

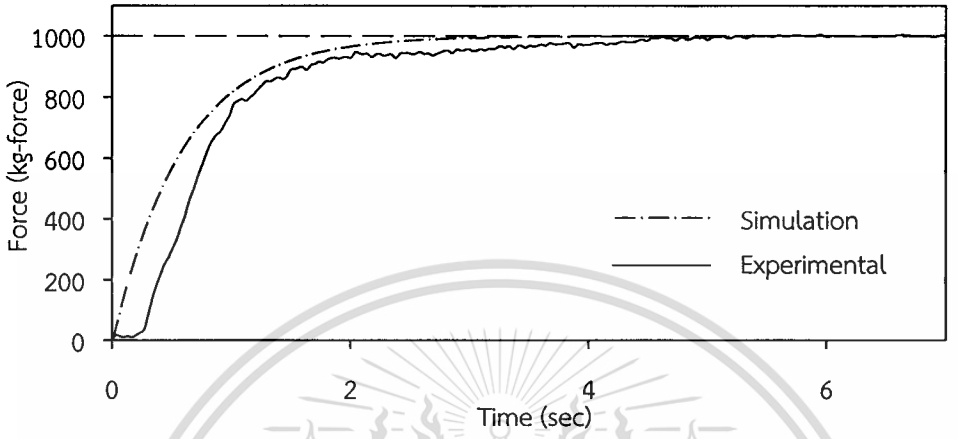

Figure 6.10 Comparison between simulation and experimental response of EHSS with PID controller at 1000 kg-force equilibrium point

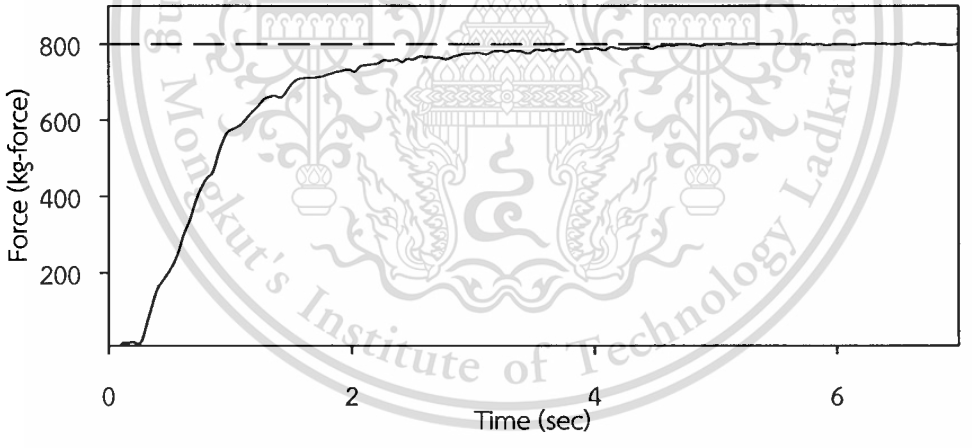

Figure 6.11 Response of 800 kg-force that force desired minimum allowed used for gain of PID controller at 1000 kg-force equilibrium

Figure 6.14 shows the response of 1200 kg-force that force desired minimum allowed used for gain of PID controller at 1500 kg-force equilibrium in Table 6.6. It can be seen that it has approximately 4.5 second settling time, 3.5 second rising time and – 2 kg-force steady state error.

Figure 6.15 shows the response of 1800 kg-force that force desired maximum allowed used for gain of PID controller at 1500 kg-force equilibrium in Table 6.6. It

can be seen that it has approximately 4.5 second settling time, 3.5 second rising time and – 3 kg-force steady state error.

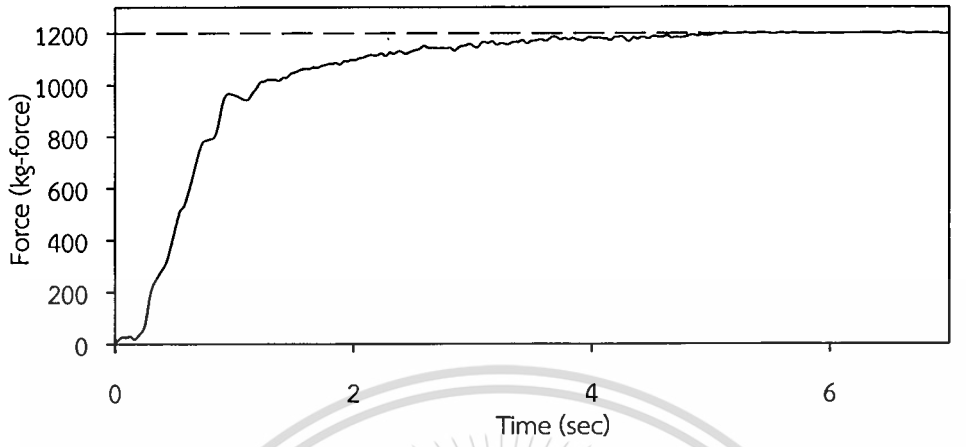

Figure 6.12 Response of 1200 kg-force that force desired maximum allowed used for gain of PID controller at 1000 kg-force equilibrium

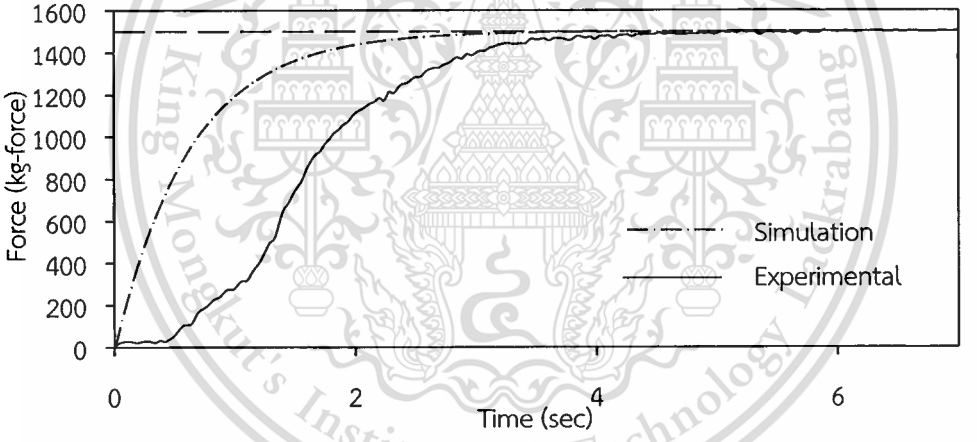

Figure 6.13 Comparison between simulation and experimental response of EHSS with PID controller at 1500 kg-force equilibrium point

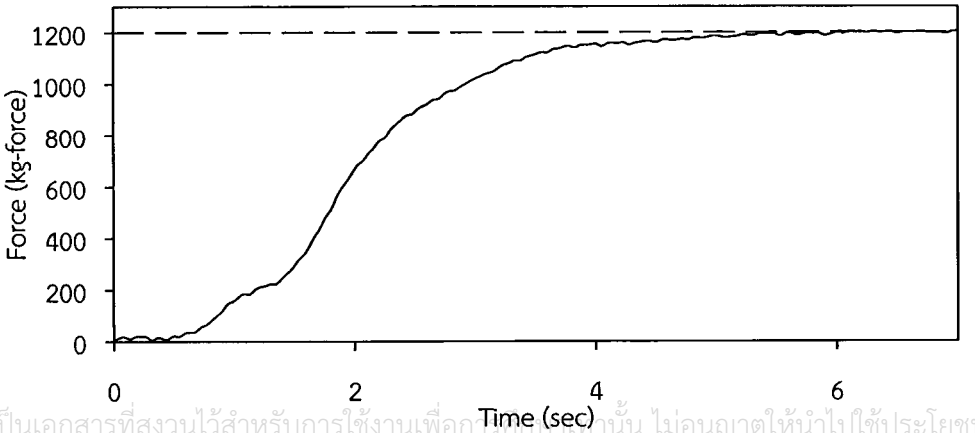

Figure 6.14 Response of 1200 kg-force that force desired minimum allowed used for gain of PID controller at 1500 kg-force equilibrium

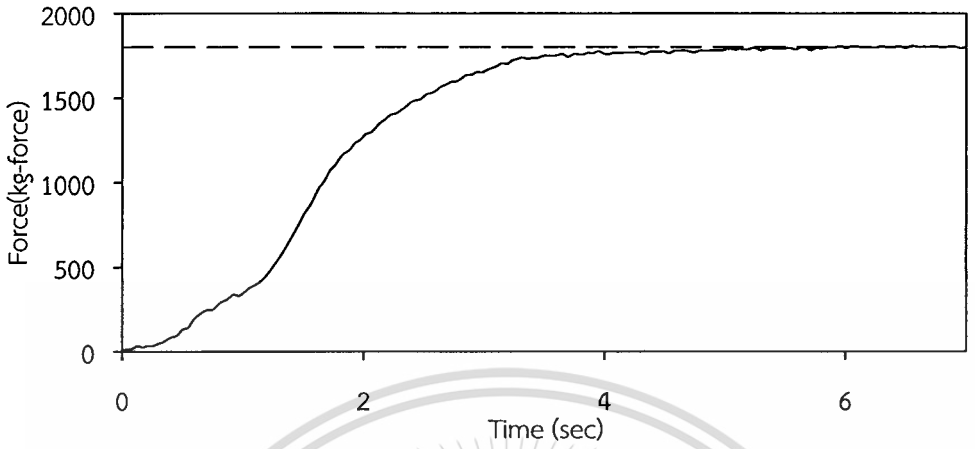

Figure 6.15 Response of 1800 kg-force that force desired maximum allowed used for gain of PID controller at 1500 kg-force equilibrium

Figure 6.16 shows the response of system with PID controller that comparison between simulation and experimental response at 2000 kg-force equilibrium point. It can be seen that in simulation response, it has approximately 4 second settling time, 3 second rising time and +1 kg-force steady state error. In experimental response, it has approximately 6.0 second settling time, 4.5 second rising time and – 4 kg-force steady state error.

Figure 6.17 shows the response of 1800 kg-force that force desired minimum allowed used for gain of PID controller at 2000 kg-force equilibrium in Table 6.6. It can be seen that it has approximately 4.5 second settling time, 4 second rising time and – 2.5 kg-force steady state error.

Figure 6.18 shows the response of 2200 kg-force that force desired maximum allowed used for gain of PID controller at 2000 kg-force equilibrium in Table 6.6. It can be seen that in Figure 6.(a), it has approximately 6.0 second settling time, 5.0 second rising time and – 3 kg-force steady state error.

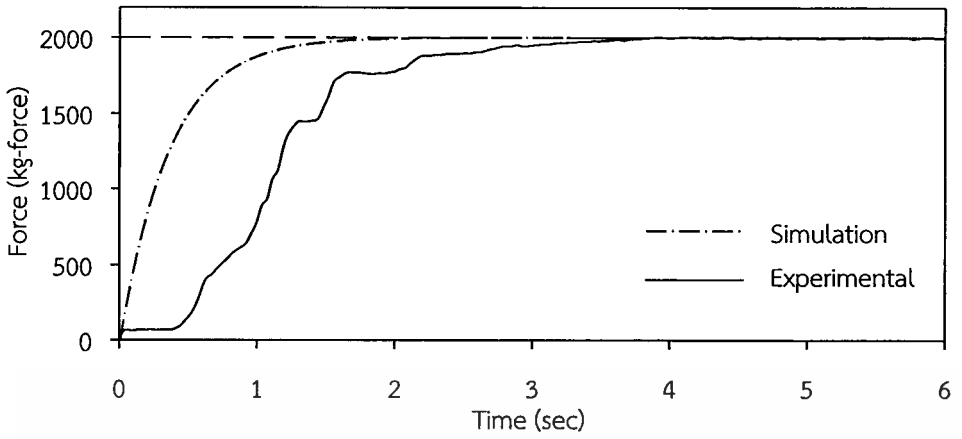

Figure 6.16 Comparison between simulation and experimental response of EHSS with PID controller at 2000 kg-force equilibrium point

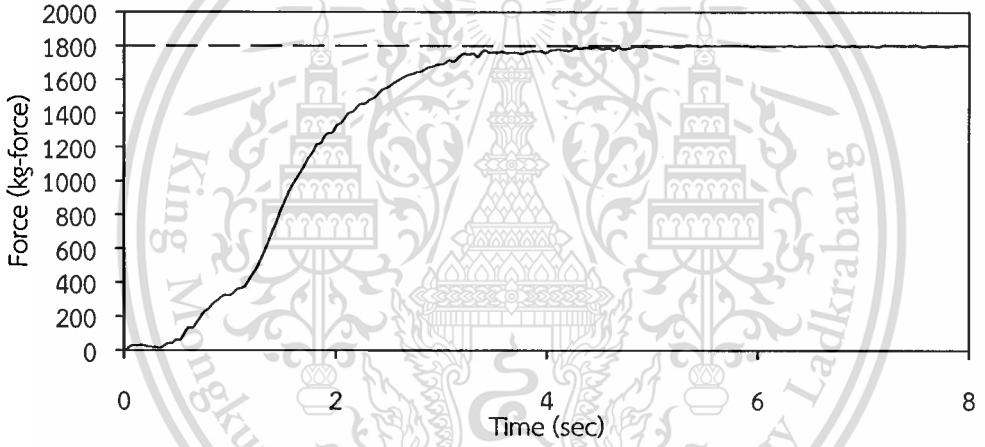

Figure 6.17 Response of 1800 kg-force that force desired minimum allowed used for gain of PID controller at 2000 kg-force equilibrium

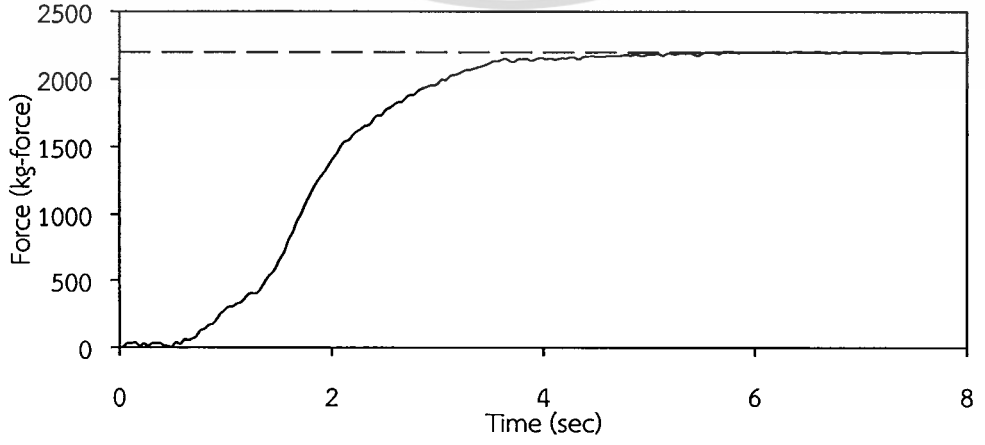

Figure 6.18 Response of 2200 kg-force that force desired maximum allowed used for gain of PID controller at 2000 kg-force equilibrium

6.3.2 Nominal Stability and Performance with Fuzzy Logic Controller

In this section, the nominal stability and performance with fuzzy logic controller result that comparison between simulation result and experimental result are shown as Figure 6.19 to Figure 6.22. In this section, the 500, 1000, 1500 and 2000 kg-force force desired is shown, and the other results are shown as Appendix A.

Figure 6.19 shows the response of EHSS with Fuzzy logic controller at 500 kg-force force desired. It can be seen that in simulation response, it has approximately 1.5 second settling time, 1 second rising time and +1 kg-force steady state error. In experimental response, it has approximately 2.5 second settling time, 2 second rising time and – 2 kg-force steady state error.

Figure 6.20 shows the response of EHSS with Fuzzy logic controller at 1000 kg-force force desired. It can be seen that in simulation response, it has approximately 1.5 second settling time, 1 second rising time and +1 kg-force steady state error. In experimental response, it has approximately 2.8 second settling time, 2.3 second rising time and – 1.5 kg-force steady state error.

Figure 6. shows the response of EHSS with Fuzzy logic controller at 1500 kg-force force desired. It can be seen that in Figure 6.(a), in simulation response, it has approximately 1.5 second settling time, 1 second rising time and +1 kg-force steady state error. In experimental response, it has approximately 3 second settling time, 2 second rising time and – 2 kg-force steady state error.

Figure 6. shows the response of EHSS with Fuzzy logic controller at 2000 kg-force force desired. It can be seen that in Figure 6.(a), in simulation response, it has approximately 1.5 second settling time, 1 second rising time and +1 kg-force steady state error. In experimental response, it has approximately 4 second settling time, 3.5 second rising time and – 2 kg-force steady state error.

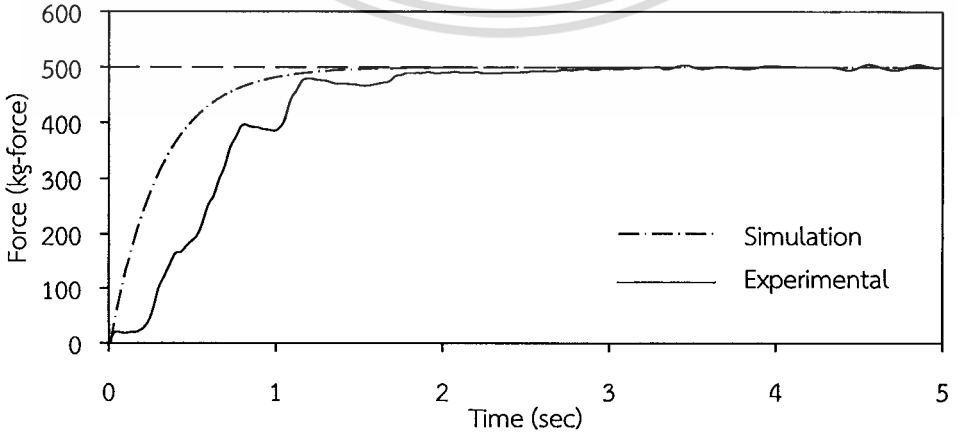

Figure 6.19 Comparison between simulation and experimental response of EHSS with Fuzzy logic controller at 500 kg-force force desired

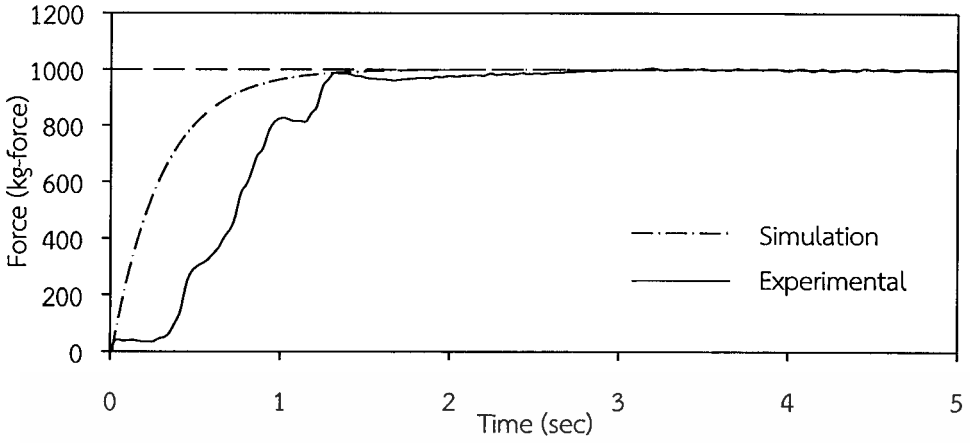

Figure 6.20 Comparison between simulation and experimental response of EHSS with Fuzzy logic controller at 1000 kg-force force desired

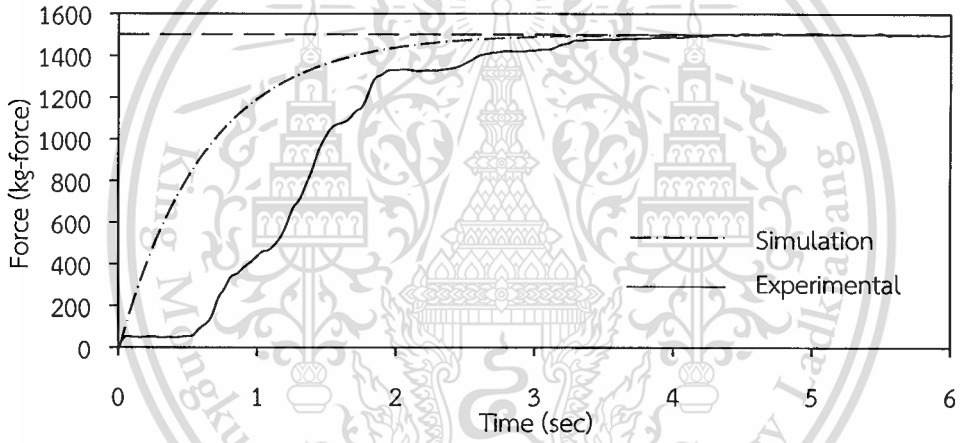

Figure 6.21 Comparison between simulation and experimental response of EHSS with Fuzzy logic controller at 1500 kg-force force desired

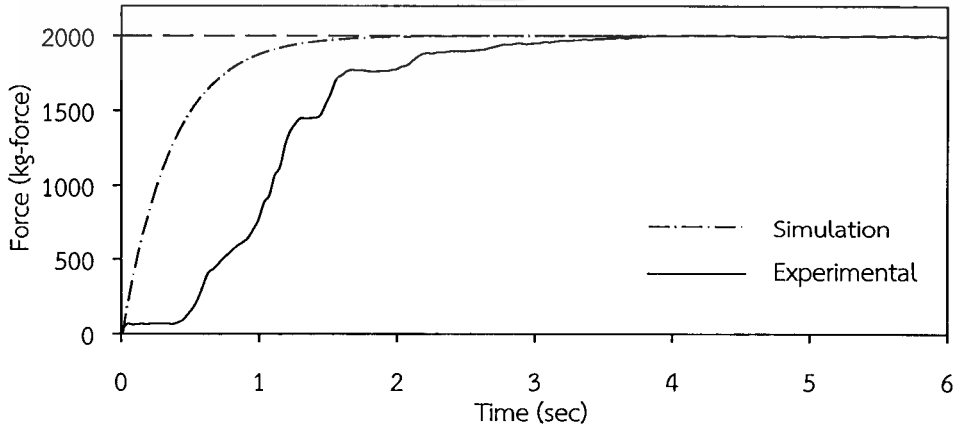

Figure 6.22 Comparison between simulation and experimental response of EHSS with Fuzzy logic controller at 2000 kg-force force desired

6.3.3 Comparison Nominal Stability and Performance between Fuzzy Logic Controller and PID Controller

In this section, the responses of EHSS with fuzzy logic controller compare with the response of EHSS with PID controller. The nominal stability and performance of each controller are compared and analyzed.

Figure 6.23 to Figure 6.26 show the responses of EHSS with fuzzy logic controller compare with the responses of EHSS with PID controller at 500, 1000, 1500 and 2000 kg-force desired, respective.

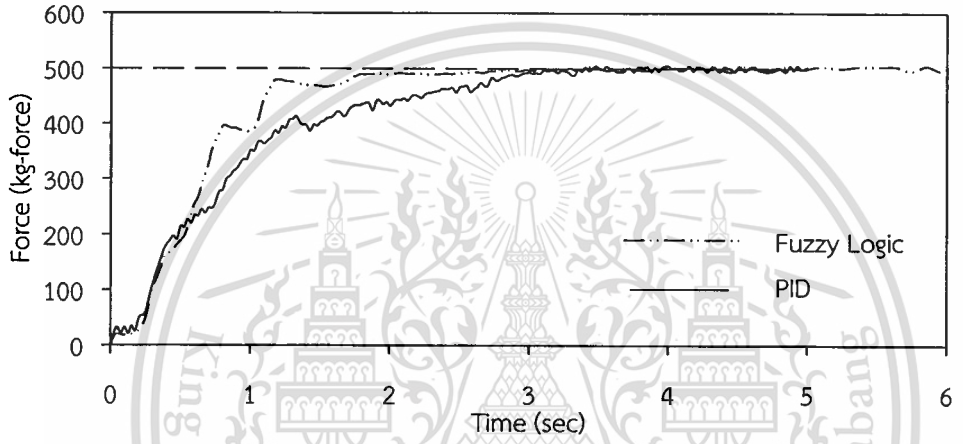

Figure 6.23 Responses of EHSS with fuzzy logic controller compare with responses of EHSS with PID controller at 500 kg-force force desired

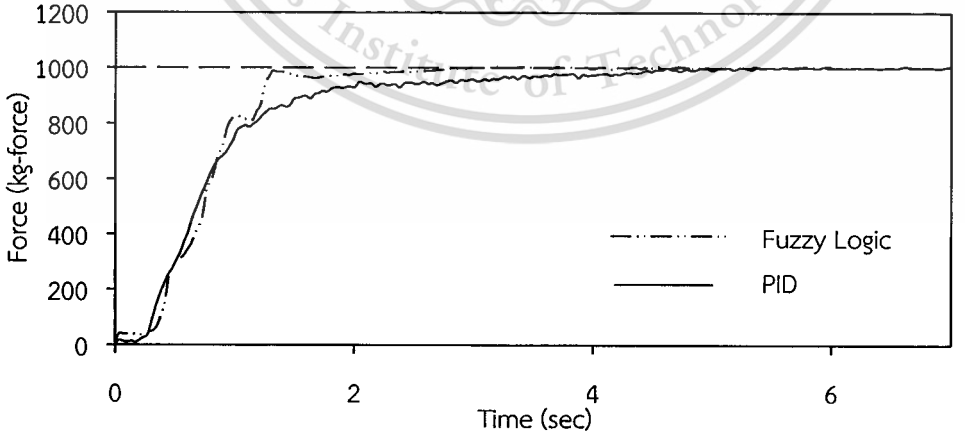

Figure 6.24 Responses of EHSS with fuzzy logic controller compare with responses of EHSS with PID controller at 1000 kg-force force desired

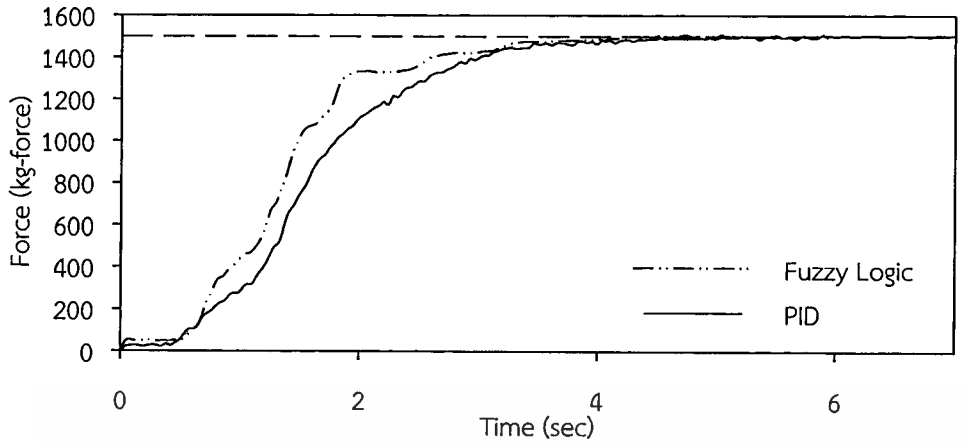

Figure 6.25 Responses of EHSS with fuzzy logic controller compare with responses of EHSS with PID controller at 1500 kg-force force desired

Figure 6.26 Responses of EHSS with fuzzy logic controller compare with responses of EHSS with PID controller at 2000 kg-force force desired

It can be seen that the performance on settling time achieved by fuzzy logic controller and PID controllers are similar. At 500 kg-force and 1000 kg-force desired pressing forces; fuzzy logic gave a faster settling time than the designed value of 3.0 - 4.0 seconds. But at 1000 kg-force and 1500 kg-force desired forces, PID gave a slower settling time than the designed value. In all cases, fuzzy logic controller yields a slightly better steady state error. The PID controller needs individual tuning at each desired pressing force level in order to achieve good performance. Whereas the fuzzy logic controller that once tuned, could work under a wider range of desired pressing forces. Note that the both fuzzy and PID controllers described in this paper were tuned for a settling time of 3.0 - 4.0 seconds. Were the settling time different values, both controllers need design revision and tuning.

Chapter 7
Concluding Comments

7.1 Conclusions

As presented in section 1.2, objectives of this thesis was constructing and model the electro – hydraulic servo system for tabletting press machine test with force control and improve upon the performance of the model/system through feedback control design.

The first, perform lab tests to create a dynamic model of the servo system is presented. In this step was met for valve modulation curve that relationship between input signal and opening area of orifice valve, in that final valve modulation curve described in section 6.1, the opening area of orifice valve range from 0.00 mm^2 to 1.38 mm^2 in port p to port a that input signal range 0.0 volt to 8.0 volt, respectively, at the difference pressure across valve approximately 10.0 MPa, and from 0.00 mm^2 to 2.75 mm^2 in port b to port t that input signal range 0.0 volt to 8.0 volt, respectively, at the difference pressure across valve approximately 9.0 MPa. In the other hand, there are range from 0.00 mm^2 to 1.37 mm^2 in port p to port b that input signal range 0.0 volt to – 8.0 volt, respectively, at the difference pressure across valve approximately 10.0 MPa, and from 0.00 mm^2 to 2.78 mm^2 in port a to port t that input signal range 0.0 volt to – 8.0 volt, respectively, at the difference pressure across valve approximately 9.0 MPa.

Second, dynamic system test is performed. The ranges of operation point command input to proportional valve in this thesis are between from 0.0 volt to 4.0 volt. The result of dynamic system test compare with simulation results is described in section 6.2. In the displacement state (x_1), the simulation results are the similar to the experimental results in the total voltage input. In the velocity state (x_2), the simulation results are the similar to the average results of experimental in the total voltage input. In this state, because of the data from potential sensor has with noise, so the results of experimental must be average data. In the pump pressure state (x_3), the simulation results are the similar to the experimental results in the total voltage input. It has pressure constant approximately 13.7 MPa. In the head end pressure state (x_4), the simulation results are higher than the experimental results in the total voltage input. The pressures of simulation results are higher than the experimental results approximately 1.5 MPa, because in mathematical model, the friction force and leak of hydraulic oil in cylinder are neglected. And, in the rod end pressure state (x_5), the simulation results are similar to the experimental results in the total voltage input. The simulation results have pressure constant at 1.5, 2.3,

2.5 and 2.6 MPa when cylinder moving but the experimental results have pressure increase from 1.2, 2.0, 2.2 and 2.5 MPa to 1.6, 2.3, 2.5 and 2.8 MPa when cylinder moving. So, the mathematic model that improves from physical property is accuracy for used to design the controller in the operation point.

Finally, tests were performed to determine the ability of the EHSS to track force target. In this thesis, there are two controller for control the EHSS with force control system that the tradition PID controller and Fuzzy logic controller. The first, in tradition PID controller, the mathematic model must be linearization at operation point for used to design the controller while in this thesis, operation points is 500, 1000, 1500 and 2000 kg-force. Therefore, each operation point has range of operation and gain of PID controller, described as Table 6.4 and Table 6.6. A reference target force was selected step input to test at each target force. At 500 kg-force equilibrium point and its range of operation, the steady state error was found to be ± 5 kg-force, and the other hand, the steady state error was found to be approximately ± 5, ± 3 and ± 8 kg-force at 1000, 1500 and 2000 kg-force equilibrium point and its range of operation, respective. The second, in Fuzzy logic controller, the range of operation was 0.0 kg-force to 2000 kg-force and a reference target force was selected step input to test at each target force. The steady state error was found to be approximately ± 8 kg-force with the Fuzzy logic controller.

Considering the response results, the EHSS system with PID controller and fuzzy logic force controllers were implemented and tested at various desired pressing force values. The responses of the EHSS with Fuzzy logic controller are approximately 1.5 sec to 5 sec settling time and approximately 1.5 sec to 4 sec rising time in 0.0 to 2000 kg-force operating point, described as section 6.3. In addition, the responses of the EHSS PID with controller are 2.0 sec to 6.0 sec settling time and 1.5 sec to 5.5 sec rising time in 0.0 to 2000 kg-force operating point, described as section 6.3.

The conclusions reached by the study are as follows. First, the valve modulation as it existed at the end of the study that performed for defined the characteristic of proportional valve is accuracy. Second, the mathematic model that improved from physical property is accuracy in the range of operation point. This was due to the implementation of the dynamic performed presented in this study. Third, the system is able to track force desired both in PID controller and Fuzzy logic controller. The PID controller is accuracy by around the equilibrium point that designed. So, when the range of operation is wide, the gain scheduling of PID controller is selected for used in this thesis. Designing with fuzzy logic control has a range of designs available in a range of applications because the configuration of the membership function is a constant. If a membership function can be custom designed or designed to control many of the control it can also be controlled in a wider range

and with fewer errors. The finally conclusion drawn was that it is difficult to state which controller is superior to the other. PID needs proper tuning at each value of desired pressing force. While fuzzy logic, once tuned, could work well over all the values of pressing forces tested in the study.

7.2 Future Work

Although the EHSS with PID controller is accuracy around the equilibrium point that designed, when the range of operation is wide, the gain scheduling is selected for each operating point. For example, if the force desired is 500 kg force and range of operation at 500 kg-force equilibrium is 300 – 800 kg-force, the gain of PID controller is the one. But when the force desired change to out of the range, the gain of PID controller must be changed to the other. It is believed that the gain of PID controller is changed by using fuzzy logic controller that used for sleeted the gain of PID controller for PID controller.

The other hand, the friction force in actuator in the mathematic model is neglected. It is believed that the mathematic model is more accuracy than the old for more accuracy of mathematic model is more accuracy; the friction force in actuator must be defined in the $\dot{x}_2$ term.

Reference

[1] Y.M. Wang, G. Zhou and Sh. G. Wang. *"Design and optimization of electro-hydraulic force servo system based on MATLAB."* **Journal Mechanical Transmission.** Vol 29(4). April 2005. pp. 46-49.

[2] Zhao, T. and T. Virvalo. *"Fuzzy control of a hydraulic position servo with unknown load."* **Proceeding of the 2nd IEEE International Conference on Fuzzy Systems.** IEEE Xplore Press, San Francisco, USA., Mar 28-Apr 1. pp.785-788.

[3] Li, C.C., X.D. Liu, X. Zhou, X. Bao and J. Huang. *"Fuzzy control of electro-hydraulic servo systems based on automatic code generation."* **Proceeding of the 6th International Conference on Intelligent Systems Design and Applications.** IEEE Computer Society, Washington DC., USA., Oct 16-18, pp. 244-247.

[4] Chuang, C.W. and L.C. Shiu. *"CPLD based DIVSC of hydraulic position control systems."* J. **Comput. Elect. Eng.** Vol 30. Aug 2004. pp. 527-541.

[5] G. P. Liu. *"Optimal-tuning nonlinear PID control of hydraulic systems."* **J. Control Engineering Practice.** Vol 8. Mar 2000. pp. 1045-1053.

[6] R. Liu and A. Alleyne. *"Nonlinear force/pressure tracking of an electro-hydraulic actuator."* **J. ASME Journal of Dynamic Systems, Measurement and Control.** Vol. 122, No.3, March 2000. pp. 232-237,

[7] A. Alleyne and R. Liu. *"A simplified approach to force control for electro-hydraulic systems."* **J. Control Engineering Practice.** No. 8. August 2000. pp.1347-1356.

[8] Y. Q. Cai, L. H. Qiu and Zh. L. Wang. *"Predictive robust control for electro-hydraulic control force loading system."* **J. Chinese Journal of Mechanical Engineering.** Vol. 35, No. 6. June 1999. pp. 81-84.

[9] Y. B. He, H. Zhao and Y. Zhu. *"Neural network self-learning variable robustness adaptive tracking control for electro-hydraulic servo system."* **C. 3rd International Symposium on Test and Measurement.** June 1999.

[10] B. Šulc, J. A. Jan. *"Non Linear Modelling and Control of Hydraulic Actuators."* **J. Acta Polytechnica.** Vol. 42, No. 3.

[11] Chen, Y. N., Lee, B. C. and Tseng, C. H. A. *"Variable-structure controller design for an electro-hydraulic force control servo system."* **J. Chin. Soc. Mech. Engrs.** Vol. 11, No. 6. pp. 520-526.

[12] Conrad, F. and Jensen, C. J. D. *"Design of hydraulic force control systems with state estimate feedback."* **In Proc. of the IFAC 10th Triennial Congress,** Munich, Germany. pp. 307-312.

[13] Alleyne, A., Liu, R. and Wright, H. *"On the limitation of force tracking control for hydraulic active suspensions."* **In Proc. of the American Control Conf.** pp. 43-47.

[14] J. Guo, J.Zhou and T. Cui. *"The application of the hybrid fuzzy control of the furnace."* **The Information of microcomputer**. Vol. 21. pp. 106-109.

[15] Herbert E. Merritt. **Hydraulic Control Systems.** John Wiley & Sons Inc. 1967.

[16] Jalali, M. and Kroll, A. Hydraulic Servo-Systems, Modeling, Identification and Control. Springer. 2004.

[17] Munson, B.R., Okiishi, T. H. and Young, D. F. **A Brief Introduction to Fluid Mechanics**. John Wiley and Sons Inc. 1996.

[18] MATLAB: Reference Guide. The MathWorks, Inc,. 1992.

[19] Jędrzykiewicz Z., Pluta J., Stojek J. **Application of the MATLAB – Simulink package in the simulation tests on hydrostatic systems**. Acta Montanistica Slovaca, Ročnik. 1998.

[20] K. Passino and S. Yurkovich. **Fuzzy Control**. Addison – Wesley Longman, Inc., Menlo Park, California. 1998.

APPENDIX

APPENDIX A
Results

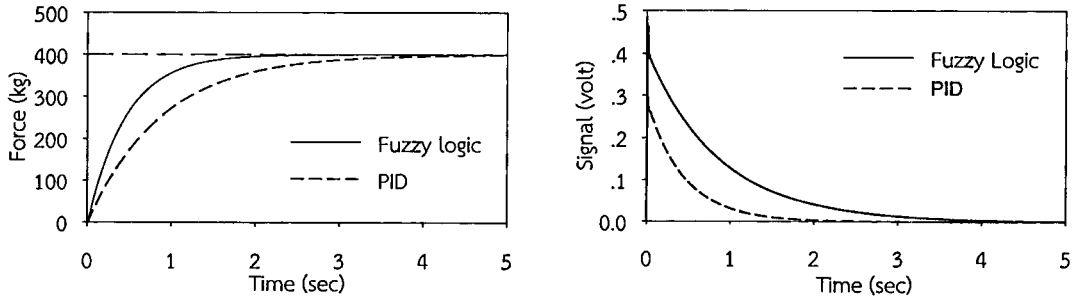

Force and signal response at 400 kg force desired

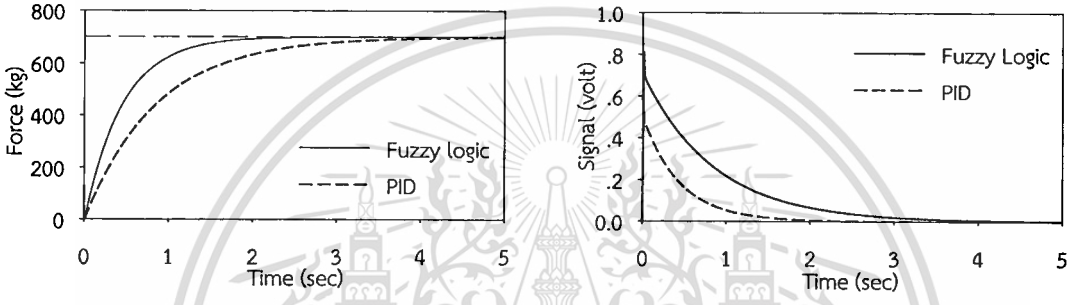

Force and signal response at 700 kg force desired

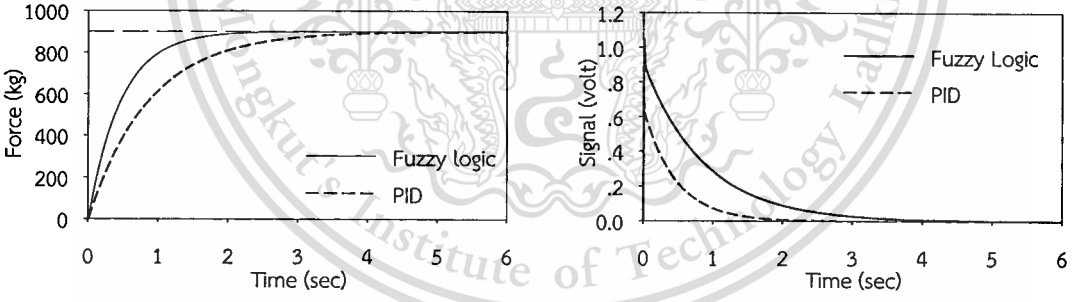

Force and signal response at 900 kg force desired

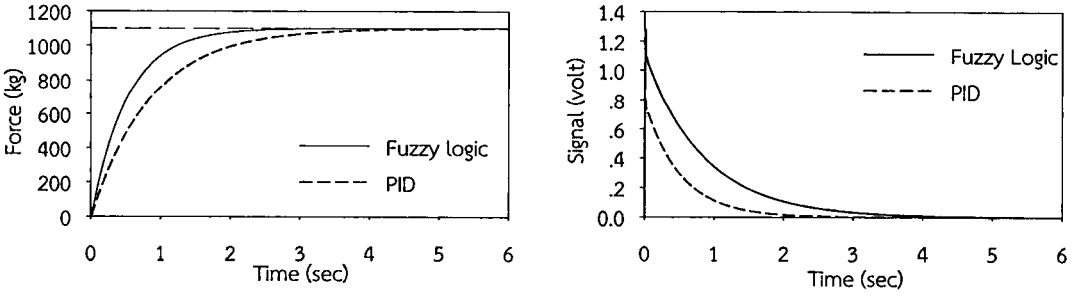

Force and signal response at 1100 kg force desired

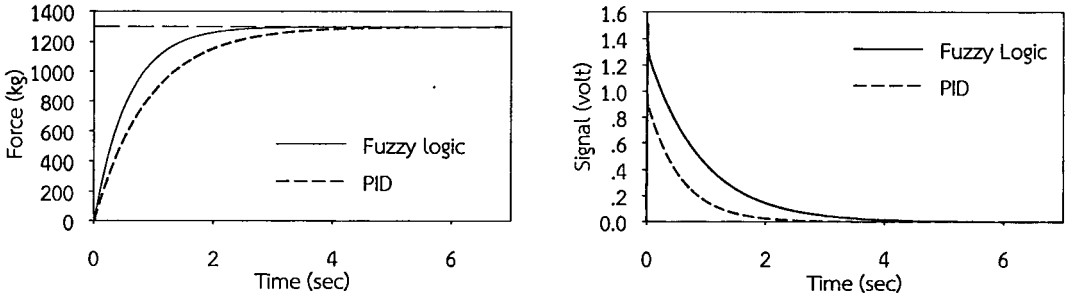

Force and signal response at 1300 kg force desired

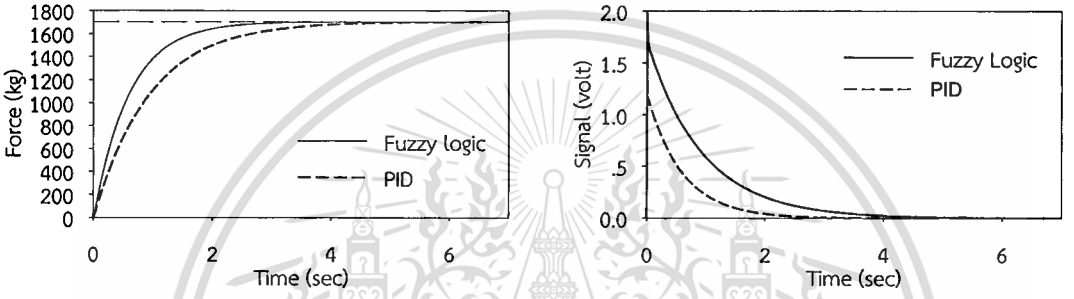

Force and signal response at 1700 kg force desired

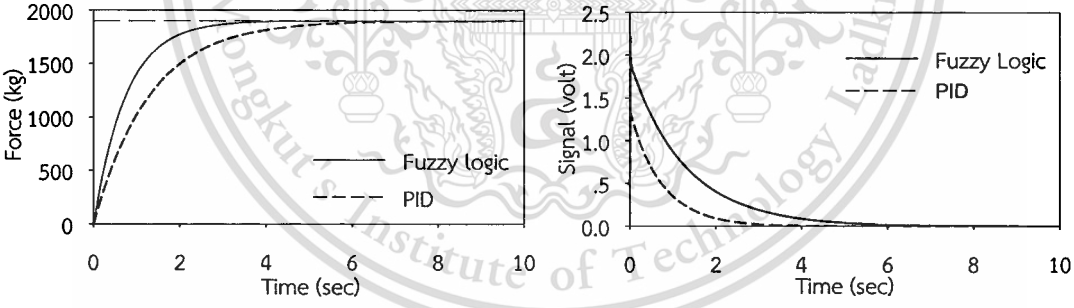

Force and signal response at 1900 kg force desired

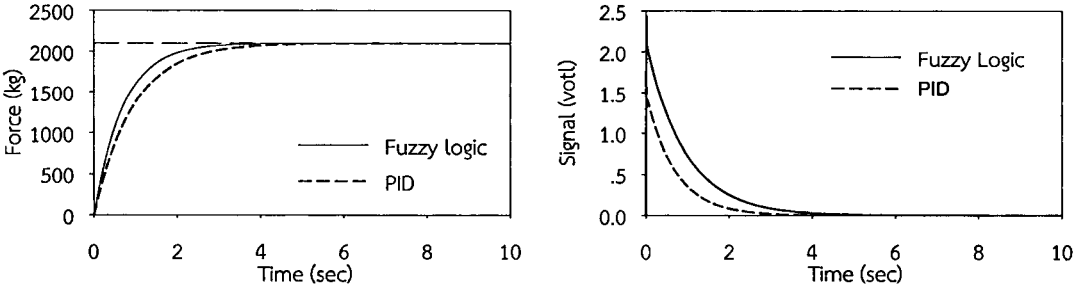

Force and signal response at 2100 kg force desired

APPENDIX B

Block Diagram

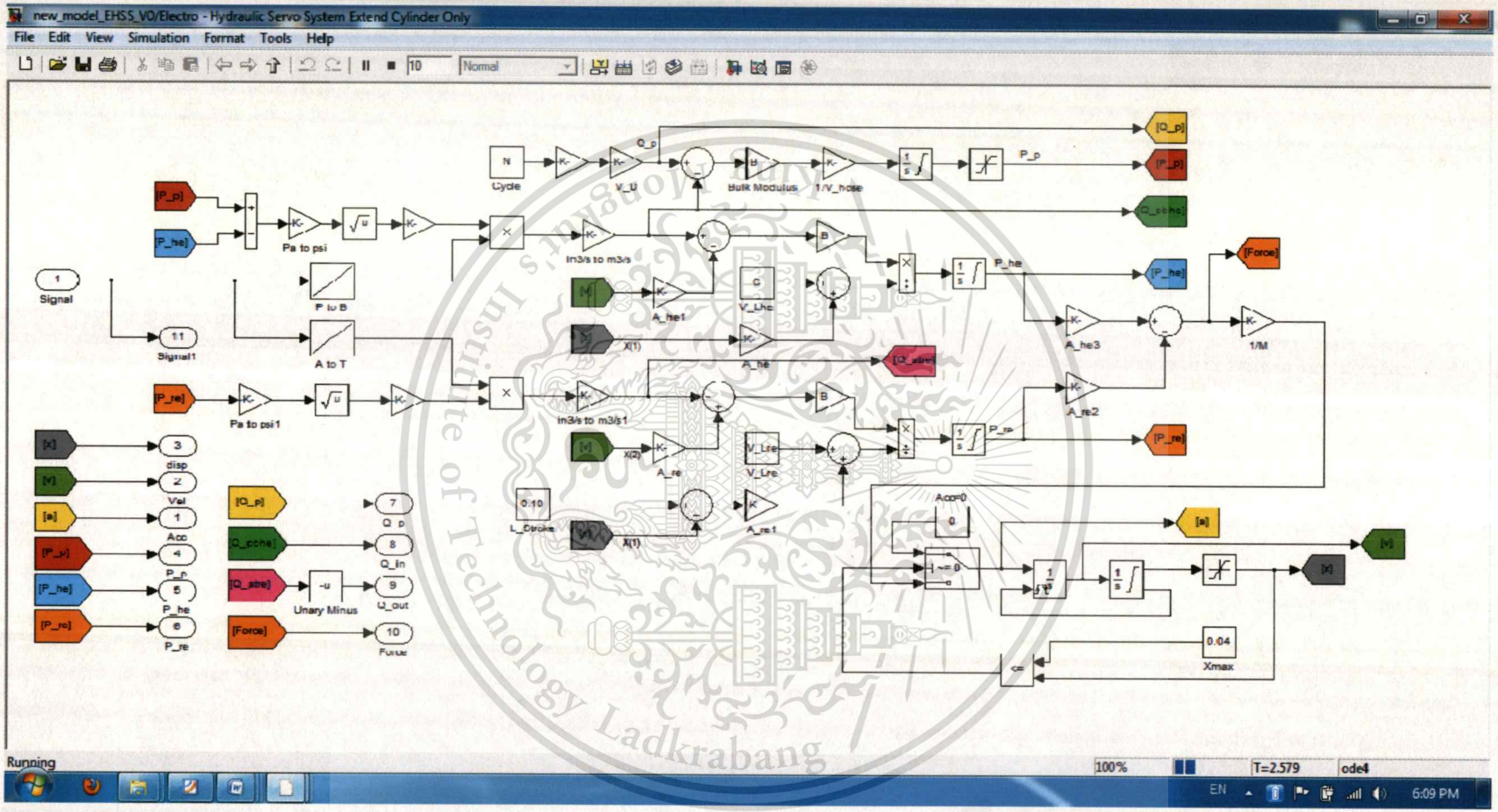

Mathematical model of electro – hydraulic servo system (EHSS)

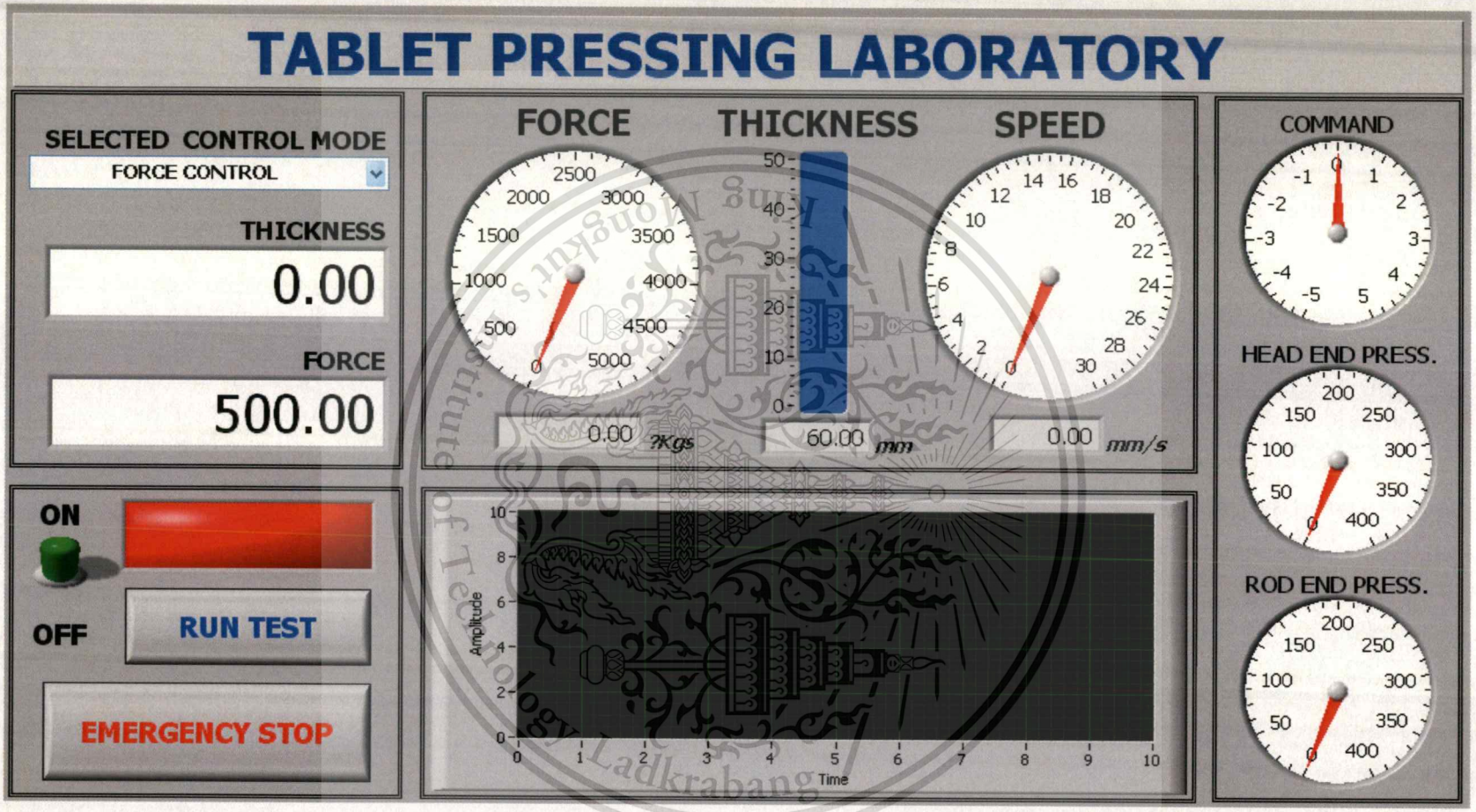
TABLET PRESSING LABORATORY
SELECTED CONTROL MODE
FORCE CONTROL
THICKNESS
0.00
FORCE
500.00
ON
OFF
RUN TEST
EMERGENCY STOP
FORCE
THICKNESS
SPEED
0.00 Kgs
60.00 mm
0.00 mm/s
Amplitude
Time
COMMAND
HEAD END PRESS.
ROD END PRESS.

Fornt panel

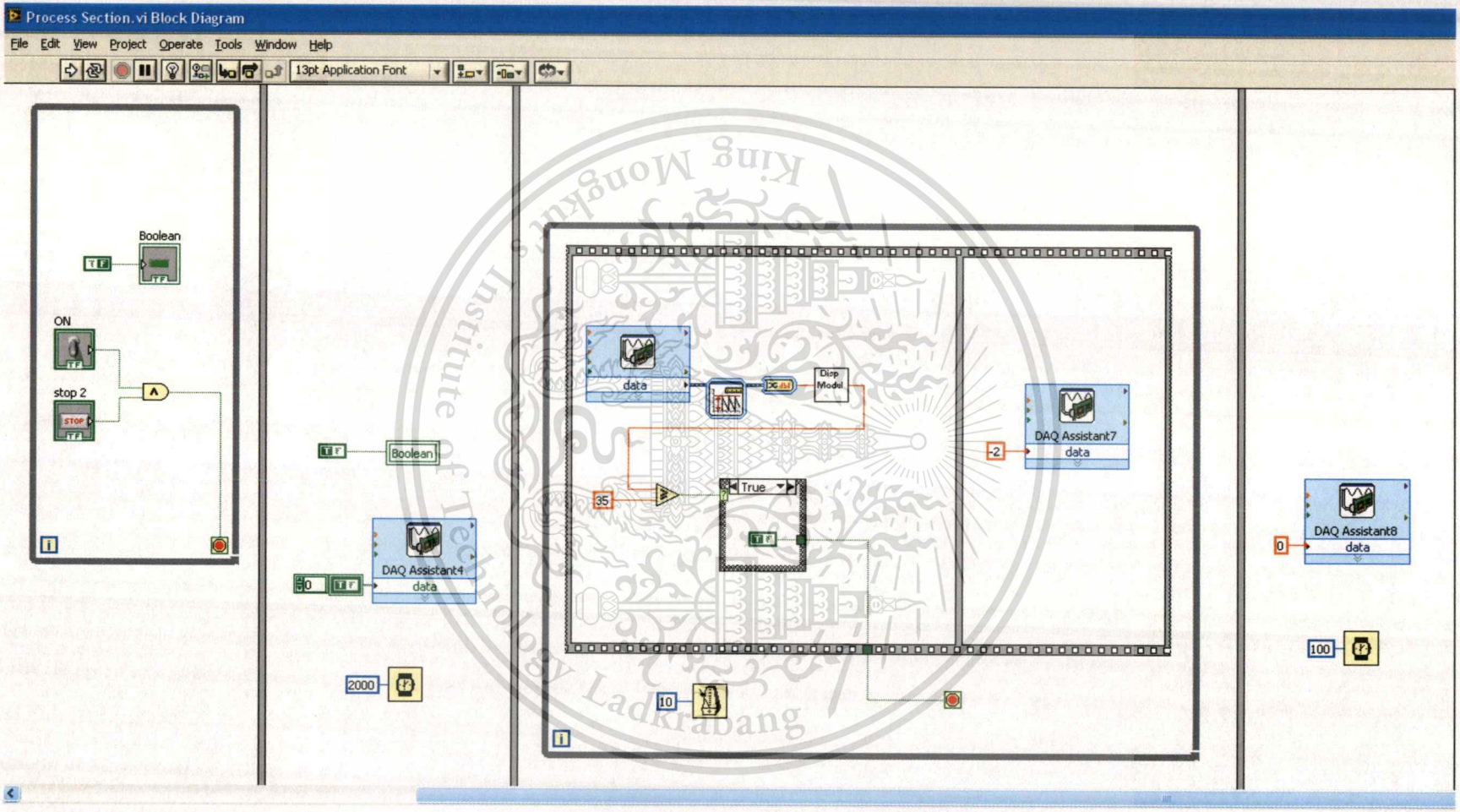

Labview Block Diagram of Pre – Process Program

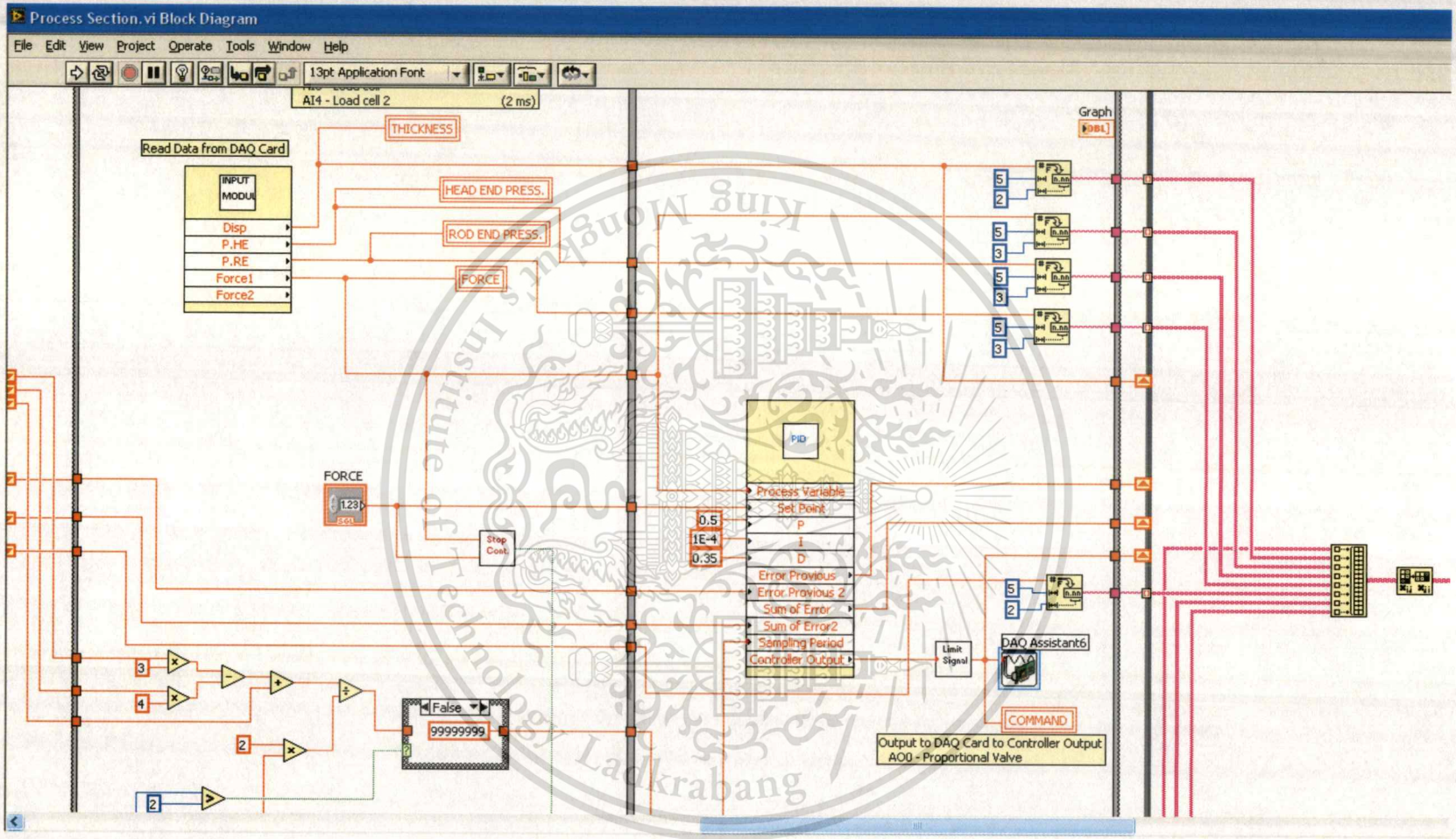

Labview Block Diagram of PID Controller

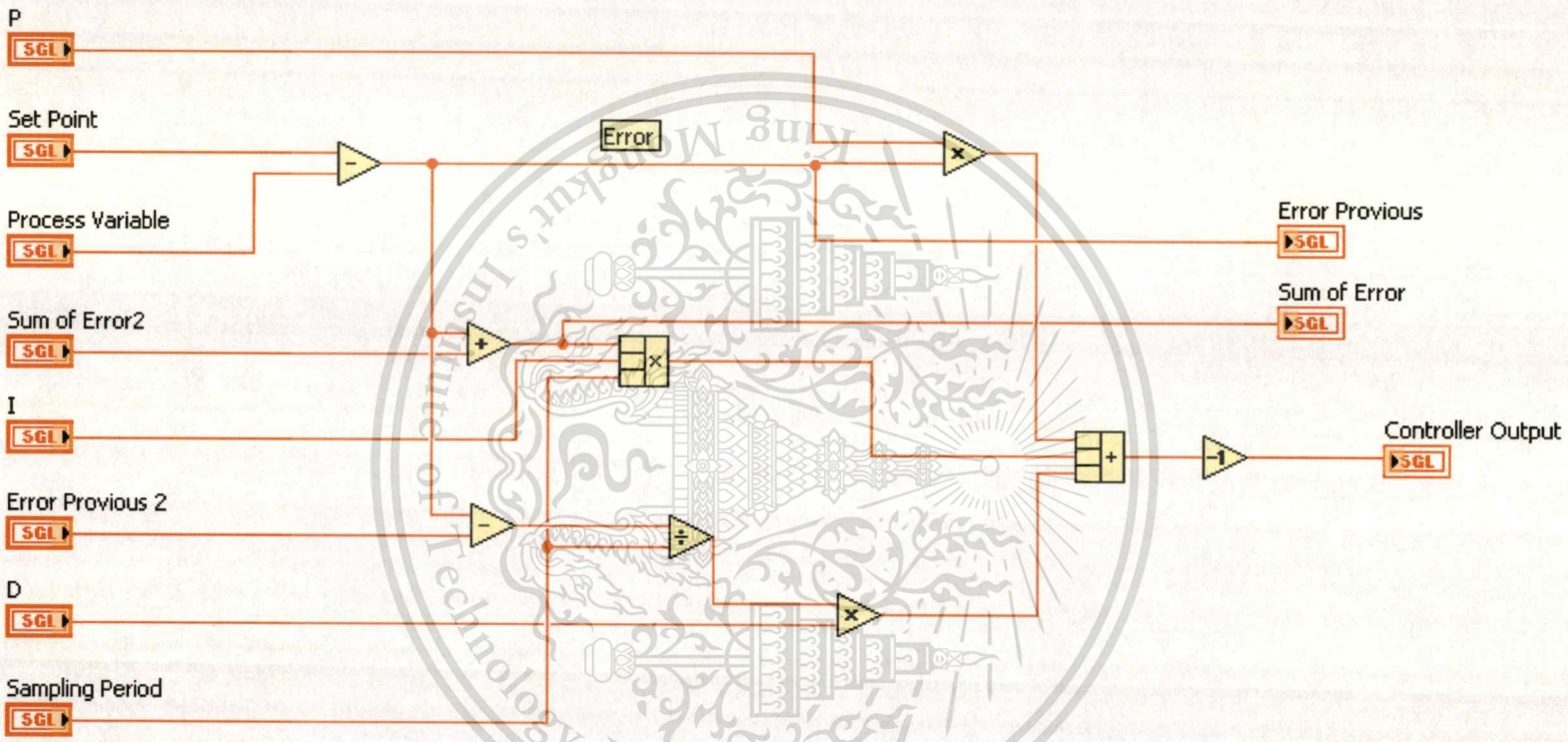

Labview Block Diagram of PID Controller Sub VI

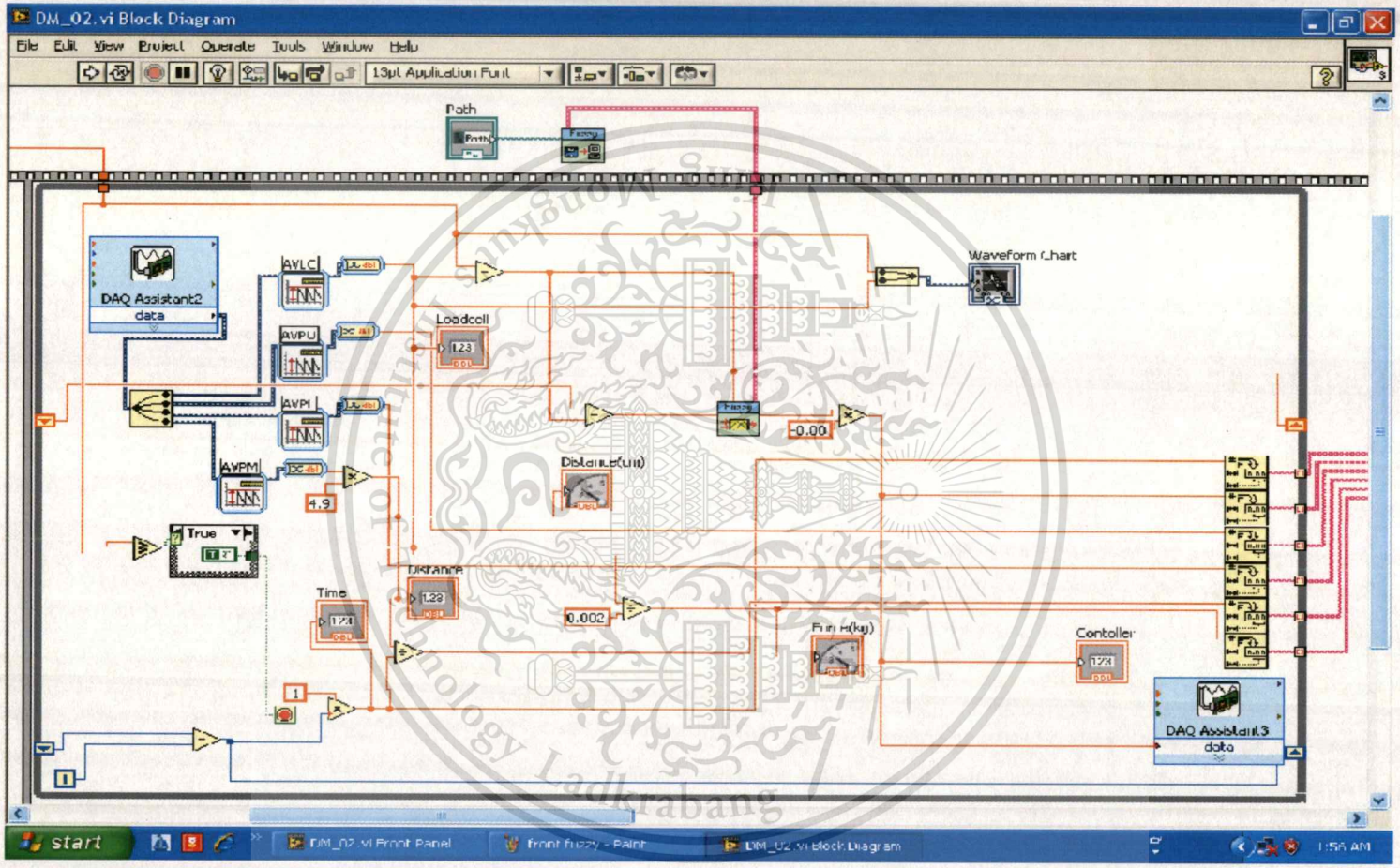

Labview Block Diagram of Fuzzy Logic Controller

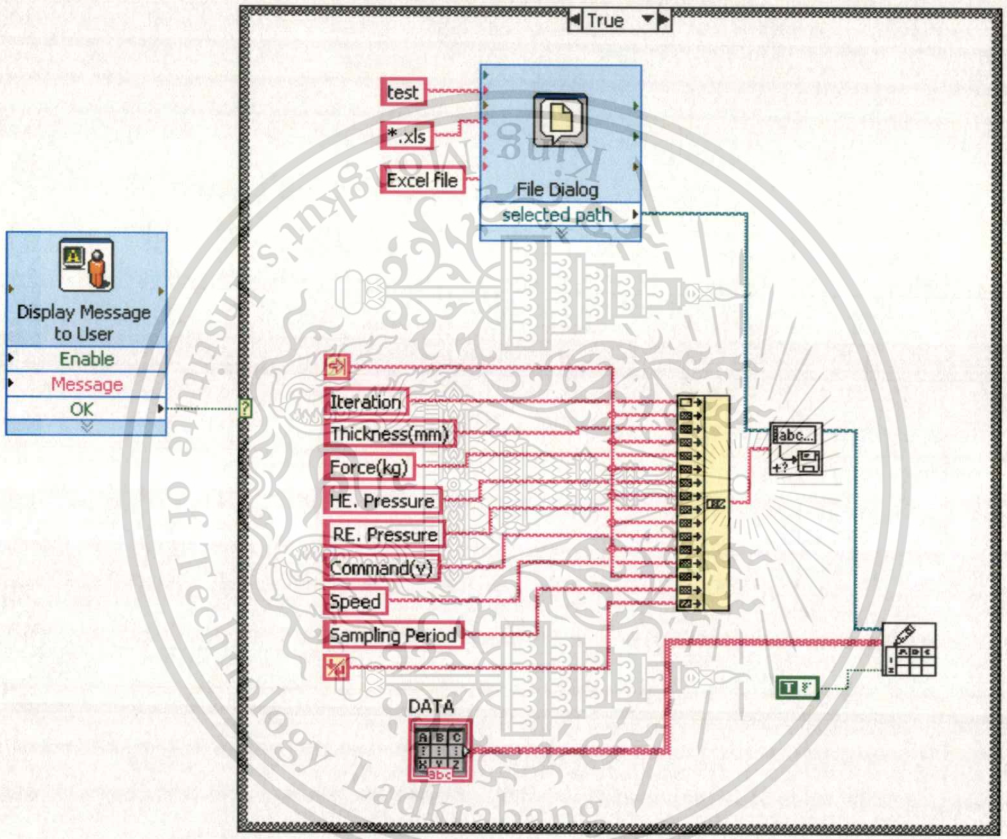

Labview Block Diagram of Data Record

APPENDIX C
Publish Paper

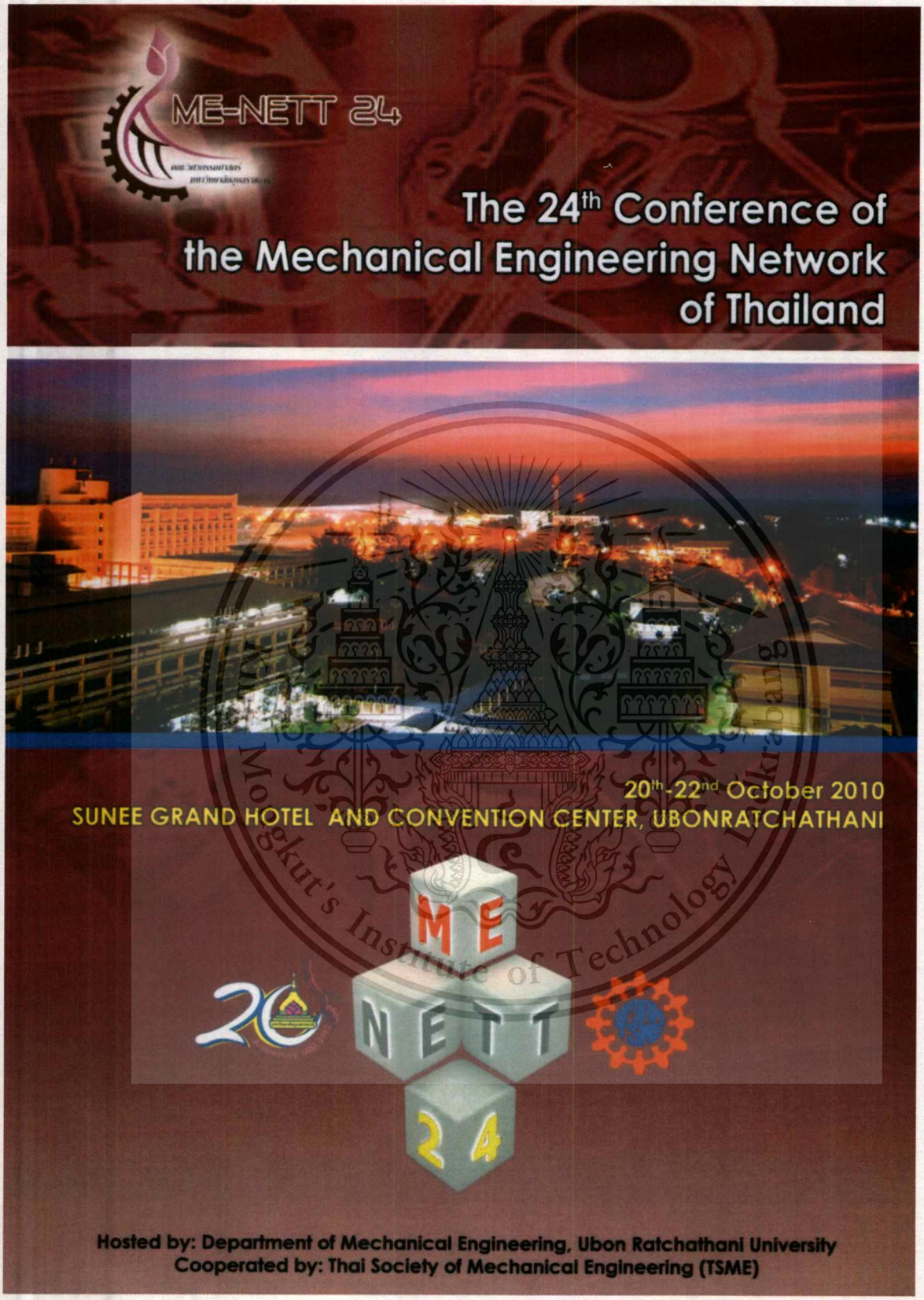

The 24th Conference of the Mechanical Engineering Network of Thailand
October 20 – 22, 2010, Ubon Ratchathani

A Hybrid Fuzzy – PID Controller for Tabletting Machine with Force Control

Pijirawuch Weingchanda[1,*], Nattawoot Depaiwa[1], Unnat Pinsopon[1], Naren chaithanee[2], Sujimon Tunvichien[3] and Duangratana Shuwisitkul[3]

[1]School of Mechanical Engineering, Faculty of Engineering, King Mongkut's Institute of Technology Ladkrabang, Bangkok, 10520
[2]Department of Automotive, Faculty of Engineering, Thai-Nichi Institute of Technology, Bangkok, 10250
[3]Department of Pharmaceutical, Faculty of Pharmacy, Srinakharinwirot University, Ongkharak, Nakornayok, 26120
* Corresponding Author: E-mail: eng4198@hotmail.com, Tel: 0-2326-4197, Fax: 0-2326-4198

Abstract

In this paper, the dynamics modeling applied to force control of tabletting machines with electro - hydraulic and a hybrid of Fuzzy – PID controller is presented. This system includes a hydraulic cylinder/piston, an electronic servo valve, a force sensor and a controller. Flow rate that flows through the valve is a function of voltage signal and a square root of pressure drop across the valve. Therefore, linearization technique is employed to solve this nonlinear function. The transfer function that relates directly between output force and input reference voltage signal can be developed. The controller is a PC computer that sends a control signal through Data Acquisition Card (DAQ) to the servo valve. The feedback control signal is directly measured by the force sensor that is installed upper the tabletting block. The control law is a hybrid Fuzzy – PID controller. Fuzzy controller is used to control force far away from the target force. PID controller is applied when the force is near the desired force reference. The control results in both computer simulation and actual hardware system are shown. The controller that is designed in this paper is able to control the magnitude of the force as desired. In conclusion, the performance of the control system is satisfactory.

Keywords: Tabletting Machine with force control, Electro – hydraulic, Servo valve, Hybrid of Fuzzy - PID.

1. Introduction

Many tabletting machines used of experiment with pressing process the tablet in some Pharmacy Department of Thailand are imported from foreign countries. The conventional machine cannot control a pressing force that may cause directly to the quality of the tablet, for example, the solubility, hardness, rough of surface, etc. In this project, the tabletting machine which can control the pressing force will be developed and used to analyze the effect of controller–parameter onto the quality of the tablet.

Due to their high force to weight ratio, small size, flexible, ease of setting speed, force and torques, and high precision control etc., [1,2] electro – hydraulic system is for use in mainly

system of the tabletting machine. The accurate design and high performance of the control system have importance as requirement, so the mathematic model of hydraulic system firstly will be developed. They are the highly nonlinear phenomena such as fluid compressibility, the flow/pressure relationship and the many uncertainties of hydraulic system due to linearization. Therefore, it seems to be quite difficult to perform a high precision control by using linear control method.

Classical PID controller that can improve both the transient response and steady error of the system at the same time has parameters containing K_P, K_I, K_D that are usually fixed during operation. Consequently, a controller is inefficient for control a system while the system is disturbed by unknown facts, or the surrounding environment of the system is changed.

Fuzzy controller that has a short rise time and a small overshoot has been successfully used in the complex ill-defined process with better performance than a PID controller. It is robust to the system with variation of system dynamics and the system of model free or the system which precise information is required. One of the important problems involved with the design of fuzzy logic controller is the complexity of fuzzy controller that increases exponentially when the number of input variable increases. The hybrid of Fuzzy – PID controller takes advances of the nonlinear characteristics of the Fuzzy controller and the accuracy near a set point which is guaranteed by the classical PID controller [3].

2. Mathematic model of Electro-hydraulic force control system

The specification of the Tabletting machine is depicted in Fig.1 that is shown a diagram of the system. The force control of the tabletting machine procedure is described as follows: Upon the intended initial and force from the end of piston are given, the computer receives the feedback signal though DAQ card (A/D) from force sensor, realizes various control algorithm and transmits a control signal though DAQ card (D/A) and amplifier card to servo valve. The force from the end of piston is proportional to the input signal.

In order to provide mathematic basic for choosing control strategy, the mathematic model of electro-hydraulic force control system was built and analyzed.

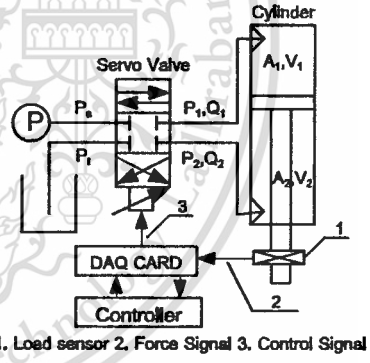

1. Load sensor 2. Force Signal 3. Control Signal

Figure 1: Diagram of Tabletting Machine and Electro-hydraulic force control system.

In the Fig. 1, P_s is the supply pressure, P_t is the reservoir pressure, P_1 and P_2 are pressure in side 1 and 2 of the cylinder, Q_1 and Q_2 are fluid flow, A_1 and A_2 are the piston area of side 1 and 2, V_1 and V_2 are the cylinder volume of side 1 and 2, and U is the control signal.

While the mathematic model is obtained, hydraulic pipe and valve dynamics are neglected

and it is considered that there is no leakage between the piston and the cylinder. Besides, it is assumed that the supply pressure is constant and reservoir pressure is zero. The orifice equation simplify to [4]

$$Q_1 = \begin{cases} +C_d U\sqrt{|P_s - P_1|}, & U \geq 0 \\ -C_d U\sqrt{|P_s - P_2|}, & U < 0 \end{cases} \quad (1)$$

$$Q_2 = \begin{cases} +C_d U\sqrt{P_2}, & U \geq 0 \\ -C_d U\sqrt{P_1}, & U < 0 \end{cases} \quad (2)$$

So only the supply or the return orifice is open at the given time.

The signs which are in the right-hand of equations assign by the control signal, can be rewritten as in [5]

$$Q_1 = C_d U\sqrt{P_s - P_1} = f_1(U, P_1) \quad (3)$$

$$Q_2 = C_d U\sqrt{P_2} = f_2(U, P_2) \quad (4)$$

Eq. (3) and (4) are lineraized by using Taylor's expansion theory. The first differentials are more dominance than the other terms.

$$\delta Q_1 = \left.\frac{\partial Q_1}{\partial U}\right|_{P_{1(0)}} \delta U + \left.\frac{\partial Q_1}{\partial P_1}\right|_{\substack{U_{(0)} \\ P_{1(0)}}} \delta P_1 \quad (5)$$

$$\delta Q_2 = \left.\frac{\partial Q_2}{\partial U}\right|_{P_{2(0)}} \delta U + \left.\frac{\partial Q_2}{\partial P_2}\right|_{\substack{U_{(0)} \\ P_{2(0)}}} \delta P_2 \quad (6)$$

In this project, the servo valve which is symmetry, is designed, and relationship directly between flow-rate and control signal are variation [6]. With their assumes are

$$\left.\frac{\partial Q_1}{\partial U}\right| = \left.\frac{\partial Q_1}{\partial P_1}\right| = K$$

$$\left.\frac{\partial Q_1}{\partial P_1}\right|_{\substack{U_{(0)} \\ P_{1(0)}}} \delta P_1 \text{ and } \left.\frac{\partial Q_2}{\partial P_2}\right|_{\substack{U_{(0)} \\ P_{2(0)}}} \delta P_2 \approx 0$$

Finally, the linear equation of servo valve can be rewritten as in

$$Q_1 = Q_2 = KU \quad (7)$$

Where K is the flow constant of servo valve, it is obtained from the manufacturer's data.

Using Newton's law, the piston force balance result in differential equation is as in (8). Applying the continuity equation to both side of cylinder, the following (9) and (10) can be derived [6,7].

$$\ddot{z} = (P_1 A_1 - P_2 A_2 - c\dot{z} - F_s)/M \quad (8)$$

$$\dot{P}_1 = \frac{\beta}{V_1}(Q_1 - A_1\dot{z}) \quad (9)$$

$$\dot{P}_2 = \frac{\beta}{V_2}(-Q_2 + A_2\dot{z}) \quad (10)$$

It is assumed that the initial total volume is

$$V_1 = V_{01} + A_1 z \quad (11)$$

$$V_2 = V_{02} - A_2 z \quad (12)$$

When β is the bulk modulus of the fluid, it is obtained from the manufacturer's datasheet.

Substituting of Eq. (7), (9), (10), (11), (12) and $F_s = k_s z$ into Eq. (8), we have

$$\dddot{F} = \left(\frac{\beta K U A_1 k_s}{k_s V_{01} + A_1 F} - \frac{\beta A_1^2 \dot{F}}{k_s V_{01} + A_1 F} - \frac{\beta A_2^2 \dot{F}}{k_s V_{02} + A_2 F} + \frac{\beta K U A_2 k_s}{k_s V_{02} + A_2 F} - \frac{c\ddot{F}}{k_s} - \dot{F}\right)\frac{k_s}{M} \quad (13)$$

So that is the non-linear equation of electro-hydraulic force control system.

It is considered that the piston works at the center of cylinder. Therefore, the displacement of motion of piston controlling the pressing force is ultrashot. The volumes of the both sides of the cylinder are changed very little. From Eq. (11) and (12), we obtain

$$V_1 = V_{01} \quad \text{and} \quad V_2 = V_{02} \quad (14)$$

Thus, substituting of Eq. (7), (9), (10) and (14) into Eq. (8), and rearranging, we have

$$\frac{M\dddot{F}}{k_s} = \frac{\beta KUA_1}{V_1} - \frac{\beta A_1^2 \ddot{F}}{k_s V_1} - \frac{\beta A_2^2 \ddot{F}}{k_s V_2} + \frac{\beta KUA_2}{V_2} - \frac{c\ddot{F}}{k_s} - \dot{F} \quad (15)$$

Consequently, using the Laplace transformation, we have the transfer function

$$\frac{F(s)}{U(s)} = \frac{\frac{\beta K k_s}{M}\left(\frac{A_1}{V_1} + \frac{A_2}{V_2}\right)}{s^3 + \frac{c}{M}s^2 + \left(\frac{\beta A_1^2}{MV_1} + \frac{\beta A_2^2}{MV_2} + \frac{k_s}{M}\right)s} \quad (16)$$

Substituting of β =1.5x10^9 N/m^2, K = 5x10^{-5}, A_1= 3.117x10^{-3} m^2, A_2=5.726x10^{-4} m^2, V_1= 2.182x10^{-3} m^3, V_2= 1.718x10^{-4} m^3, M is the mass of piston = 5 kg, c is the viscous friction coefficient = 3x10^4 N/ms^{-1}, k_s is spring coefficient = 1.489x10^9 N/m into Eq. (16), we obtain

$$P(s) = \frac{F(s)}{U(s)} = \frac{1.063\times10^{15}}{s^3 + 6000s^2 + 1.458\times10^{10}s} \quad (17)$$

We can get the electro-hydraulic force servo control system open loop bode figure as Fig. 2 from Eq. (17) and related parameter simulation. We can know from Fig. 2 that the amplitude margin and phase margin of the system are not adequacy, and they cannot satisfy the system steady condition, the open loop gain of the system is no steady, and we must design controller to proofread the system.

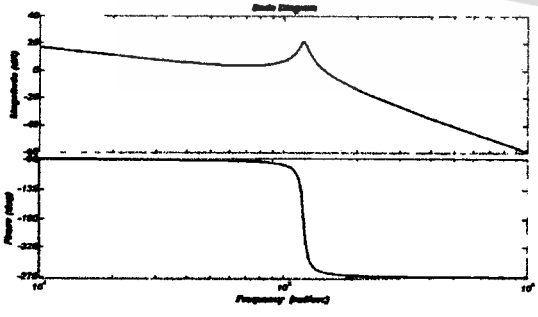

Figure 2: The open loop figure of electro-hydraulic force servo control system

3. Control system design.

There are various types of control system used in classical control, modern control and intelligent control systems. Each has been study and implement in many industrial applications. Every control system method has its advantage and disadvantages. Consequently, the trend is to implement hybrid system consisting of more than one type of control technique. The hybrid of Fuzzy – PID controller is presented. Fuzzy controller is used to control force far away from the target force. PID controller is applied when the force is near the desired force reference.

3.1 PID controller design.

The PID control method has been widely used in industry during last several decades because of its simplicity. The implementation of PID control logic, as shown in Eq. (18), requires finding suitable values for the gain parameters K_P, K_I and K_D.

$$U(s) = K_P + \frac{K_I}{s} + K_D s \quad (18)$$

Rearranging Eq. (18), we obtain

$$U(s) = \frac{K_c(s^2 + as + b)}{s} \quad (19)$$

$$U(s) = \frac{K_c(s + z_1)(s + z_2)}{s} \quad (20)$$

When $K_c = K_D$, $a = K_P/K_D$ and $b = K_I/K_D$.

The PID controller is designed by root locus method. The performances of system as requires are no overshoot and less than 3 second of setting time. Designed and simulated in the computer by Matlab program. In the PID controller, the two zero that the first zero is 0.005 and the second zero is 4.5 are added in the PID. In the root locus plot, we have $K_c = 0.00001$. Thu, the PID controller is

$$U(s) = \frac{0.00001(s+0.005)(s+4.5)}{s} \qquad (21)$$

Comparing Eq. (21) with Eq. (19), we have $K_D = 0.00001$, $K_I = 4.505\times10^{-5}$ *and* $K_P = 2\times10^{-7}$

We can know from Fig.5 that the amplitude margin and phase margin of the system are adequacy, and the system is steady, and the low frequency gain of the system is increased, but we can find the slop of the frequency response curve of the system crossing 0 decibel line is bigger than 20dB, when the elastic load rise to definite extent. The phase margin of the system is decrease very rapid. So PID control cannot provide very good control performance. Aiming at this reason, fuzzy control algorithm is designed and adopted in the controller design process.

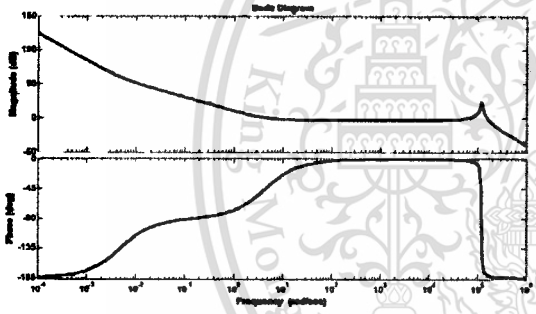

Figure 3: The open loop figure of electro-hydraulic force servo control system corrected by PID – controller

3.2 Fuzzy controller design.

Fuzzy control is a kind of expert control and the control rule of it fully reflect person's intelligent activity. It can control difficult process by simulating person's fuzzy controller, input and output port, actuator, controlling object and sensor, etc usually. The basic of fuzzy control principle is shown as Fig.4. The part including in the dotted line in Fig.4 is fuzzy controller, we can also find from Fig.4 that the main part of fuzzy controller is fuzzification process, knowledge base, fuzzy reasoning decision and exactness.

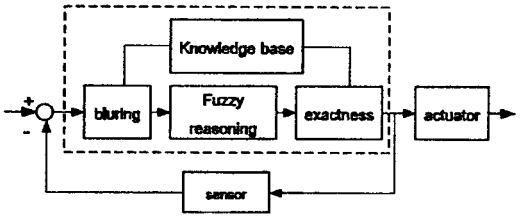

Figure 4: The basic structure of fuzzy control

In this project, input of model is the derivation e and it change rate $\dot{e}$ of output force and their fuzzy subset are (1, 2, 3) and their linguistic value and universe division grade receptivity is *{negative, zero, positive}* and *{negative big, negative middle, negative small, zero, positive small, positive middle, positive big}*

= {NB, NM, NS, Z, PS, PM, PB}

= {-3, -2, -1, 0, 1, 2, 3}.

Let linguistic variable of output control variable u is U, and its fuzzy subset is (1,2,...,5) and its linguistic value respectively and universe division grade receptivity is

{quick close, slow close, no move, slow open, quick open} and *{negative big, negative middle, negative small, zero, positive small, positive middle, positive big}*

= {NB, NM, NS, Z, PS, PM, PB}

= {-3, -2, -1, 0, 1, 2, 3}

Fuzzy set is described by membership function, and common membership function in fuzzy system is gaussmf style membership function. The curve shape of gaussmf is normal distribution curve, and expression of it is

$$\mu(x) = \exp[-((x-c)/\sigma)^2] \qquad (22)$$

The membership functions of three variable of fuzzy controller design in this paper are all gaussmf style membership function, in both

parameter σ and c, the numerical value of σ directly influence the shape of the membership function curve, and the parameter c is the center of the membership function curve.

Table 1. The parameter value of membership function of e and $\dot{e}$

Parameter valve		name		
		negative	zero	positive
variable	e	[1.4,-3]	[1.4,0]	[1.4,3]
	$\dot{e}$	[1.4,-3]	[1.4,0]	[1.4,3]

Table 2. The parameter values of membership function of U

Parameter value		name				
		Quick close	Slow close	No move	Slow open	Quick open
variable	U	[0.13, -2.5]	[0.13, -1.5]	[0.13, 0]	[0.13, 1.5]	[0.13, 2.5]

Table 3. Fuzzy control rule table

U		$\dot{e}$						
		NB	NM	NS	Z	PS	PM	PB
e	NB	PB	PB	PB	PB	PM	Z	z
	NM	PB	PB	PB	PB	PM	Z	Z
	NS	PM	PM	PM	PM	Z	NS	NS
	Z	PM	PM	PS	Z	NS	NM	NM
	PS	PS	PS	Z	NM	NM	NM	NM
	PM	Z	Z	NM	NB	NB	NB	NB
	PB	Z	Z	NM	NB	NB	NB	NB

The parameter values of the membership function adopted in this paper are shown as table 1 and table 2. According to expert experiment, we can get fuzzy control rule, and the fuzzy control rule table are shown as table 3.

Mamdani reasoning method is adopted during fuzzy reasoning designed. Mamdani reasoning method is introduced briefly as follow.

Let error gotten after a certain time sampling is e, the variety of error is $\dot{e}$. e is belong to fuzzy sets A_1 and A_2, and the membership degree of A_1 and A_2 respectively is $\mu_{A_1}(e)$ and $\mu_{A_2}(e)$. $\dot{e}$ is belong to fuzzy sets B_1 and B_2, and the membership degree of B_1 and B_2 respectively is $\mu_{B_1}(\dot{e})$ and $\mu_{B_2}(\dot{e})$.

If hypothesis of two reasoning rules following is tenable

IF $e = A_1$ and $\dot{e} = B_1$, then $U = C_1$

IF $e = A_2$ and $\dot{e} = B_2$, then $U = C_2$

Then according to Mamdani reasoning method we can get fuzzy set of U is

$$n_1 \vee n_2 \tag{23}$$

Where

$$n_1 = [m_1 \wedge \mu_{C_1}(U)], \quad n_2 = [m_2 \wedge \mu_{C_2}(U)]$$

$$m_1 = \mu_{A_1}(e) \wedge \mu_{B_1}(\dot{e}), \quad m_2 = \mu_{A_2}(e) \wedge \mu_{B_2}(\dot{e})$$

The production of membership function degree, fuzzy rule and fuzzy reasoning can be realized by Matlab tool box.

3.3 A hybrid Fuzzy – PID controller design.

While convention PID controllers are sensitive to variation in the system parameter, fuzzy controllers do not need precise information about the system variable in order to be effective. However, PID controllers are better able to control and minimize the steady state error of the system. Hence, a hybrid system, shown as Fig.3, was developed to utilize the advantages of both PID controller and fuzzy controller.

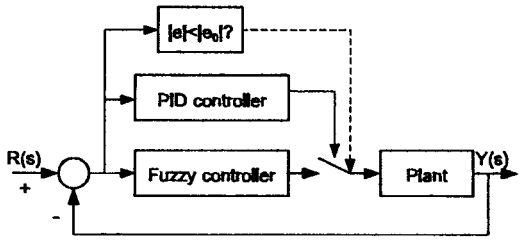

Figure 5: Diagram of a hybrid Fuzzy PID controller

Fig. 5 shows a switch between the fuzzy controller and PID controller, where the force of the switch depends on the error between the actual value and set point value.

If the error in force reaches a value higher than that of the threshold e_0, the hybrid system applies the fuzzy controller, which has fast rise time and small amount overshoot, to the system in order to correct the force with respect to the set point. When the force is below the threshold e_0 or close to the set point, the hybrid system shifts control to the PID, which has better accuracy near the set force.

4. Results

In order to verify the effectiveness PID controller and hybrid Fuzzy – PID controller, and compare analyzing the three controllers; the simulation of system is done. Simulink module of Matlab is adopted in the simulation. The unit step responses simulation curve is shown as Fig.7. The simulation results show that adjusting time is longer when PID controller is adopted and rising time is shorter than PID controller when fuzzy controller is adopted. The rapidity performance of system controlled by fuzzy controller is greatly improved, but oscillation of system is relatively violent, and stability performance is not better, the stability value is 0.962. Therefore, The hybrid Fuzzy – PID controller is improved. There are short rising time that is characteristics of fuzzy controller and the good stability performance. In this project, the stability value is 1.001.

In order to validate the validity PID controller and hybrid Fuzzy – PID controller in fact use and compare practical controlling effects of two controllers, experiment study is done on the tabletting machine shown as Fig. 6.

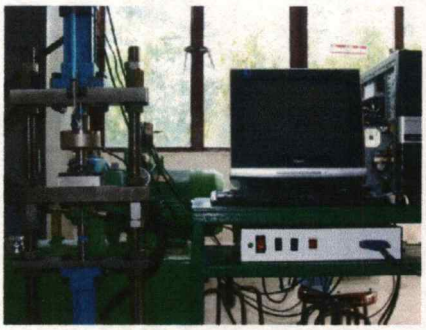

Figure 6: Tabletting Machine

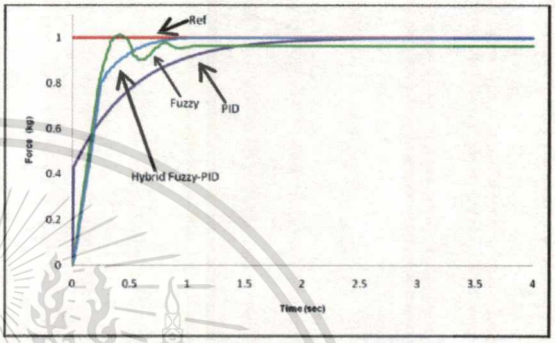

Figure 7: Simulation curve of unit step response

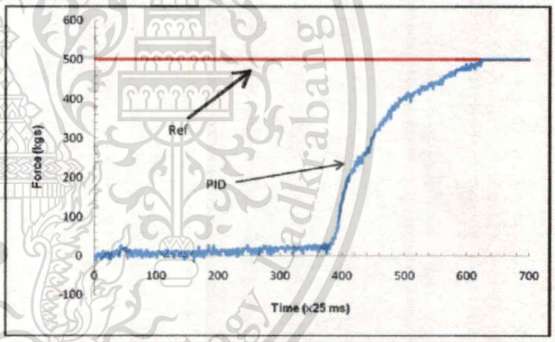

Figure 8: Unit step response experimental curve of PID controller

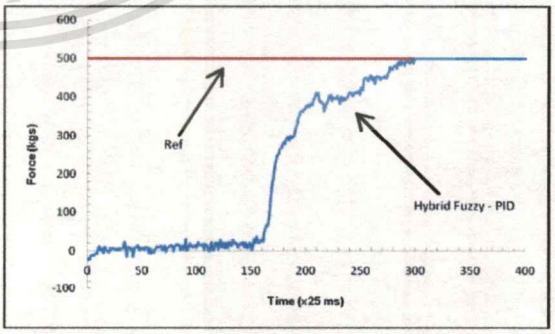

Figure 9: Unit step response experimental curve of Hybrid Fuzzy - PID controller

Fig. 8 is unit step response experimental curve of the tabletting machine controller by PID controller. There are 5.5 sec of rising time, 6.75 sec of setting time and 2 kgs of error.

Fig. 9 is unit step response experimental curve of the tabletting machine controller by hybrid Fuzzy - PID controller. There are 2.5 sec of rising time, 3 sec of setting time and 1 kg of error.

5. Conclusions

Aiming at the characteristics of electro-hydraulic force servo control itself, building model and simulation are done. We find the problem that the open loop gain of system is less and frequency width of system is low and easy to be unsteadily. The object of the project was to develop a control scheme for the tabletting machine. First, a PID controller was individually applied to the tabletting machine. The PID controller accurately controller the steady – state error but did not robustly handle parameter variation in the system while the fuzzy controller provided a fast rise time and low overshoot of the dynamic response output of the system. Then, the hybrid Fuzzy – PID controller proposed in this project was tested experimental and the results were compared with that of individually applied PID and hybrid Fuzzy – PID controllers. The experimental results show that the proposed controller has superior performance compared to individual PID controller. Hence, it can be concluded that the hybrid fuzzy – PID controller is suited for the tabletting machine.

6. Reference

[1] Esposito, A. (1994). *Fluid Power with Application.* Prentice Hall International, Englewood Cliff.

[2] S. Cetin and A. V. Akkaya. (2010). *Simulation and hybrid fuzzy-PID control for positioning of a hydraulic system,* Nonlinear dynamic, vol. 59(3), February 2010, pp. 515-527.

[3] Pronjit P., Siripun T. and Surapun T. (2010). *A hybrid of fuzzy and proportional-integral-derivation controller for electro-hydraulic position servo System,* Energy Research Journal, vol. 1(2), March 2010, pp.62-67.

[4] B. Eryilmaz and B. H. Wilson. (2006). *Unified modeling and analysis of a proportional valve,* Journal of the Franklin Institute, vol. 343, January 2006, pp. 48-46.

[5] Prakob S. (2003). *Mathematical modeling analysis of positional control system for hydraulic cylinder,* Engineering Journal Kasetsart, April 2003, vol. 49, pp. 92-107.

[6] Mccloy D. and Martin H.R. (1980). *Control of Fluid Power Analysis and Design,* Ellis Horwood, Chichester.

[7] Becan R.M., Kuzucu A. and Kutlu K. (1998). *The realistic model and simulation of hydraulic position control systems,* Turk. J. Eng. Environ. Sci. vol. 22, March 1998, pp.125-130.

[8] J. Yan, M. Ryan and J. Power. (1994).*Using fuzzy logic: Towards intelligent systems*, Prentice Hall International, Hertfordshire.

[9] Y.M. Wang, G. Zhou and Sh. G. Wang. (2005). *Design and optimization of electro-hydraulic force servo system based on MATLAB,* Journal Mechanical Transmission, vol. 29(4), April 2005, pp. 46-49.

[10] *MATLAB/Simulink*, The Mathworks INC., www.mathworks.com

Author Biography

Name	LT.Pijirawuch Wiengchanda, RTN.
Date of birth	April 1, 1982.
Place of birth	Khonkean.
Education	B.Eng (Mechanical Engineering) (Second Honor)
	Royal Thai Naval academy, Thailand.
Experience	Main Propulsion Assistant, H.T.M.S.Rattanakosin, RTN.
	Deputy Chief Engineer, H.T.M.S.Thayanchol, RTN.